



Politecnico  
di Torino

ScuDo

Scuola di Dottorato ~ Doctoral School  
WHAT YOU ARE, TAKES YOU FAR

Doctoral Dissertation

Doctoral Program in Civil and Environmental Engineering (36<sup>th</sup> cycle)

# Fish Swimming Performance: Insights from Theory and Experiments

By

**Muhammad Usama Ashraf**

\*\*\*\*\*

**Supervisor(s):**

Prof. Costantino Manes, Supervisor

Prof. Claudio Comoglio, Co-Supervisor

**Doctoral Examination Committee:**

Prof. Valentina di Santo, Referee, Stockholm University, Sweden

Dr. Luiz Silva, Referee, ETH Zürich, Switzerland

Prof. Fulvio Boano, Politecnico di Torino, Italy

Prof. Stefania Tamea, Politecnico di Torino, Italy

Prof. Stefano Fenoglio, Università di Torino, Italy

Politecnico di Torino

2024

## Declaration

I hereby declare that, the contents and organisation of this dissertation constitute my own original work and does not compromise in any way the rights of third parties, including those relating to the security of personal data.

Muhammad Usama Ashraf  
2024

\* This dissertation is presented in partial fulfilment of the requirements for **Ph.D. degree** in the Graduate School of Politecnico di Torino (ScuDo).

*I dedicate this thesis to all the children worldwide who have been  
kept from their education by war and injustice.*

## Acknowledgements

With a mix of joyful and sad emotions, I write this acknowledgements section. Joy because I have reached a much-needed milestone in my career. Sadness because these three and a half years were among the best periods of my life while, now, they are only memories. First, I would like to sincerely thank three people, without whom none of what I have achieved during my PhD would have been possible: Costa, Claudio, and Daniel. Your supervision, support, kindness, encouragement, and hope in low times were the most important ingredients in the completion of this degree. The relationship that has developed with each of you over the years is unique and extremely valuable to me. I will always reflect on the lessons I have learnt from you, and they will continue to guide me in the years to come. I would also like to thank Paolo Domenici, Prof. Andrea Marion, and Prof. Vladimir Nikora for their scientific support during my PhD. I am delighted to have collaborated with all of you, and your inputs significantly contributed to my research work. Furthermore, I would like to thank Paolo Lo Conte (and others from the Incubatoio di Porte) and Alessandro Candiotta for their remarkable support during the experimental campaigns.

Moving on, I thank all 15 ESRs from the RIBES project who were like a family to me during these years. I had the opportunity to spend more time with only a few ESRs, which naturally resulted in stronger connections, but I acknowledge all of them as I believe they gave me support (direct or indirect) in this beautiful journey. In particular, I would like to thank Gloria. Her support as a colleague and as a friend has immensely helped me, and it was a pleasure working with her. Fieldworks were tiring, uncertain, and at times frustrating, but we always managed to finish them successfully. Without your help, I would have been lost, especially in the first year. So, a big thank to you for all your help. Thanks to Sophia for her assistance during the experimental campaign in 2021. Thank you, Alfredo, for your good company, unwavering support in fieldwork, and fun times at conferences. Thank you, Ali, for being a good roommate during conferences. Thank you Marcelo for your company, particularly during our secondment period in Aberdeen, and a special thanks to Miriam for her kindness and help during our visit to Scotland.

Outside of the RIBES family, I would like to thank Fabio for his support, particularly during the summer experiments in 2022. A big thank you to Andrea Cagninei and

Roberto Bosio for their consistent help and availability in lab works during my whole PhD. You both do such an excellent job in the lab, that I believe Artificial Intelligence will never be able take over your positions. And a special thanks to all the colleagues who made my time in the office worthwhile: Lorenzo, Filippo, Elisabetta, Elia, Davide, Roberta, Oliver, Nathan, Bert, Gigi, Ahmed, Hamed, Natalia, Silvia, and others.

A big thank you to my three friends: Aun, Mohammed, and Saurabh. Our friendship did not end with our master's degree but grew even stronger afterwards. Those trips in the summer and winter vacations provided the much-needed break from work. Many thanks to my mother, father, and three siblings. Their support and belief in me have fuelled my success, and their continuous prayers have worked wonders. Finally, I would like to say thank you so much to my wife, Fiammetta, for being a constant support day in, day out. It still seems surreal to think that in just three years, which feel like an entire life with you, we have been through so much together. Throughout these years, your love, appreciation, and support have been instrumental in my success. A simple thank you does not justify your efforts, love, and support for me. I look forward to creating even more beautiful memories as a family and achieving greater success together.

~ Usama  
17/06/2024

## **Abstract**

Fish swimming performance is crucial for activities like migration, habitat selection, reproduction, and predator-prey interactions, as well as in designing fish passage systems. Estimating fish swimming performance, using different experimental facilities, is influenced by subjective choices made by scientists. This includes use of different fatigue definitions, flume lengths, and habituation times, among others. These subjective choices not only hinder the comparison of results across studies but also impede the development of a unifying methodology for studying fish swimming performance. Moreover, fish fatigue curves, which quantify swimming performance as a relationship between time-to-fatigue and steady flow velocity, rely solely on empirical observations as obtained from time-consuming and expensive experiments, without much theoretical support. And lastly, there exists a significant knowledge gap in our understanding of fish swimming patterns and behaviour in fast-moving waters, commonly experienced by fish when navigating velocity barriers or holding position in swift streams.

In this PhD work, systematic experiments were carried out to test over 1100 juvenile fish belonging to five small-sized Cypriniformes using a fixed velocity testing protocol. Experiments were conducted to study the effect of different flume lengths, fatigue definitions, and habituation times on fish swimming performance and behaviour. Results show that fish swimming performance is a product of both capability and behaviour and is influenced by all three studied variables. Moreover, a theoretical framework is proposed that builds upon concepts of fish hydrodynamics to derive scaling laws linking statistical properties of time-to-fatigue to flow velocity in burst range. Experimental data on five fish species supports theoretical predictions reasonably well. Finally, fish velocity data was analysed for fish swimming in burst activity level, revealing persistent swimming patterns at time scales of about 1 sec, which are consistent with fish reaction times to visual stimuli.

# Contents

<b>List of Figures</b>	<b>ix</b>
<b>List of Tables</b>	<b>xii</b>
<b>Nomenclature</b>	<b>xiii</b>
<b>1. Introduction</b>	<b>1</b>
1.1 Background .....	2
1.2 Aim and objectives.....	4
1.3 Thesis structure .....	5
<b>References</b>	<b>6</b>
<b>2. Fish Swimming Performance: Effect of Flume Length and Different Fatigue Definitions</b>	<b>9</b>
2.1 Abstract .....	10
2.2 Introduction.....	11
2.3 Materials and Methods.....	13
2.4 Results .....	16
2.5 Discussion .....	18
<b>References</b>	<b>20</b>
<b>3. The Effect of In-Flume Habituation Time and Fish Behaviour on Estimated Swimming Performance</b>	<b>24</b>
3.1 Abstract .....	25
3.2 Introduction .....	26
3.3 Materials and Methods .....	29
3.4 Results .....	32
3.5 Discussion .....	35
<b>References</b>	<b>38</b>
<b>4. Decoding Burst Swimming Performance: A Scaling Perspective on Time-to-Fatigue</b>	<b>45</b>

4.1 Abstract .....	46
4.2 Introduction .....	47
4.3 Theoretical framework .....	50
4.4 Materials and Methods .....	52
4.5 Experimental results .....	56
4.6 Discussion .....	61
<b>References</b>	<b>64</b>
<b>5. Exploring Fish-Velocity Statistics in Burst Swimming Activity Level</b>	<b>70</b>
5.1 Abstract .....	71
5.2 Introduction .....	72
5.3 Materials and Methods .....	74
5.4 Results .....	79
5.5 Discussion .....	85
<b>References</b>	<b>87</b>
<b>6. Conclusions</b>	<b>92</b>
<b>References</b>	<b>95</b>
<b>Appendix A</b>	<b>97</b>
<b>References</b>	<b>100</b>
<b>Appendix B</b>	<b>101</b>
<b>Reference</b>	<b>103</b>
<b>Appendix C</b>	<b>104</b>
<b>Appendix D</b>	<b>105</b>
<b>Appendix E</b>	<b>107</b>



# List of Figures

Figure 2.1 Kaplan-Meier curves for tapped and untapped fatigue definition.....	17
Figure 3.1 Experimental flume used for swimming performance studies with all components connected.....	30
Figure 3.2 Box plot of time-to-fatigue for 0.5 min ( $n = 7$ ), 5 min ( $n = 27$ ), and 20 min ( $n = 31$ ) habituation time treatments.....	32
Figure 3.3 Box plot of time-to-fatigue for the fish swimming or resting in the flume ( $n = 21$ ) or resting on the grid ( $n = 37$ ) at the end of habituation/beginning of transition.....	33
Figure 3.4 Box plot of time-to-fatigue for fish swimming voluntarily in response to flow (“no tap”, $n = 29$ ) or swimming first after having been externally motivated by tapping (“tapped”, $n = 29$ ).....	34
Figure 4.1 Illustration of the relationship between fish time-to-fatigue ( $T_f$ ) and flow velocity ( $U_f$ ).....	49
Figure 4.2 Box plot of all experimentally collected time-to-fatigue ( $T_f$ ) data, without subsampling, for all five fish species.....	57
Figure 4.3 Kernel Density Estimation (KDE) of time-to-fatigue ( $T_f$ ) against flow velocity $U_f$ for the best fit subsampled group (with the highest reliability index value) for the five fish species.....	58
Figure 4.4 Data for time-to-fatigue mean $\bar{T}_f$ (panel (a)) and variance $\overline{T_f'^2}$ (panel (b)) versus flow velocity $U_f$ for the subsampled group with the highest Reliability Index ( $Rel$ ) value.....	59

Figure 4.5 Empirical estimates of scaling exponent $\beta$ obtained from the linear regression analysis between (a) $\ln (\bar{T}_f)$ and $\ln (U_f)$ and (b) $\ln (\bar{T}_f'^2)$ and $\ln (U_f)$ plotted against reliability index ( $Rel$ ).....	60
Figure 5.1 Sketch of the open channel flume with location of the points where longitudinal flow velocity measurement were carried out using LDA. ....	76
Figure 5.2 Validation of CFD simulated flow velocity data against LDA measurements for a treatment with an averaged cross-sectional flow velocity of 50 $\text{cm s}^{-1}$ .....	77
Figure 5.3 Lateral cross sections of the flow domain showing the longitudinal flow velocity magnitude obtained using the CFD $k-\epsilon$ model for mean $U_f$ of 50 $\text{cm s}^{-1}$ .....	79
Figure 5.4 Longitudinal cross section, in the middle of flume width, showing the development of boundary layer along the bottom flume wall.....	79
Figure 5.5 Fish velocity ( $U_r$ ) time-series signal for fish swimming at a mean $U_f$ of 55 $\text{cm s}^{-1}$ .....	80
Figure 5.6 Boxplot of maximum fish swimming velocity $U_{max}(n = 10)$ for all mean flow velocity treatments. ....	81
Figure 5.7 Frequency distributions of fish velocity ( $U_r$ ) at four mean flow velocity treatments. ....	82
Figure 5.8 Power Spectra of longitudinal (panel (a) and (b)) and lateral (panel (c) and (d)) fish velocity time series at four mean $U_f$ values. ....	83
Figure 5.9 Plots of power spectra and its pre-multiplied form for time-averaged single-point longitudinal flow velocity measurements, as obtained from the LDA, at four locations in the flow domain.....	84
Figure A.1 Sketch of an idealized fish swimming.....	98
Figure A.2 Experimental data measurements highlighting the dependence of Strouhal number ( $St$ ) on Reynolds number ( $Re_L$ ).....	99
Figure B.1 Distribution plot of fish fork length ( $L_f$ ) for five fish species.....	101

Figure C.1 Fish allometric relationships for five fish species ..... 104

Figure D.1 Plots between  $\overline{T_f'^3}$  and  $U_f$  for the subsampled data with the highest Reliability Index (*Rel*). ..... 106

# List of Tables

Table 2.1 Cox Proportional-Hazard Model summary table output for untapped and tapped fatigue models.....	16
Table 4.1 Summary of experimental data for five tested Cypriniformes fish species.....	56
Table B.1 Summary of subsampled groups .....	102
Table E.1 List of candidate models for (a) Tapped and (b) Untapped fatigue definitions with their AIC values.....	107

# Nomenclature

## Roman Symbols

$\bar{E}$	Mean fish energy [ $\text{Kg.m}^2\text{s}^{-2}$ ]
$\bar{T}_f$	Mean time-to-fatigue [s]
$\overline{T_f'^2}$	Variance of time-to-fatigue [ $\text{s}^2$ ]
$\overline{T_f'^3}$	Third-order central moment of time-to-fatigue [ $\text{s}^3$ ]
$\vec{Z}$	Flow velocity vector [ $\text{cms}^{-1}$ ]
$\bar{u}$	Time-averaged longitudinal flow velocity component [ $\text{cms}^{-1}$ ]
$\bar{v}$	Time-averaged lateral flow velocity component [ $\text{cms}^{-1}$ ]
$\bar{w}$	Time-averaged vertical flow velocity component [ $\text{cms}^{-1}$ ]
$A$	Fish tail beat amplitude [cm]
$a$	Acceleration [ $\text{ms}^{-2}$ ]
$C_D$	Drag coefficient of rigid body [-]
$C_{DU}$	Drag coefficient of undulating body [-]
$D_g$	Fish ground distance [cm]
$D_{smax}$	Maximum fish swimming distance [cm]
$E$	Fish energy [ $\text{Kg.m}^2\text{s}^{-2}$ ]
$E'_i$	Individual fish energy deviations from mean fish energy [ $\text{Kg.m}^2\text{s}^{-2}$ ]

$f$	Fish tail beat frequency [ $s^{-1}$ ]
$F_D$	Drag force [N]
$F_{DS}$	Drag force per unit of fish depth [ $Nm^{-1}$ ]
$\vec{F}_t$	Inertial force [N]
$F_{tx}$	Thrust force component in longitudinal direction [N]
$h$	Fish height [cm]
$K$	Turbulent kinetic energy [ $m^2s^{-2}$ ]
$k$	Order of central moment [-]
$L$	Fish length [cm]
$L_f$	Fish fork length [cm]
$L_{means}$	Vector of mean fish length [cm]
$L_{variation}$	Vector of variation in fish length [cm]
$l_{ms}$	Upstream mesh grid size [mm]
$m$	Fish mass [g]
$n$	Number of successful fish trials [-]
$p(T_f)$	Probability function of time-to-fatigue [-]
$P$	Power [ $Kg.m^2s^{-3}$ ]
$p$	Total number of time-to-fatigue data points [-]
$Q$	Volume flow rate [ $cm^3s^{-1}$ ]
$Re$	Reynolds number [-]
$Re_L$	Reynolds number with fish length as characteristic length scale [-]
$Re_s$	Reynolds number with fish depth as characteristic length scale [-]
$R^2$	Coefficient of determination [-]
$S$	Fish body depth [cm]
$St$	Fish Strouhal number [-]

$T$	Water temperature [°C]
$T_f$	Time-to-fatigue [s]
$T'_{fi}$	Individual time-to-fatigue deviation from mean time-to-fatigue [s]
$U_f$	Average cross sectional flow velocity [cms <sup>-1</sup> ]
$U_g$	Fish ground velocity [cms <sup>-1</sup> ]
$U_M$	Maximum tested flow velocity [cms <sup>-1</sup> ]
$U_m$	Minimum tested flow velocity [cms <sup>-1</sup> ]
$U_r$	Fish-water relative velocity [cms <sup>-1</sup> ]
$U_{rx}$	Longitudinal fish velocity [cms <sup>-1</sup> ]
$U_{ry}$	Lateral fish velocity [cms <sup>-1</sup> ]
$U_{CFD}$	Numerically modelled flow velocity [cms <sup>-1</sup> ]
$U_{crit}$	Critical fish swimming velocity [cms <sup>-1</sup> ]
$U_{gopt}$	Optimal fish ground velocity [cms <sup>-1</sup> ]
$U_{max}$	Maximum fish swimming velocity [cms <sup>-1</sup> ]
$U_{ropt}$	Optimal fish-water relative velocity [cms <sup>-1</sup> ]
$u$	Single-point longitudinal flow velocity [cms <sup>-1</sup> ]
$V$	Transverse velocity of fish body undulations [cms <sup>-1</sup> ]
$w$	Fish width [cm]
$X$	Cross-sectional area of flume [cm <sup>2</sup> ]

### **Greek Symbols**

$\Delta t$	Fixed time interval [s]
$\Delta U$	Fixed flow velocity increment [cms <sup>-1</sup> ]
$\alpha$	Scaling function
$\beta$	Scaling exponent [-]
$\theta$	Local angle between the fish tail and direction of motion [deg]

$\sim$	Scales as [-]
$\rho$	Fluid density [ $\text{Kg}\cdot\text{m}^{-3}$ ]
$\mu$	Water dynamic viscosity [ $\text{Kg}\cdot\text{m}^{-1}\text{s}^{-1}$ ]
$\nu$	Water kinematic viscosity [ $\text{m}^2\text{s}^{-1}$ ]
$\varepsilon$	Turbulent dissipation rate [ $\text{m}^2\text{s}^{-3}$ ]

### **Acronyms / Abbreviations**

<i>1-D</i>	One-Dimensional
<i>AIC</i>	Akaike Information Criterion
<i>ANOVA</i>	Analysis of variance
<i>BL/s</i>	Fish body length per second
<i>CFD</i>	Computational Fluid Dynamics
<i>CNN</i>	Convolutional Neural Network
<i>IQR</i>	Interquartile range
<i>KDE</i>	Kernal Density Estimation
<i>LDA</i>	Laser Doppler Anemometer
<i>ln</i>	Natural logarithm
<i>PDF</i>	Probability Density Function
<i>PSD</i>	Power Spectral Density
<i>Rel</i>	Reliability Index
<i>sd</i>	Standard deviation
<i>se</i>	Standard error



# **Chapter 1**

## **Introduction**

This chapter is subdivided into three sections: Section 1.1 contains a general brief background of the study problem, Section 1.2 presents the aim and objectives, and Section 1.3 outlines the thesis structure.

## 1.1 Background

In recent decades, there has been a global surge in studies investigating fish swimming performance as it plays a vital role in fish migration, habitat selection, reproduction, and predator-prey interactions, as well as fish passage design. (Beamish, 1978; Castro-Santos, 2002; Domenici & Blake, 1997; Katopodis, 1992; Videler, 1993). To date, scientists have explored various interlinked attributes of fish swimming performance such as swimming velocities, manoeuvrability, energy expenditure, and time-to-fatigue, among others (Domenici & Kapoor, 2010; Videler, 1993). From an applied perspective, understanding these different attributes and their responses to environmental changes enables informed decision-making in fish habitat management and restoration plans in rivers and streams (Cano-Barbacid et al., 2020; Peake, 2008; Silva et al., 2021). One particularly significant example is the use of swimming performance estimates in the design and development of effective fish passage to allow fish to pass dams, weirs, culverts, and other anthropogenic barriers to their movement (Barbarossa et al., 2020; Belletti et al., 2020; Nilsson et al., 2005).

Two commonly employed testing methodologies, which use an open channel flume or a water tunnel, to estimate various metrics of fish swimming performance are: increasing velocity and fixed velocity method (Beamish, 1978; Katopodis & Gervais, 2012). In the former, a fish is forced to swim at a regularly increasing flow velocity at fixed time intervals until the fish fatigues whereas, in the latter, a fish is forced to swim against a steady flow velocity until fatigued. Despite their widespread use, significant variations in important details of both testing protocols are found in the scientific literature (Deslauriers & Kieffer, 2011; Farlinger & Beamish, 1977; Tudorache et al., 2013). Three such examples include the use of arbitrarily chosen definition of fish fatigue, flume length, and habituation period. A few earlier studies have highlighted the potential negative impact of these variables on measured fish performance and behaviour (Deslauriers & Kieffer, 2011; Tudorache et al., 2007, 2010). However, there is still a significant need for further research to test various fish species and testing protocols as a step toward developing a unified methodology that reduces the subjectivity involved in estimating fish swimming performance. In an effort to address this knowledge gap, chapters two and three investigate the effect of the choice of fatigue definition, flume length, and the duration of habituation period on estimated swimming performance.

Fixed velocity tests have been traditionally used to obtain fatigue curves which quantify fish swimming performance by examining the relationship between time-to-fatigue ( $T_f$ ) and steady flow velocity ( $U_f$ ). Fatigue curves serve as a cornerstone in the design of fish passage structures, allowing the evaluation of fish swimming performance across various flow velocities and associated swimming activity levels (Katopodis, 1992;

Katopodis & Gervais, 2012). Our current ability to model fatigue curves primarily relies on empirical observations as obtained by testing fish at varying velocities in time-consuming and costly experiments. Given the vast fish biodiversity worldwide, this is a daunting task. Moreover, an enormous and largely unexplored variability in swimming performance estimates exists even among conspecifics of similar sizes (Goerig & Castro-Santos, 2017; Jones et al., 2020; Videler, 1993; Wardle, 1975). This presents a challenge, in the use of results from fatigue curves for practical applications, as empirically modelled fatigue curves only provide information about the average trend of the data without any clue about the distribution of  $T_f$  at each tested velocity and how it varies with  $U_f$ . Therefore, relying solely on an empirical approach limits our ability to model and understand fatigue curves. This highlights the necessity of employing theoretical approaches to bridge the knowledge gap. One such theoretical framework based on fish drag and hydrodynamics, describing a statistical relationship between  $T_f$  and  $U_f$ , is presented in Chapter 4, thereby opening up new avenues for experimental research aimed at quantifying endurance in fish.

Fatigue curves in burst swimming range, where fish use white muscles and fatigue within a few tens of seconds, hold significant ecological importance (Wolter & Arlinghaus, 2004). This is particularly true for species that need to maintain their position in swiftly moving waters or cross barriers with high velocity during migration. Their survival and successful journey may ultimately depend on their ability to perform burst swimming (Beamish, 1978; Burnett et al., 2014). However, interpreting fatigue curves is a difficult task as estimated performance is a product of both physiological capability and behaviour (Deslauriers, 2011; Peake & Farrell, 2006). Fish are clever swimmers as they are known to exploit turbulence by harnessing the energy from vortices (Liao, 2007), low drag flow regions (Kerr et al., 2016), and inertia by means of burst-and-coast behaviour (Videler & Weihs, 1982; Weihs, 1974; Wu et al., 2007). However, our knowledge about these intelligent fish behaviours is limited to the case of standing or slow-moving waters. Instead, it is unclear whether fish encountering fast-flowing waters use any swimming strategies or ways to either minimise energy expenditure, stabilise the visual field, and/or enhance their sensory abilities. This is important because burst swimming capacity is essential to the design of fish passage infrastructure. Chapter 5, therefore, explore fish velocity statistics in burst activity level to investigate swimming patterns in fixed velocity fatigue tests.

## 1.2 Aim and objectives

The general aim of the present thesis is to improve our current understanding of fish fatigue in the burst swimming activity level, combining theoretical and empirical methods. To fulfil this aim, the following objectives are set:

1. To identify and quantify the effect of two different fatigue definitions and three different flume lengths on the estimated swimming performance of Italian riffle dace (*Telestes muticellus*).
2. To investigate, in North Italian roach (*Leucos aula*), the effects on time-to-fatigue of (i) habituation time, (ii) fish behaviour during habituation, and (iii) external stimuli to provoke swimming.
3. To develop a theoretical framework that can statistically describe the relation between time-to-fatigue and mean flow velocity in fixed velocity tests and test it on five small-sized Cypriniformes: Italian riffle dace (*Telestes muticellus*), common minnow (*Phoxinus phoxinus*), European bitterling (*Rhodeus amarus*), North Italian roach (*Leucos aula*), and common bleak (*Alburnus alburnella*).
4. To investigate swimming patterns and maximum sprinting velocities of Italian riffle dace (*Telestes muticellus*) during fixed velocity fatigue tests within the burst swimming velocity range.

The five experimentally investigated small-sized riverine Cypriniformes were chosen because they are all common within their geographic range (Freyhof & Kottelat, 2007), are classified as least concerned in the IUCN red lists (IUCN, 2023), and were expected to display interspecific variation in swimming abilities.

## 1.3 Thesis structure

The thesis is organised into chapters, with chapters 2 to 5 each addressing one of the aforementioned study objectives. A brief outline of the thesis structure is given below:

Chapter 2, addressing study objective 1, has been published as a book chapter in *Advances in Hydraulic Research, GeoPlanet: Earth and Planetary Sciences*.

Chapter 3 is dedicated to study objective 2 and has been published as an article in the *Journal of Ecohydraulics*.

Chapter 4 focuses on study objective 3 and is under revision in the *Journal of Royal Society Interface*.

Chapter 5 is devoted to study objective 4 and has not been submitted for publication yet.

Chapter 6 summarises and concludes the overall thesis work with potential future research directions.

In addition, Appendix A to D are provided as supplemental to Chapter 4, while Appendix E supplements Chapter 2.

## References

- Barbarossa, V., Schmitt, R. J. P., Huijbregts, M. A. J., Zarfl, C., King, H., & Schipper, A. M. (2020). Impacts of current and future large dams on the geographic range connectivity of freshwater fish worldwide. *Proceedings of the National Academy of Sciences*, 117(7), 3648–3655. <https://doi.org/10.1073/pnas.1912776117>
- Beamish, F. W. H. (1978). *Fish Physiology* (W. S. Hoar & D. J. Randall, Eds.; 1st ed., Vol. 7). Academic Press, London.
- Belletti, B., Garcia De Leaniz, C., Jones, J., Bizzi, S., Börger, L., Segura, G., Castelletti, A., Van De Bund, W., Aarestrup, K., Barry, J., Belka, K., Berkhuysen, A., Birnie-Gauvin, K., Bussetini, M., Carolli, M., Consuegra, S., Dopico, E., Feierfeil, T., Fernández, S., ... Zalewski, M. (2020). More than one million barriers fragment Europe's rivers. *Nature*, 588(7838), 436–441. <https://doi.org/10.1038/s41586-020-3005-2>
- Burnett, N. J., Hinch, S. G., Braun, D. C., Casselman, M. T., Middleton, C. T., Wilson, S. M., & Cooke, S. J. (2014). Burst Swimming in Areas of High Flow: Delayed Consequences of Anaerobiosis in Wild Adult Sockeye Salmon. *Physiological and Biochemical Zoology*, 87(5), 587–598. <https://doi.org/10.1086/677219>
- Cano-Barbacid, C., Radinger, J., Argudo, M., Rubio-Gracia, F., Vila-Gispert, A., & García-Berthou, E. (2020). Key factors explaining critical swimming speed in freshwater fish: A review and statistical analysis for Iberian species. *Scientific Reports*, 10(1), 18947. <https://doi.org/10.1038/s41598-020-75974-x>
- Castro-Santos, T. (2002). *Swimming performance of upstream migrant fishes: New methods, new perspectives* [University of Massachusetts Amherst]. <https://scholarworks.umass.edu/dissertations/AAI3056208/>
- Deslauriers, D. (2011). *Factors influencing swimming performance and behaviour of the shortnose sturgeon (Acipenser brevirostrum)*. University of New Brunswick, Saint John.
- Deslauriers, D., & Kieffer, J. D. (2011). The influence of flume length and group size on swimming performance in shortnose sturgeon *Acipenser brevirostrum*. *Journal of Fish Biology*, 79(5), 1146–1155. <https://doi.org/10.1111/j.1095-8649.2011.03094.x>
- Domenici, P., & Blake, R. (1997). The kinematics and performance of fish fast-start swimming. *Journal of Experimental Biology*, 200(8), 1165–1178. <https://doi.org/10.1242/jeb.200.8.1165>
- Domenici, P., & Kapoor, B. G. (Eds.). (2010). *Fish locomotion: An eco-ethological perspective*. Science Publishers.
- Farlinger, S., & Beamish, F. W. H. (1977). Effects of Time and Velocity Increments on the Critical Swimming Speed of Largemouth Bass (*Micropterus salmoides*). *Transactions of the American Fisheries Society*, 106(5), 436–439. [https://doi.org/10.1577/1548-8659\(1977\)106<436:EOTAVI>2.0.CO;2](https://doi.org/10.1577/1548-8659(1977)106<436:EOTAVI>2.0.CO;2)

- Freyhof, J., & Kottelat, M. (2007). Handbook of European freshwater fishes. <https://portals.iucn.org/library/node/9068>
- Goerig, E., & Castro-Santos, T. (2017). Is motivation important to brook trout passage through culverts? *Canadian Journal of Fisheries and Aquatic Sciences*, 74(6), 885–893. <https://doi.org/10.1139/cjfas-2016-0237>
- Jones, P. E., Svendsen, J. C., Börger, L., Champneys, T., Consuegra, S., Jones, J. A. H., & Garcia De Leaniz, C. (2020). One size does not fit all: Inter- and intraspecific variation in the swimming performance of contrasting freshwater fish. *Conservation Physiology*, 8(1), coaa126. <https://doi.org/10.1093/conphys/coaa126>
- IUCN. 2023. The IUCN Red List of Threatened Species. Version 2023-1. <https://www.iucnredlist.org>.
- Katopodis, C. (1992). Introduction to fishway design. Freshwater Institute, Central and Arctic Region Department of Fisheries and Oceans, Manitoba, Canada.
- Katopodis, C., & Gervais, R. (2012). Ecohydraulic analysis of fish fatigue data. *River Research and Applications*, 28(4), 444–456. <https://doi.org/10.1002/rra.1566>
- Kerr, J. R., Manes, C., & Kemp, P. S. (2016). Assessing hydrodynamic space use of brown trout, *Salmo trutta*, in a complex flow environment: A return to first principles. *Journal of Experimental Biology*, jeb.134775. <https://doi.org/10.1242/jeb.134775>
- Killen, S. S., Christensen, E. A. F., Cortese, D., Závorka, L., Norin, T., Cotgrove, L., Crespel, A., Munson, A., Nati, J. J. H., Papatheodoulou, M., & McKenzie, D. J. (2021). Guidelines for reporting methods to estimate metabolic rates by aquatic intermittent-flow respirometry. *Journal of Experimental Biology*, 224(18), jeb242522. <https://doi.org/10.1242/jeb.242522>
- Liao, J. C. (2007). A review of fish swimming mechanics and behaviour in altered flows. *Philosophical Transactions of the Royal Society B: Biological Sciences*, 362(1487), 1973. <https://doi.org/10.1098/rstb.2007.2082>
- Nilsson, C., Reidy, C. A., Dynesius, M., & Revenga, C. (2005). Fragmentation and Flow Regulation of the World's Large River Systems. *Science*, 308(5720), 405–408. <https://doi.org/10.1126/science.1107887>
- Peake, S. J. (2008). Swimming performance and behaviour of fish species endemic to Newfoundland and Labrador: A literature review for the purpose of establishing design and water velocity criteria for fishways and culverts. *Can. Manuscr. Rep. Fish. Aquat. Sci.* 2843: V + 52p.
- Peake, S. J., & Farrell, A. P. (2006). Fatigue is a behavioural response in respirometer-confined smallmouth bass. *Journal of Fish Biology*, 68(6), 1742–1755. <https://doi.org/10.1111/j.0022-1112.2006.01052.x>

Roche, D. G., Tytell, E. D., & Domenici, P. (2023). Kinematics and behaviour in fish escape responses: Guidelines for conducting, analysing and reporting experiments. *Journal of Experimental Biology*, 226(14), jeb245686. <https://doi.org/10.1242/jeb.245686>

Silva, S. S., Alexandre, C. M., Quintella, B. R., & de Almeida, P. R. (2021). Seasonal environmental variability drives the swimming performance of a resident Iberian fish. *Ecology of Freshwater Fish*, 30(3), 366–374. <https://doi.org/10.1111/eff.12587>

Tudorache, C., de Boeck, G., & Claireaux, G. (2013). Forced and Preferred Swimming Speeds of Fish: A Methodological Approach. In A. P. Palstra & J. V. Planas (Eds.), *Swimming Physiology of Fish* (pp. 81–108). Springer Berlin Heidelberg. [https://doi.org/10.1007/978-3-642-31049-2\\_4](https://doi.org/10.1007/978-3-642-31049-2_4)

Tudorache, C., O’Keefe, R. A., & Benfey, T. J. (2010). Flume length and post-exercise impingement affect anaerobic metabolism in brook charr *Salvelinus fontinalis*. *Journal of Fish Biology*, 76(3), 729–733. <https://doi.org/10.1111/j.1095-8649.2009.02513.x>

Tudorache, C., Viaenen, P., Blust, R., & De Boeck, G. (2007). Longer flumes increase critical swimming speeds by increasing burst-glide swimming duration in carp *Cyprinus carpio*, L. *Journal of Fish Biology*, 71(6), 1630–1638. <https://doi.org/10.1111/j.1095-8649.2007.01620.x>

Videler, J. J. (1993). *Fish Swimming*. Springer Netherlands. <https://doi.org/10.1007/978-94-011-1580-3>

Videler, J., & Weihs, D. (1982). Energetic advantages of burst-and-coast swimming of fish at high speeds. *The Journal of Experimental Biology*, 97, 169–178.

Wardle, C. S. (1975). Limit of fish swimming speed. *Nature*, 255(5511), 725–727. <https://doi.org/10.1038/255725a0>

Weihs, D. (1974). Energetic advantages of burst swimming of fish. *Journal of Theoretical Biology*, 48(1), 215–229. [https://doi.org/10.1016/0022-5193\(74\)90192-1](https://doi.org/10.1016/0022-5193(74)90192-1)

Wolter, C., & Arlinghaus, R. (2004). Burst and critical swimming speed of fish and their ecological relevance in waterways. In *Berichte des IGB* (Vol. 20, pp. 77–93). <https://www.ifishman.de/publikationen/einzelansicht/599-burst-and-critical-swimming-speed-of-fish-and-their-ecological-relevance-in-waterways/>

Wu, G., Yang, Y., & Zeng, L. (2007). Kinematics, hydrodynamics and energetic advantages of burst-and-coast swimming of koi carps (*Cyprinus carpio koi*). *Journal of Experimental Biology*, 210(12), 2181–2191. <https://doi.org/10.1242/jeb.001842>



## **Chapter 2**

# **Fish Swimming Performance: Effect of Flume Length and Different Fatigue Definitions**

## 2.1 Abstract

Swimming performance is important for a range of fish behaviours. Quantifying fish swimming performance in experimental facilities is influenced by channel geometry, size, and length. Also, the lack of a standard fatigue definition potentially affects the assessment of the fish swimming performance. Experiments on juvenile Italian ruffe dace (*Telestes muticellus*) were conducted to elucidate the effect of different flume lengths and fatigue definitions on swimming performance estimates using a fixed velocity protocol. Three swimming arena lengths of 15, 30, and 100 cm in an open channel flume were tested under two different mean flow velocities, 35 and 45  $\text{cm s}^{-1}$ . The effect of two different criteria for determining time-to-fatigue was studied: (1) untapped fatigue, i.e. fish were considered fatigued when resting on the downstream grid for  $\geq 3\text{s}$ . (2) tapped fatigue, i.e. when fish rested on the grid it was gently tapped to encourage swimming. The third time it returned to the downstream grid, it was considered fatigued. The difference in time-to-fatigue of Italian ruffe dace was statistically significant between the two treatment velocities, i.e. 35 and 45  $\text{cm s}^{-1}$ . The flume length affected swimming performance based on untapped but not on tapped fatigue definition. It is concluded that the criteria used to define fatigue may have an influence on the conclusions drawn from the fish swimming experiments.

## 2.2 Introduction

Fish swimming performance has received substantial attention in the last 30-40 years owing to its importance in fish passage design, fish migration, habitat selection, reproduction, and predator-prey interaction (Castro-Santos, 2002; Domenici & Blake, 1997; Katopodis & Gervais, 2012; Peake et al. 1997; Watson et al., 2019). Since the early work on the swimming performance of juvenile sockeye salmon (*Oncorhynchus nerka*) by Brett (1964), a plethora of information about fish swimming performance of different species has been made available by researchers around the world (Katopodis & Gervais, 2012).

At the general level, fish swimming activity levels have been categorized as sustained, prolonged, and burst (Beamish, 1978; Hammer, 1995). The sustained swimming is powered by red muscle fibres, also known as aerobic swimming, and can theoretically be maintained indefinitely. Burst swimming is entirely fuelled by white muscle fibres and is measured to last no more than 15-30 seconds (Nikora et al. 2003). Prolonged swimming, as an intermediate activity level, employs both red and white muscle fibres and lasts from seconds up to 200 mins before fatigue (Brett, 1964). As an energy-saving mechanism, fish may also deploy a mix of swimming activity levels, the so-called burst-and-coast or intermittent locomotion (Paoletti & Mahadevan, 2014; Videler & Weihs, 1982).

Currently, the increasing velocity and fixed velocity tests are two widely used methods to quantify fish swimming performance. As the name suggests, in the increasing velocity test, the fish is forced to swim against stepwise increasing mean flow velocity ( $\Delta U$ ) over a fixed time interval ( $\Delta t$ ) until fatigued. Whereas in the fixed velocity testing, the fish is forced to swim at a constant mean flow velocity until fatigued (Tudorache et al. 2013). While the increasing velocity tests are quick to run and reveal information about fish performance through a unique parameter, commonly referred to as the critical swimming velocity ( $U_{crit}$ , approximately the velocity at which maximum sustainable oxygen uptake occurs), the fixed velocity tests at a range of velocities result in a fatigue curve covering different fish swimming activity levels for the species under investigation (Brett, 1964; Farrell & Steffensen, 1987).

Swimming performance tests typically end when a fish is declared as fatigued. So far, numerous fatigue definitions have been reported in published articles, including when a fish impinges to the downstream grid for 3 sec (Tudorache et al. 2010a), 5 sec (Peake & Farrell, 2006), or 15 sec (Veza et al. 2020). Sometimes fish are encouraged to swim by physically tapping, visual stimulation, abrupt change of water velocity, or even repeated electric shocks for a pre-decided number of times, or until the fish simply stop responding, before fatigue is declared (Bestgen et al. 2010; McFarlane & McDonald, 2002; Nelson et al. 2003; Romão et al. 2012). Since fish behaviour plays a critical role in performance tests (Peake 2008a; Peake & Farrell, 2006), the total fatigue time, and related conclusions, could potentially differ depending on the use of fatigue definition. Nevertheless, the effect

of the use of encouraging stimuli on the estimated swimming performance is lacking in the literature.

Swimming performance tests are typically carried out in closed respirometry tunnels or open channel flumes (Katopodis & Gervais, 2012). The size and geometry of such testing apparatus are arbitrarily chosen to restrict the fish motions within a specified flow domain. The length of such a domain, in particular, varies extensively between studies with potential effects on the estimated fish swimming performance. In fact, several studies have shown that decreasing flume lengths has a negative influence on the measured performance, presumably by restricting fish swimming behaviour such as intermittent locomotion and gait transitions, along with blocking and wall effects (Bell & Terhune, 1970; Deslauriers & Kieffer, 2011; Tudorache et al. 2007, 2008, 2010a).

Considering the aforementioned remarks about the choice of fatigue definition and flume length in forced performance tests, the main goal of this study is to elucidate the effect of these variables on the estimated swimming performance. Experiments were conducted on Italian riffle dace (*Telestes muticellus*), a small-sized riverine cyprinid using a fixed velocity testing protocol. Results were statistically analysed to test (i) if the flume length affects swimming performance by using three different swimming arena lengths at two different flow velocities and (ii) if the definition of fatigue affects the experiment results by using two different definitions, with or without physical encouragement (tapping).

## 2.3 Materials and Methods

### 2.3.1 Fish

Juvenile *T. muticellus* with fork length  $L_f$ ,  $5 \pm 0.3$  cm (mean  $\pm$  standard deviation (sd)) and mass  $m$ ,  $1.6 \pm 0.3$  g (mean  $\pm$  sd) were captured from the Noce stream near Pinerolo, Italy ( $44^\circ 56' 17.9''$  N  $7^\circ 23' 09.1''$  E) using electrofishing on the morning of 31 May 2021. Fish were transported in 10L buckets to a hatchery facility in Porte di Pinerolo. Fish were kept in two flow-through spring-fed tanks divided into 6 perforated compartments (20L) with c. 15 fish in each. Water temperature was recorded using a HOBO MX-2202 data logger at regular time intervals of 10 minutes until the end of the experimental campaign. Temperature varied between 12.5-13.2 °C. The first trial started 4 days after electrofishing to allow the fish to acclimatise to the hatchery environment. Fish were not fed (Cai et al. 2014; Penghan et al. 2016) and remained healthy looking throughout the experimental campaign. The study was performed in accordance with the Protection of Flora and Fauna Department of the Metropolitan City of Turin (authorization D.D. n.4457 of 29 October 2020).

### 2.3.2 Flume description

Fish were tested in an open-channel recirculating flume with a cross-section area of 900 cm<sup>2</sup> (30 cm by 30 cm) and a total length of 260 cm. The walls of the flume are made of transparent plexiglass. An inlet that feeds the water to the main flume is connected to a pump with a maximum frequency of 50 Hz. The flow rate in the system is controlled manually through an inverter (DGFIT MT 12) installed with the pump. Water is received by a 600L reservoir tank and is then recirculated back to the flume through the pump. A flow meter sensor (AquaTrans<sup>TM</sup> AT600) is attached to the outlet pipe from the reservoir tank and measures the flow rate (Ashraf et al. 2024).

Water in the system was kept at a relatively constant temperature  $T$ ,  $12.6 \pm 0.3$  °C (mean  $\pm$  sd) during testing times and was cooled when necessary using an ad-hoc designed chiller unit (TECO TK-2000). The temperature difference between the holding tanks and the testing flume was never more than 1°C to avoid any potential effects of extreme temperature change on swimming performance (Tudorache et al. 2010b; Vezza et al. 2020). The swimming tests were video recorded from underneath and from the side using two Sony AX43 Handycam at a resolution of 1920x1080p and 50 fps.

### 2.3.3 Fixed velocity testing

A movable grid was used to modify the flume length available to the fish. Three flume lengths, 15, 30, and 100 cm, were tested at two different mean flow velocities: 35 and 45 cms<sup>-1</sup>. Three flume lengths, corresponding to 3, 6, and 20 fish body lengths, were used to study the potential reduction in swimming performance in smaller flumes due to restricted intermittent and burst-and-coast behaviour, as well as the enhanced performance in larger

flumes (Deslauriers & Kieffer, 2011; Tudorache et al. 2007). The selection of flow velocities was made, based on preliminary trials, to evaluate fish swimming performance at two different activity levels: prolonged swimming at  $35 \text{ cm s}^{-1}$  and burst swimming at  $45 \text{ cm s}^{-1}$ . Only fish actively swimming, i.e. those oriented against the flow and not displaying signs of stress, were included in the study. 10 fish were successfully tested for each of the six treatments, and each fish was tested only once. Fish were tested in a randomised-block design, each block including all 6 treatments. At the beginning of the experiment, fish were allowed to habituate for 10 minutes: 5 minutes at  $10 \text{ cm s}^{-1}$  followed by another 5 minutes at  $20 \text{ cm s}^{-1}$  (Ashraf et al. 2024). This allowed the fish to habituate to the flume environment prior to being exposed to the experimental velocity. Following the habituation period, the flow rate was increased to achieve the testing velocity within 30 seconds. The maximum trial time was limited to 1800 seconds (Veza et al. 2020).

### 2.3.3.1 Time-to-fatigue

To study the effect of fatigue definition, in fixed velocity fatigue tests, on swimming performance estimates, two different definitions of fatigue were used: tapped fatigue and untapped fatigue. For untapped fatigue, a fish was considered as fatigued when it rested on the downstream grid for  $\geq 3$  sec, for the first time. For the tapped fatigue, fish were physically encouraged to swim, using a gentle tap with a stick to the downstream grid, three times in a row before being considered fatigued. By watching the recorded videos, the total time a fish swam was calculated. The time a fish rested on the grid before tapping or fatigue was subtracted from the total swimming time to obtain the active swimming time. The total active swimming time and the time a fish swam before first resting on the downstream grid were recorded as times-to-fatigue under the tapped and untapped fatigue definitions, respectively. At the end of each trial, fish were anaesthetised, and the fork length  $L_f$  [cm] and mass  $m$  [g] were recorded.

### 2.3.3.2 Statistical analysis

A Cox proportional-hazards model, a type of survival analysis, was used to test the effect of flume length on time-to-fatigue for the two different fatigue definitions separately. The Cox proportional-hazards model is a type of regression model which allows to investigate the link between fatigue and one or more predictor variables, taking both fatigue (yes/no) and the time-to-fatigue into account (Cox, 1972). Fish still swimming after the 30 min trial were treated as right censored observations (Rao et al. 2000). The assumption of proportionality of hazard was explicitly tested for the selected models (Fox, 2002).

All combinations of flume length, flow velocity, and their interactions were included among the candidate models. To control for acclimatisation in the hatchery and any starvation effects, the day of the experiment (starting from 0 on the day of capture) was also included among the candidate models. The Akaike information criterion (AIC) method was used to choose the best model among possible candidate models. AIC values were calculated for each candidate model (Appendix E contains list of all candidate models with their AIC values). A model with the lowest AIC value ( $\text{AIC}_{\min}$ ) is considered

the best. However, any model with an AIC value within 2 units of difference from the  $AIC_{\min}$  is regarded as good (Burnham & Anderson, 2004). In the case of two or more good models, the one with the least number of covariates was chosen (Richards, 2007). Results were considered significant at  $p\text{-value} < 0.05$ . The Kaplan-Meier curves were plotted to graphically represent the proportion of non-fatigued fish for both tapped and untapped fatigue definitions, and for all six treatments. The differences between the length and mass of fish in the different treatments were tested using ANOVA. All statistical analyses were run using R version 4.1.2 (R Foundation for Statistical Computing, Vienna, Austria. URL <https://www.R-project.org>). Package *dplyr* was used for data management (<https://CRAN.R-project.org/package=dplyr>). *Survminer* package was used for time-to-event analysis (<https://CRAN.R-project.org/package=survminer>), and *ggplot2* was used for plotting.

## 2.4 Results

There was no significant difference in fish length or mass between treatments (two-way ANOVA,  $p > 0.05$ ). For all three flume lengths and for both fatigue definitions, the time-to-fatigue was significantly shorter for  $45 \text{ cms}^{-1}$  velocity compared to  $35 \text{ cms}^{-1}$  and flume length did not influence the time-to-fatigue at  $45 \text{ cms}^{-1}$  velocity ( $p < 0.05$ ). At  $35 \text{ cms}^{-1}$ , however, a large proportion of fish swam more than the testing time limit of 1800 seconds: 40% at untapped and 63% at tapped fatigue definition (Fig. 2.1 (a) and (c)). On the other hand, fish fatigued within 2 to 206 seconds in all flume lengths at  $45 \text{ cms}^{-1}$  (Fig. 2.1 (b) and (d)).

### 2.4.1 Untapped fatigue

For the untapped fatigue definition, the time-to-fatigue at  $35 \text{ cms}^{-1}$  flow velocity depended on the flume length. As shown in Table 2.1, the results indicate that the time-to-fatigue was significantly higher ( $p < 0.05$ ) in the 100 cm flume length compared to 15 cm and 30 cm. Moreover, the day of testing had a significant effect on the time-to-fatigue. From Table 2.1 it can be seen that with every passing day, the chances of earlier fatigue increased by a factor of 1.38. For fish fatiguing, median fatigue times were 103 seconds (Interquartile Range, IQR = 846.5 seconds) at  $35 \text{ cms}^{-1}$  and 34.5 seconds (IQR = 33.75 seconds) at  $45 \text{ cms}^{-1}$ .

### 2.4.2 Tapped fatigue

For the tapped fatigue definition, there was no significant difference between time-to-fatigue and flume length at the lower flow velocity ( $p > 0.05$ ). For fish fatiguing, the median fatigue times were 287 seconds (IQR = 869.5 seconds) and 56.5 seconds (IQR = 42.75 seconds) for  $35 \text{ cms}^{-1}$  and  $45 \text{ cm s}^{-1}$ , respectively.

Table 2.1 Cox Proportional-Hazard Model summary table output for untapped and tapped fatigue models. The “se(coef)” column shows the standard error of the estimated regression coefficient, whereas the “exp(coef)” column gives the effect size of covariates. Significant results are marked with an asterisk symbol in the p-value column. The dash (-) symbol is used for the reference treatment group against which other treatments are compared.

Fatigue definition	Dependent variable	Independent variables	Treatments	p-value	se(coef)	exp(coef)
Untapped	Time-to-fatigue	Flume length	15 cm	-	-	-
			30 cm	0.174	0.52	0.49
			100 cm	0.001*	0.73	0.09
		Flow velocity	35 $\text{cms}^{-1}$	-	-	-
			45 $\text{cms}^{-1}$	0.031*	0.53	3.14
		Day	0.009*	0.12	1.38	
Tapped	Time-to-fatigue	Flume length	15 cm	-	-	-
			30 cm	0.871	0.38	1.06
			100 cm	0.618	0.41	0.82
		Flow velocity	35 $\text{cms}^{-1}$	-	-	-
			45 $\text{cms}^{-1}$	<0.001*	0.53	22.67



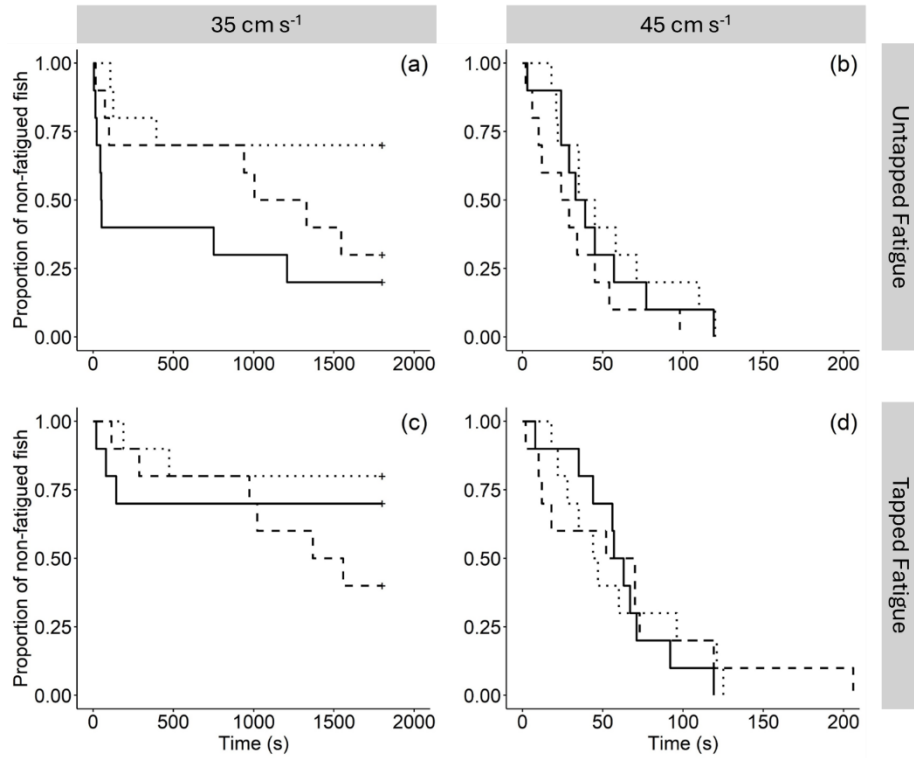


Figure 2.1 Kaplan-Meier curves for tapped and untapped fatigue definition. Plots (a) and (b) are Kaplan-Meier curves for untapped fatigue definition for 35 and 45  $\text{cm s}^{-1}$  flow velocities, respectively. Plots (c) and (d) are Kaplan-Meier curves for tapped fatigue definition for 35 and 45  $\text{cm s}^{-1}$  flow velocities, respectively. X-axis represents the time elapsed from the beginning of testing velocity in seconds whereas the Y-axis shows the proportion of non-fatigued fish. In all plots, solid, dashed, and dotted lines represent the flume length of 15, 30, and 100 cm, respectively. Censored data is marked with a plus (+) symbol for the fish swimming at 1800 seconds (the end of testing time).

## 2.5 Discussion

The swimming performance of *Telestes muticellus* depends on the flume length but only when the fish were allowed to independently choose to stop swimming (untapped fatigue). When encouraged i.e. tapped to swim, on the other hand, no effect of flume length was seen in the result. At the higher velocity, with shorter fatigue times, flume length did not influence the result regardless of fatigue definition. The time-to-fatigue was always lower at higher flow velocities.

The difference in result depending on fatigue definition highlights the importance of behaviour in fish swimming capability estimates. It is acknowledged that the motivation state of the fish can influence swimming performance (Goerig & Castro-Santos, 2017; Videler, 1993), and fish actively choosing to enter the swimming trial sometimes outperform forced swimmers (Castro-Santos et al. 2013; Peake, 2008b). In our experiment, some of the fish chose to stop swimming before exhaustion. By tapping, an external drive to swim was added to any internal motivation, forcing the fish to resume swimming. In this case, the difference in time-to-fatigue between the untapped and tapped fish was enough to change the outcome of the experimental test – the conclusions drawn on the effect of flume length on time-to-fatigue.

In our experiment, the fish were more likely to stop swimming in a shorter flume, while no difference in performance for the different flume lengths was seen when the fish was encouraged (tapped) to swim. The difference between the untapped and tapped fatigues could be viewed as a difference between behavioural and physiological fatigue; for the former, the fish chooses to stop swimming while in the latter it is unable to swim despite being intimidated by tapping. The fish are physically unable to keep swimming when they have used up their energy reserves, per definition in the burst or prolonged swimming regime, whereas little is known about what causes the fish to stop swimming before that (McFarlane & McDonald, 2002; Videler, 1993). It could be that a more confined environment and less room to display a range of swimming behaviour caused the fish to give up faster in the shorter flumes (Deslauriers & Kieffer, 2011; Tudorache et al. 2007). Importantly, however, most fish did not fatigue in this experiment, and it cannot be ruled out that a similar effect would also be seen in relation to the physiological fatigue (tapped fish) with longer trial times and a higher proportion of fish fatiguing.

At the higher velocity, all fish fatigued within a short period of time, with no effect of flume length and no difference in result between the two fatigue definitions. At these faster flow velocities, fish swim in the burst activity level utilising white muscle fibres and anaerobic processes (Videler, 1993). Fish accumulate lactate in blood and muscles, resulting in the depletion of energy reserves, causing fish to fatigue and be unable to swim (Beamish, 1978; Hammer, 1995). The main advantage of a longer flume should be the possibility to increasingly use intermittent swimming (Tudorache et al. 2007). At much higher velocities, however, fish may need to continuously perform burst swimming,

preventing the use of burst-and-coast and reducing the advantage of a longer flume (Castro-Santos, 2005).

For the untapped swimming trials, fish stopped swimming at a higher rate later in the study. The day of trial was included among the candidate models to control for any effect of acclimatisation time in the hatchery and time without eating. Time to acclimatisation to captivity varies enormously in fish swimming studies, from hours to days or weeks (e.g. Enders et al. 2003; Jain et al. 1997; Nikora et al. 2003; Tritico & Cotel, 2010), with little known about effects on swimming performance. On the other hand, although fish may lose white muscle energy reserves within days of starvation (Kieffer & Tufts, 1998), cyprinids have been reported to maintain swimming performance for 2 weeks without eating (Cai et al. 2014; Penghan et al. 2016). Perhaps multiple fish captures in the relatively small fish holding compartments caused a decrease in motivation to swim (O'Connor et al. 2010). Under the tapped fatigue definition, no effect of time since capture was seen, potentially indicating that time since capture did not affect the physiological swimming performance. Future studies should integrate time-to-fatigue data with measurements of fish physiological attributes, such as oxygen consumption, heart rate, and gill movements. This approach will provide a clearer understanding of whether fish fatigue in forced performance experiments, as defined by the tapped fatigue definition, is truly a physiological necessity.

To conclude, this paper highlights the importance of testing protocols in fish swimming performance experiments. It confirms the potential effect of flume length on swimming behaviour and performance, and underscores the potential bias intrinsic in the fatigue definition used when estimating swimming capabilities. Although a “true” swimming performance is difficult, not to say impossible, to measure in the laboratory, being aware of potential pitfalls will help us to achieve better approximations. Further work with a higher sample size and increased maximum testing time limit is required to assess the geometrical limitations beyond which swimming performance results do not change significantly.

## References

- Ashraf, M. U., Nyqvist, D., Comoglio, C., & Manes, C. (2024). The effect of in-flume habituation time and fish behaviour on estimated swimming performance. *Journal of Ecohydraulics*. <https://doi.org/10.1080/24705357.2024.2306411>.
- Beamish, F. W. H. (1978). *Fish Physiology* (W. S. Hoar & D. J. Randall, Eds.; 1st ed., Vol. 7). Academic Press, London.
- Bestgen, K. R., Mefford, B., Bundy, J. M., Walford, C. D., & Compton, R. I. (2010). Swimming performance and fishway model passage success of Rio Grande silvery minnow. *Transactions of the American Fisheries Society*, 139(2), 433–448.
- Bell, W. H. & Terhune, L. D. B. (1970). Water tunnel design for fisheries research. *Journal of the Fisheries Research Board of Canada* 195, 55–59.
- Brett, J. R. (1964). The Respiratory Metabolism and Swimming Performance of Young Sockeye Salmon. *Journal of the Fisheries Research Board of Canada*, 21(5), 1183–1226. <https://doi.org/10.1139/f64-103>
- Burnham, K. P., & Anderson, D. R. (Eds.). (2004). *Model Selection and Multimodel Inference*. Springer New York. <https://doi.org/10.1007/b97636>
- Cai, L., Fang, M., Johnson, D., Lin, S., Tu, Z., Liu, G., & Huang, Y. (2014). Interrelationships between feeding, food deprivation and swimming performance in juvenile grass carp. *Aquatic Biology*, 20(1), 69–76. <https://doi.org/10.3354/ab00546>
- Castro-Santos, T. (2002). *Swimming performance of upstream migrant fishes: New methods, new perspectives*.
- Castro-Santos, T. (2005). Optimal swim speeds for traversing velocity barriers: An analysis of volitional high-speed swimming behavior of migratory fishes. *Journal of Experimental Biology*, 208(3), 421–432. <https://doi.org/10.1242/jeb.01380>
- Castro-Santos, T., Sanz-Ronda, F. J., & Ruiz-Legazpi, J. (2013). Breaking the speed limit—Comparative sprinting performance of brook trout ( *Salvelinus fontinalis* ) and brown trout ( *Salmo trutta* ). *Canadian Journal of Fisheries and Aquatic Sciences*, 70(2), 280–293. <https://doi.org/10.1139/cjfas-2012-0186>
- Cox, D. R. (1972). Regression Models and Life-Tables. *Journal of the Royal Statistical Society. Series B (Methodological)*, 34(2), 187–220.
- Deslauriers, D., & Kieffer, J. D. (2011). The influence of flume length and group size on swimming performance in shortnose sturgeon *Acipenser brevirostrum*. *Journal of Fish Biology*, 79(5), 1146–1155. <https://doi.org/10.1111/j.1095-8649.2011.03094.x>

- Domenici, P., & Blake, R. (1997). The kinematics and performance of fish fast-start swimming. *Journal of Experimental Biology*, 200(8), 1165–1178. <https://doi.org/10.1242/jeb.200.8.1165>
- Enders, E. C., Boisclair, D., & Roy, A. G. (2003). The effect of turbulence on the cost of swimming for juvenile Atlantic salmon (*Salmo salar*). *Canadian Journal of Fisheries and Aquatic Sciences*, 60(9), 1149–1160.
- Farrell, A. P., & Steffensen, J. F. (1987). An analysis of the energetic cost of the branchial and cardiac pumps during sustained swimming in trout. *Fish Physiology and Biochemistry*, 4(2), 73–79. <https://doi.org/10.1007/BF02044316>
- J. Fox, “Cox proportional-hazards regression for survival data,” An R and S-PLUS companion to applied regression, vol. 2002, 2002.
- Goerig, E., & Castro-Santos, T. (2017). Is motivation important to brook trout passage through culverts? *Canadian Journal of Fisheries and Aquatic Sciences*, 74(6), 885–893. <https://doi.org/10.1139/cjfas-2016-0237>
- Hammer, C. (1995). Fatigue and exercise tests with fish. *Comparative Biochemistry and Physiology Part A: Physiology*, 112(1), 1–20. [https://doi.org/10.1016/0300-9629\(95\)00060-K](https://doi.org/10.1016/0300-9629(95)00060-K)
- Jain, K., Hamilton, J., & Farrell, A. (1997). Use of a ramp velocity test to measure critical swimming speed in rainbow trout (*Onchorhynchus mykiss*). *Comparative Biochemistry and Physiology Part A: Physiology*, 117(4), 441–444.
- Katopodis, C., & Gervais, R. (2012). ECOHYDRAULIC ANALYSIS OF FISH FATIGUE DATA: ECOHYDRAULIC ANALYSIS OF FISH FATIGUE DATA. *River Research and Applications*, 28(4), 444–456. <https://doi.org/10.1002/rra.1566>
- Kieffer, J. D., & Tufts, B. L. (1998). Effects of food deprivation on white muscle energy reserves in rainbow trout (*Oncorhynchus mykiss*): The relationships with body size and temperature. *Fish Physiology and Biochemistry*, 19(3), 239.
- McFarlane, W. J., & McDonald, D. G. (2002). Relating intramuscular fuel use to endurance in juvenile rainbow trout. *Physiological and Biochemical Zoology*, 75(3), 250–259.
- Nelson, J. A., Gotwalt, P. S., & Snodgrass, J. W. (2003). Swimming performance of blacknose dace (*Rhinichthys atratulus*) mirrors home-stream current velocity. *Canadian Journal of Fisheries and Aquatic Sciences*, 60(3), 301–308.
- Nikora, V. I., Aberle, J., Biggs, B. J. F., Jowett, I. G., & Sykes, J. R. E. (2003). Effects of fish size, time-to-fatigue and turbulence on swimming performance: A case study of *Galaxias maculatus* : SWIMMING PERFORMANCE OF INANGA. *Journal of Fish Biology*, 63(6), 1365–1382. <https://doi.org/10.1111/j.1095-8649.2003.00241.x>

O'Connor, C. M., Gilmour, K. M., Arlinghaus, R., Hasler, C. T., Philipp, D. P., & Cooke, S. J. (2010). Seasonal carryover effects following the administration of cortisol to a wild teleost fish. *Physiological and Biochemical Zoology*, 83(6), 950–957.

Paoletti, P., & Mahadevan, L. (2014). Intermittent locomotion as an optimal control strategy. *Proceedings of the Royal Society A: Mathematical, Physical and Engineering Sciences*, 470(2164), 20130535.

Peake, S. J. (2008a). Behavior and passage performance of northern pike, walleyes, and white suckers in an experimental raceway. *North American Journal of Fisheries Management*, 28(1), 321–327.

Peake, S. J. (2008b). Gait transition speed as an alternate measure of maximum aerobic capacity in fishes. *Journal of Fish Biology*, 72(3), 645–655. <https://doi.org/10.1111/j.1095-8649.2007.01753.x>

Peake, S. J., & Farrell, A. P. (2006). Fatigue is a behavioural response in respirometer-confined smallmouth bass. *Journal of Fish Biology*, 68(6), 1742–1755. <https://doi.org/10.1111/j.0022-1112.2006.01052.x>

Peake, S., McKinley, R. S., & Scruton, D. A. (1997). Swimming performance of various freshwater Newfoundland salmonids relative to habitat selection and fishway design. *Journal of Fish Biology*, 51(4), 710–723. <https://doi.org/10.1111/j.1095-8649.1997.tb01993.x>

Penghan, L.-Y., Pang, X., & Fu, S.-J. (2016). The effects of starvation on fast-start escape and constant acceleration swimming performance in rose bitterling (*Rhodeus ocellatus*) at two acclimation temperatures. *Fish Physiology and Biochemistry*, 42(3), 909–918. <https://doi.org/10.1007/s10695-015-0184-0>

Rao, P. V., Hosmer, D. W., & Lemeshow, S. (2000). Applied Survival Analysis: Regression Modeling of Time to Event Data. *Journal of the American Statistical Association*, 95(450), 681. <https://doi.org/10.2307/2669422>

Richards, S. A. (2007). Dealing with overdispersed count data in applied ecology: Overdispersed count data. *Journal of Applied Ecology*, 45(1), 218–227. <https://doi.org/10.1111/j.1365-2664.2007.01377.x>

Romão, F., Quintella, B. R., Pereira, T. J., & Almeida, P. R. (2012). Swimming performance of two Iberian cyprinids: The Tagus nase *Pseudochondrostoma polylepis* (Steindachner, 1864) and the bordallo *Squalius carolitertii* (Doadrio, 1988): Critical swimming speed of two Iberian cyprinids. *Journal of Applied Ichthyology*, 28(1), 26–30. <https://doi.org/10.1111/j.1439-0426.2011.01882.x>

Tritico, H. M., & Cotel, A. J. (2010). The effects of turbulent eddies on the stability and critical swimming speed of creek chub (*Semotilus atromaculatus*). *Journal of Experimental Biology*, 213(13), 2284–2293.

Tudorache, C., de Boeck, G., & Claireaux, G. (2013). Forced and Preferred Swimming Speeds of Fish: A Methodological Approach. In A. P. Palstra & J. V. Planas (Eds.), *Swimming Physiology of Fish* (pp. 81–108). Springer Berlin Heidelberg. [https://doi.org/10.1007/978-3-642-31049-2\\_4](https://doi.org/10.1007/978-3-642-31049-2_4)

Tudorache, C., O’Keefe, R. A., & Benfey, T. J. (2010a). Flume length and post-exercise impingement affect anaerobic metabolism in brook charr *Salvelinus fontinalis*. *Journal of Fish Biology*, 76(3), 729–733. <https://doi.org/10.1111/j.1095-8649.2009.02513.x>

Tudorache, C., O’Keefe, R. A., & Benfey, T. J. (2010b). The effect of temperature and ammonia exposure on swimming performance of brook charr (*Salvelinus fontinalis*). *Comparative Biochemistry and Physiology Part A: Molecular & Integrative Physiology*, 156(4), 523–528. <https://doi.org/10.1016/j.cbpa.2010.04.010>

Tudorache, C., Viaene, P., Blust, R., Vereecken, H., & De Boeck, G. (2008). A comparison of swimming capacity and energy use in seven European freshwater fish species. *Ecology of Freshwater Fish*, 17(2), 284–291. <https://doi.org/10.1111/j.1600-0633.2007.00280.x>

Tudorache, C., Viaenen, P., Blust, R., & De Boeck, G. (2007). Longer flumes increase critical swimming speeds by increasing burst-glide swimming duration in carp *Cyprinus carpio*, L. *Journal of Fish Biology*, 71(6), 1630–1638. <https://doi.org/10.1111/j.1095-8649.2007.01620.x>

Veza, P., Libardoni, F., Manes, C., Tsuzaki, T., Bertoldi, W., & Kemp, P. S. (2020). Rethinking swimming performance tests for bottom-dwelling fish: The case of European glass eel (*Anguilla anguilla*). *Scientific Reports*, 10(1), 16416. <https://doi.org/10.1038/s41598-020-72957-w>

Videler, J. J. (1993). *Fish Swimming*. Springer Netherlands. <https://doi.org/10.1007/978-94-011-1580-3>

Videler, J. J., & Weihs, D. (1982). Energetic advantages of burst-and-coast swimming of fish at high speeds. *Journal of Experimental Biology*, 97(1), 169–178.

Watson, J., Goodrich, H., Cramp, R., Gordos, M., Yan, Y., Ward, P., & Franklin, C. (2019). *Swimming performance traits of twenty-one Australian fish species: A fish passage management tool for use in modified freshwater systems*. <https://doi.org/10.1101/861898>

## **Chapter 3**

# **The Effect of In-Flume Habituation Time and Fish Behaviour on Estimated Swimming Performance**



### 3.1 Abstract

Swimming performance is important for fish migration, habitat selection, and predator-prey interaction, as well as for fish passage design. Procedural choices made when experimentally estimating it may influence the results. Systematic experiments were conducted to study the effect of different in-flume habituation times, habituation behaviour, and the use of external encouragement on burst swimming performance of *Leucos aula* (formerly *Rutilus aula*), a small-sized cyprinid, in a fixed velocity testing protocol. Increasing habituation times from 30 sec to 5 or 20 min substantially increased the success proportion of swimming trials and fish swimming performance, with no difference between the latter two habituation times. Fish resting on the downstream grid before the start of testing velocity outperformed those who swam during habituation and transition periods. Fish swimming voluntarily in response to flow at testing velocity showed a significantly improved performance compared to fish motivated by external tapping. The results of this study highlight that in-flume habituation time is important, and fish behaviour before actual testing may influence the outcomes of swimming performance results.

## 3.2 Introduction

Swimming performance is important for fish migration, habitat selection, and predator-prey interaction, as well as for fish passage design (Castro-Santos, 2002; Domenici & Blake, 1997; Katopodis & Gervais, 2012; Peake et al., 1997; Tudorache et al., 2008; Watson et al., 2019). Typically, fish swimming performance is categorized into three activity levels: sustained, prolonged, and burst (Beamish, 1978; Hammer, 1995). Although several techniques and devices provide fish swimming performance metrics (Katopodis et al., 2019), commonly, laboratory studies are carried out using one of the two testing methodologies: increasing velocity or fixed velocity method (Brett, 1964; Hammer, 1995). In the former, a fish is forced to swim at a regularly increasing flow velocity with fixed incremental time  $\Delta t$ , until fatigued. In the latter, a fish is forced to swim at a fixed velocity before being declared fatigued. Both methods have been widely used in the literature and provide information about fish performance and behaviour to inform both ecological theory and fisheries management, with particular focus on the design of upstream and downstream fish passage structures (Brett, 1964; Deslauriers & Kieffer, 2012; Farrell et al., 2003; Hammer, 1995; Mu et al., 2019; Schiavon et al., 2023).

Despite the wide application of fish swimming tests, significant variations in testing protocols and nomenclature are found in the scientific literature. One such example is the use of different and rather arbitrary habituation periods. In the swimming performance literature this is the time fish are allowed to adjust to laboratory conditions before testing begins, and more often is referred to as "acclimation period (or time)", "conditioning period", "settling period" or "recovery period (or time)" (Jones et al., 1974; Myrick & Cech, 2000; Nikora et al., 2003; Penghan et al., 2016; Silva et al., 2012; Tudorache et al., 2007). Time allotted to habituation varies enormously among studies, typically without empirical support: 5 min (Louison et al., 2019; Schiavon et al., 2023), 10 min (Nikora et al., 2003; Plew et al., 2007), 15 min (Lupandin, 2005), 30 min (Deslauriers & Kieffer, 2011), 1 h (Myrick & Cech, 2000; Palstra et al., 2020; Silva et al., 2021), 11 h (Tritico & Cotel, 2010), 12 h (Silva et al., 2011), and overnight habituation (Hvas & Oppedal, 2019; Tudorache et al., 2008). While such a wide variation of the habituation time may stem from the different study objectives, the choices made appear to be rather arbitrarily taken and rarely supported by either robust arguments or empirical evidence. Jones et al. (1974) studied the effect of 1, 2, 12, and 16 h habituation times at a water velocity of 10  $\text{cm s}^{-1}$  on Arctic grayling *Thymallus arcticus* and Longnose suckers *Catostomus catostomus* and found no significant difference in critical swimming velocity among different habituation times. Similarly, Peake et al. (1997) conducted a study on juvenile Rainbow trout *Oncorhynchus mykiss* and found no significant difference in the average critical swimming velocity when tested at 6°C and 18°C after different habituation times of 0, 0.5, 1, 2, 4, 8, and 16 h at a flow velocity of 26.5  $\text{cm s}^{-1}$ . Long habituation times can significantly increase the overall duration of the experimental study, and this could originate potential confounding effects on fish physiology and ontogeny. Furthermore, a longer study duration requires increased costs, leading towards a trade-off

with sample size. These elements cause many researchers optioning for short habituation times: 5-min (Louison et al., 2019), 10-min (Plew et al., 2007), and 15-min (Lupandin, 2005). However, despite their widespread use, studies on the effects of such short habituation periods are apparently lacking in the literature.

Fish behaviour during the habituation time may affect swimming performance, and is sometimes used as a criterion for inclusion in performance studies (Heuer et al., 2021). During the habituation period, fish may, for example, rest on the downstream grid or actively explore the flume. Although often not reported, in some experiments, non-cooperative fish are subject to exclusion or physical encouragement using subjective criteria. While Quintella et al. (2010) excluded the fish that showed signs of stress and poor swimming behaviour i.e. moving back and forth in the swim chamber, other research studies have also reported exclusion criteria where a fish was unable to orient to the flow (Myrick & Cech, 2000; Nikora et al., 2003), refused to swim at all (Santos et al., 2007), or declined to leave the net (which was being used to handle the fish) (Shiau et al., 2020). Sometimes, encouragements such as electric shocks are also used to prevent the fish from resting on the rear of the swim chamber during habituation period before their exclusion (Stevens, 1979).

The transition period between habituation velocity and testing velocity is another integral part of increasing and fixed velocity tests. Energy spent under the transition between habituation and increasing velocity test, is likely to affect swimming performance (Videler, 1993) but is often not described or glossed over in the fish swimming literature. Some studies have reported very short transition times of less than 2 and up to 5 sec (Deslauriers & Kieffer, 2011, 2012; Nikora et al., 2003; Plew et al., 2007). Although theoretically it may seem straightforward to minimise the swimming time and conserve energy spent during transition, fast transitions are not always possible (e.g. due to behavioural or logistic constraints). However, although typically ignored or deemed insignificant, it is unclear to what extent the behaviour of fish during the transition time affect the measured performance.

Physical tapping is often used to encourage the fish to swim during the swimming trials (Aedo et al., 2021; Karlsson-Drangsholt et al., 2018; Nikora et al., 2003; Plew et al., 2007; Schiavon et al., 2023). Alternatively the use of electric shocks is also a frequently found method in the literature to prevent fish from resting on the downstream grid (Brett, 1967; Farrell et al., 1990; Romão et al., 2012; Silva et al., 2021; Van Den Thillart et al., 2004; Webb et al., 1984). Motivation, however, is important for fish swimming performance (Goerig & Castro-Santos, 2017; Videler, 1993), and fish actively choosing to enter a swimming trial, in volitional swimming tests, sometimes outperform forced swimmers (Castro-Santos et al., 2013; Peake, 2008b). Surprisingly, in forced performance tests, the difference in swimming performance between fish swimming voluntarily at the start of testing velocity and fish that are encouraged (i.e. tapped) to swim is still unexplored in the published literature.

In this study, we investigate potential effects of habituation time and fish

behaviour on the estimated burst swimming performance. The goal of this study is to elucidate the effects on time-to-fatigue of: (1) three different, relatively short (i.e. 30 sec, 5-min, and 20-min), in-flume habituation times; (2) fish behaviour during habituation; and (3) tapping. We hypothesise that time-to-fatigue increases with: increasing habituation time, active swimming during habituation period, and the use of external stimuli (i.e. tapping) to provoke swimming. These hypotheses were tested from the results of systematic experiments that were conducted using a fixed velocity testing protocol on *Leucos aula* (formerly *Rutilus aula*), a small-sized riverine cyprinid (Fortini, 2016).

## 3.3 Materials and Methods

### 3.3.1 Fish

Juvenile *L. aula* with an average fork length of 5.19 cm (standard deviation,  $sd \pm 0.4$  cm) and average mass of 1.8 g ( $sd \pm 0.4$  g) were captured from the Orba stream in the Province of Alessandria, Italy (44°45'46.7"N 8°40'15.6"E) using electrofishing on January 30, 2023. The fish were brought to the hatchery facility in Predosa, Alessandria, Italy and were left to habituate to hatchery conditions in a spring-fed flow-through tank. After three days from their capture date, a random subset of fish was tested in a separate experimental campaign in the hatchery, and then returned to the holding tank. All fish rested at least 4 days before testing. The water temperature in the tank was measured by a HOBO MX-2202 logger at regular intervals of 10 min, with a mean temperature of 11.8 °C ( $sd \pm 0.3$ °C). The fish were fed commercial aquaria fish pellets (Tetra TabiMin) but were starved 24 hours before the experiments to ensure a post-absorptive state. The fish remained healthy looking throughout the experimental campaign, displaying active swimming behaviour, and no fish mortality was observed. The study was conducted in accordance with the Ufficio Tecnico Faunistico e Ittiofauna of the Provincia di Alessandria (permit number 1570, issued on 19th January 2023), under the provisions of art.2 of the national Decree n.26/2014 (implementation of Dir. 2010/63/EU).

### 3.3.2 Flume description

Experiments were carried out using a hydraulic flume whose channel is 280 cm long and has a 30 cm by 30 cm rectangular cross section. A pump allows for water recirculation from a small upstream tank, through the channel to a 600 L downstream tank, which is connected back to the upstream tank via a 8.5 cm diameter stainless steel pipe (see Figure 3.1), hosting a AquaTrans™ AT600 flow metre sensor for monitoring the flow rate, which was controlled by means of an inverter (DGFIT MT 12) and a flow opening valve located at the pump outlet. A flow straightener located 75 cm from the channel inlet was employed to damp the intensity of turbulence generated by the pump. The swimming arena utilized for the tests was 80 cm long and was bounded upstream by the flow straightener and downstream by a net. For all the experiments the flow depth was kept at 7.5 cm. Prior to any test with fish, hydrodynamic conditions were carefully assessed using advanced laser diagnostics (i.e. Laser Doppler Anemometry), which revealed that flow conditions were nicely uniform along the spanwise direction and that the flow straightener generated turbulence whose intensity (estimated as the standard deviation of the longitudinal velocity component normalised with its local mean) decayed along the longitudinal direction and never exceeded 10.72%.

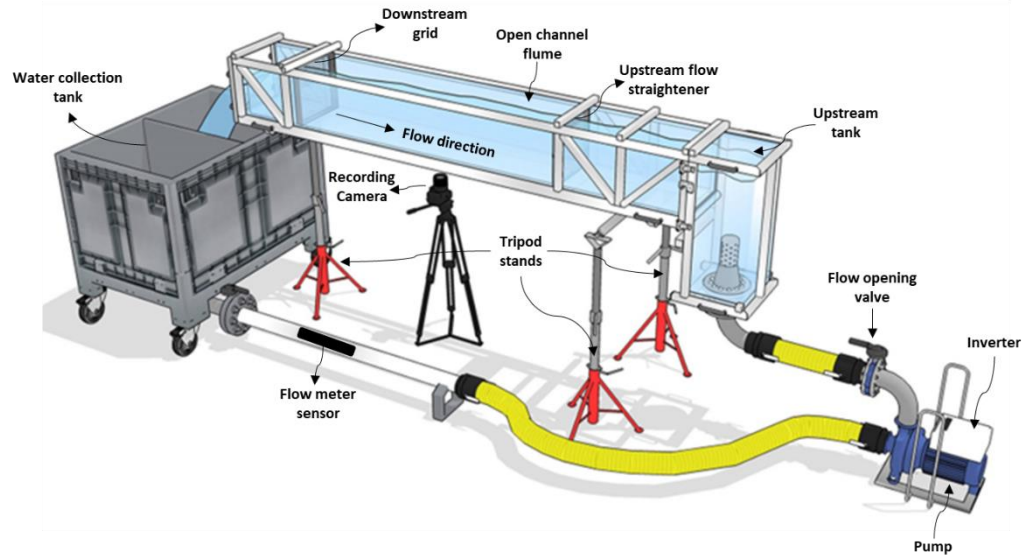


Figure 3.1 Experimental flume used for swimming performance studies with all components connected. The flume consisted of an upstream tank connected with the main open channel flume which discharges water in the downstream water collection tank. The water is recirculated using a water pump via a combination of a stainless steel and plastic pipes connecting the whole flume system.

Throughout testing, water in the system was maintained at an average temperature  $T$  of  $10.6\text{ }^{\circ}\text{C}$  ( $\text{sd} \pm 0.2\text{ }^{\circ}\text{C}$ ) and cooled intermittently with a chiller unit (TECO TK-2000). The temperature difference between the holding tanks and the testing flume was never larger than  $1^{\circ}\text{C}$  to avoid any potential adverse effects of a sudden temperature change on swimming performance (Tudorache et al. 2010b; Vezza et al. 2020). Sony AX43 Handycams were used to video record the swimming tests at a resolution of  $1920 \times 1080$  with a frame rate of 50.

### 3.3.3 Habituation times

Fish were tested using a fixed velocity testing protocol. Three different in-flume habituation times, prior to the onset of testing velocity, were used: 30 sec (Treatment 0.5), 5 min (Treatment 5), and 20 min (Treatment 20). Thirty-five fish were tested per treatment, resulting in a total sample size of 105 fish. Each fish was tested only once. The flow velocity during habituation time was set to  $5\text{ cm s}^{-1}$  (around 1 BL/s). At the end of the habituation period, the flow rate was progressively increased within 20 min transition time to achieve the mean testing flow velocity of  $50\text{ cm s}^{-1}$  (around 10 BL/s). The flow velocity value of  $50\text{ cm s}^{-1}$  was selected because, according to preliminary testing, it is within the burst swimming range of juvenile *L. auala*, whose time-to-fatigue was found to be, at most, a few seconds to tens of seconds (Beamish, 1978; Nikora et al., 2003; Videler, 1993). The 20 sec transition time was chosen to allow a gentle increase in flow rate that prevented fish from startling or losing equilibrium. Each trial concluded when the fish was fatigued. Fatigue was defined as fish resting/impinged on the downstream grid despite tapping it. The fish was tapped no more than three times to motivate it to swim. Fish were anesthetized in clove oil (Aroma Labs, Kalamazoo, MI, USA; approximately 0.2 ml clove oil / litre water) and measured at the end of each trial for fork length in centimetres [cm]

and mass in grams [g].

### 3.3.4 Fish behaviour definitions

Differences between the three habituation treatments were tested with respect to proportion of successful swimming tests (i.e. a test trial where fish actively swims against the flow until fatigued) and time-to-fatigue. Data was then pooled and effects of behaviour during habituation and the start of the swimming trial on swimming performance was evaluated. During habituation, fish were observed to either (1) swim or stay without motion, away from the downstream grid (“in the flume”) or (2) rest on the downstream grid (“on grid”). Typically, fish in the flume at the end of the habituation period were also swimming during transition, while fish resting at the end of the habituation period were also resting during transition. In addition, fish resting on the grid were observed to display two different behaviours: laterally impinged or resting on the grid with head facing the flow. Difference in success proportion and time-to-fatigue was tested between fish in the flume or on the grid at the end of habituation using the whole pool of fish, as well between fish laterally impinged and fish facing on the flow among the on the grid fish.

From the successful swimming trials, fish started to swim in response to the flow or were tapped at the start of testing velocity, and we tested difference in time-to-fatigue between fish displaying these two behaviours: swimming voluntarily in response to flow (“no tap”) or swimming first after having been externally motivated by tapping (“tapped”).

Chi-square test of independence was performed to compare the proportion of successful swimming trials between treatments and behavioural groups. Swimming performance data were non-normally distributed so Kruskal-Wallis and Wilcoxon tests were used to compare performance and behaviour outcomes among treatments and behavioural groups. Pairwise comparison between treatments were calculated using pairwise Wilcoxon rank sum test. One-way ANOVA was used to test any significant differences among treatments based on fish length and weight. All statistical tests were performed using R version 4.1.2 (R Foundation for Statistical Computing, Vienna, Austria. URL <https://www.R-project.org>). Package *dplyr* was used for data management (<https://CRAN.R-project.org/package=dplyr>), package *ggplot2* was used for plotting (<https://CRAN.R-project.org/package=ggplot2>), and package *car* was used to run ANOVA tests (<https://CRAN.R-project.org/package=car>).

### 3.4 Results

There were no difference in length or weight between fish in the different habituation treatments (ANOVA,  $p > 0.38$ ). In total 65 out of 105 swimming trials resulted in successful fish swimming tests (i.e. a fish with time-to-fatigue data). Fish with 30 sec habituation time had a substantially lower success proportion (20%) compared to fish habituated to flume for 5 min (77.14%; chi-square,  $p < 0.001$ ) and 20 min (88.57%; chi-square,  $p < 0.001$ ). There was no difference in proportion of successful trials between the 5 min and 20 min habituation treatments (chi-square,  $p = 0.34$ ).

Time-to-fatigue (median = 8 sec, Interquartile Range IQR = 7 sec; Figure 3.2) differed significantly among the three habituation treatments (Kruskal-Wallis,  $p = 0.03$ ). As shown in Figure 3.2, fish habituated for 30 sec fatigued significantly faster than fish habituated for 20 min (Wilcoxon,  $p = 0.03$ ). The same tendency was seen between fish habituated for 30 sec and fish habituated for 5 min (Wilcoxon,  $p = 0.06$ ). Habituation for 5 min or 20 min did not affect time-to-fatigue (Wilcoxon,  $p = 0.36$ ).

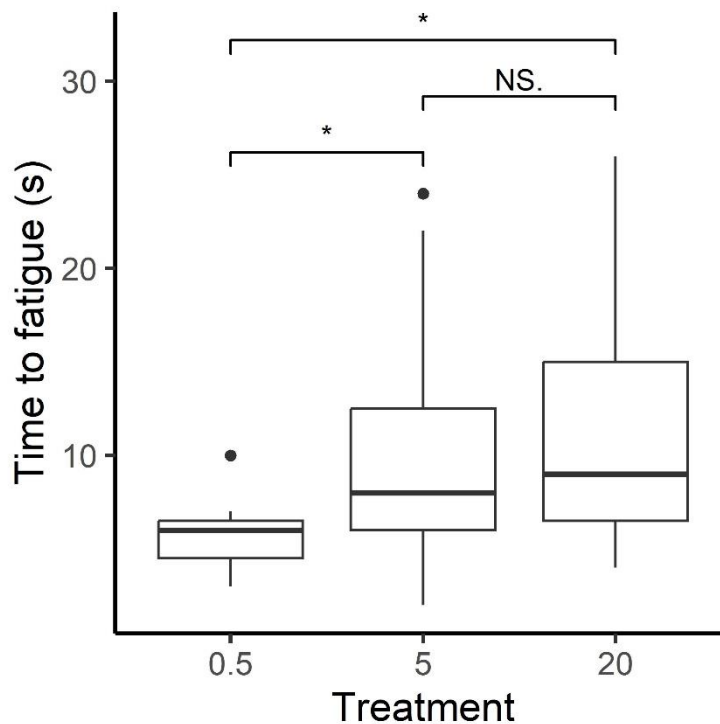


Figure 3.2 Box plot of time-to-fatigue for 0.5 min ( $n = 7$ ), 5 min ( $n = 27$ ), and 20 min ( $n = 31$ ) habituation time treatments. The solid black horizontal line inside the bounding box is the median fatigue time. The black dots represent the outliers, whereas the bounding box defines the Interquartile Range (IQR) of the time-to-fatigue data for each treatment. The vertical solid black lines mark  $Q1 - 1.5 * IQR$  (bottom end) and  $Q3 + 1.5 * IQR$  (top end), where  $Q1$  and  $Q3$  are the 25th and 75th percentiles, respectively. The asterisk symbol indicates which groups have significant differences, while NS stands for non-significant.

Due to very low proportion of success and poor swimming performance among the fish habituated for only 30 sec, these thirty-five fish were excluded from the further behavioural analysis. Therefore, the following results only include data from Treatment 5



and 20 i.e. a total of 70 test fish with 58 successful trials.

At the end of the habituation time, fish were either resting on the downstream grid ( $n = 37$ ) or present upstream in the flume arena (swimming or resting;  $n = 21$ ). The position of the fish at the end of the habituation time did not affect the proportion of successful trials (chi-square,  $p = 0.052$ ). Fish in flume (either swimming or motionless) at the end of habituation and start of transition, however, performed significantly worse than fish resting on the grid (Wilcoxon,  $p = 0.02$ ; Figure 3.3).

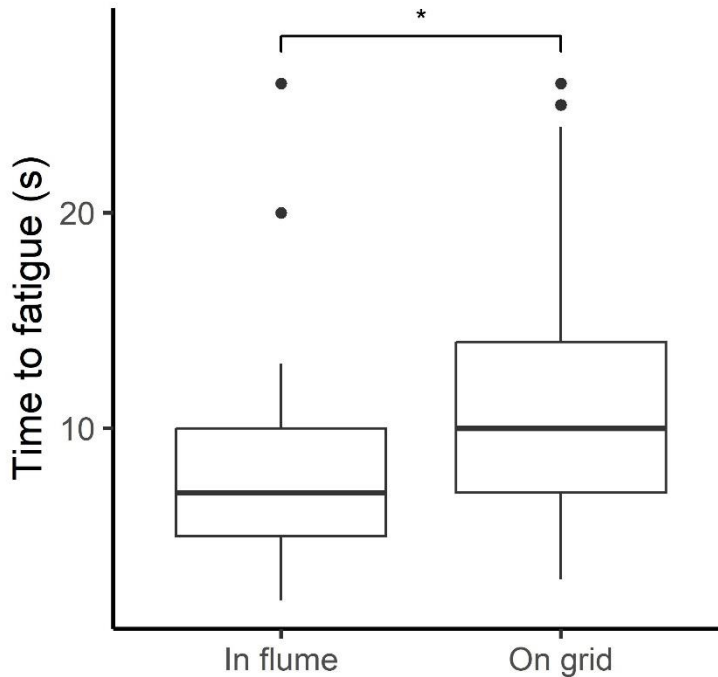


Figure 3.3 Box plot of time-to-fatigue for the fish swimming or resting in the flume ( $n = 21$ ) or resting on the grid ( $n = 37$ ) at the end of habituation/beginning of transition. The solid black line is the median fatigue time. The black dots represent the outliers, whereas the bounding box defines the Interquartile Range (IQR) of the time-to-fatigue data for each treatment. The vertical solid black lines mark  $Q1 - 1.5 \cdot IQR$  (bottom end) and  $Q3 + 1.5 \cdot IQR$  (top end), where  $Q1$  and  $Q3$  are the 25<sup>th</sup> and 75<sup>th</sup> percentiles, respectively. The asterisk symbol represents the significant differences between the two groups.

All but one fish who swam during habituation also swam during the transition period. Among the fish resting on the grid, no difference in time-to-fatigue was seen between fish facing the flow or fish being laterally impinged (Wilcoxon,  $p = 0.35$ ).

At the start of the testing velocity, Fish were either swimming voluntarily in response to flow (“no tap”,  $n = 29$ ) or first after being physically encouraged to swim (“tapped”,  $n = 29$ ). Fish swimming voluntarily in response to flow (“no tap”) displayed a significantly longer time-to-fatigue compared to fish that had to be tapped to swim (Wilcoxon,  $p = 0.01$ ; Figure 3.4).

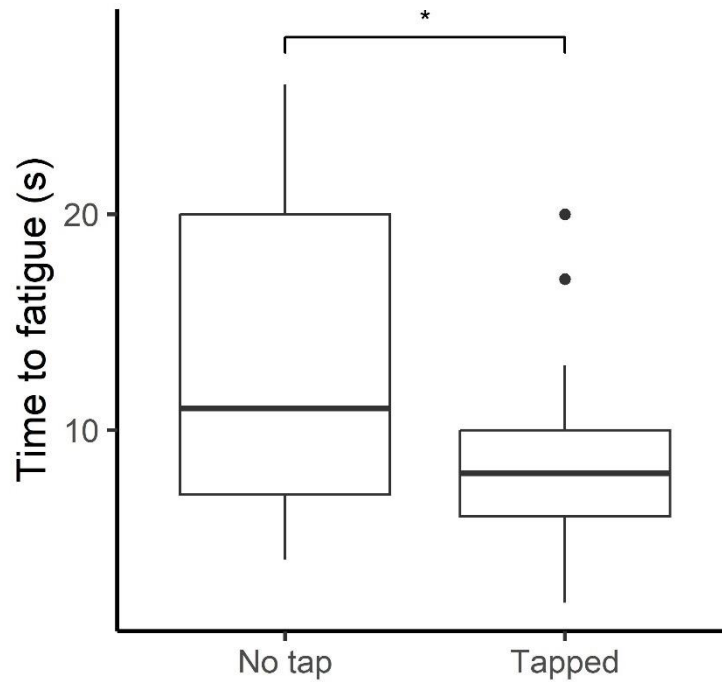


Figure 3.4 Box plot of time-to-fatigue for fish swimming voluntarily in response to flow (“no tap”,  $n = 29$ ) or swimming first after having been externally motivated by tapping (“tapped”,  $n = 29$ ). The solid black line is the median fatigue time. The black dots represent the outliers, whereas the bounding box defines the Interquartile Range (IQR) of the time-to-fatigue data for each treatment. The vertical solid black lines mark  $Q1 - 1.5 \cdot IQR$  (bottom end) and  $Q3 + 1.5 \cdot IQR$  (top end), where  $Q1$  and  $Q3$  are the 25<sup>th</sup> and 75<sup>th</sup> percentiles, respectively. The asterisk symbol represents the significant differences between the two groups.

### 3.5 Discussion

Increasing habituation time from 30 sec to 5 or 20 min substantially increased the proportion of swimming trials resulting in successful swimming tests, and also resulted in increased time-to-fatigue. No difference, however, in either success proportion and time-to-fatigue was found between fish habituating to the flume for 5 and 20 min. Fish resting on the grid performed better than fish located in the upstream area of the flume during habituation time, and fish swimming voluntarily in response to the testing velocity outperformed fish tapped to swim.

The large difference in the proportion of successful trials between the 30 sec habituation treatment and the 5 and 20 min habituation treatments highlights the importance of in-flume habituation time. Fish handling before its release in the flume causes fish stress and energy expenditure, important factors known to reduce fish performance (Arnekleiv et al., 2004; Barton & Schreck, 1987; Pickering et al., 1982; Schreck & Tort, 2016). Barton & Schreck (1987) showed the adverse effect of acute physical stress in juvenile Steelhead *O. mykiss* limiting the energy available by about one-quarter for activities such as swimming. Moreover, capture and handling are known to elevate plasma lactate concentration levels, that also limits burst swimming performance (Videler, 1993). Black (1957) reported increase in mean lactate levels in Rainbow trout *O. mykiss* from 15.7 mg% to 31.9 mg% when forced to swim slowly (9.7 -12.4 cms<sup>-1</sup>) for 15 min. Olla et al. (1992) found that juvenile Coho Salmon *O. kisutch* regained their previous ability to avoid predation in less than 90 min after significant handling (held out of water for 1 min). In our experiments, only 20% of the fish subjected to 30 sec of habituation resulted in successful swimming trials compared to 80-90% among the fish given more time to habituate to the flume and recuperate after handling. Karlsson-Drangsholt et al. (2018) highlighted in his study on Haddock *Melanogrammus aeglefinus* that it may take more than 6 h to recover the blood lactate levels. Likely, 30 sec (Treatment 0.5) were insufficient to recuperate the white muscle energy reserves allowing the fish to swim at testing velocity (McFarlane & McDonald, 2002; Videler, 1993). On the other hand, the minimal differences in the proportion of successful trials and in the time-to-fatigue between habituation times of 5 or 20 min may indicate a logarithmic relationship between habituation time and time-to-fatigue (i.e. above a certain threshold the effects of habituation time upon fish burst swimming performance become negligible or milder compared to those related to the flow velocity at which fish are exposed). This potential relationship should be further investigated with a more representative sample and testing other habituation times, since the identification of the inflection point of the logarithmic curve may eventually provide a consistent basis for planning effective and less time-consuming experimental campaigns. In any case, comparing burst swimming velocities after 20 min habituation time with even longer habituation times may clarify if also the longest habituation time tested in our study (i.e. 20 min) carries a potential cost due to insufficient habituation.

Sometimes, during habituation or transition periods, fish not showing rheotactic behaviour, orienting and swimming against the flow, are excluded from fish swimming performance experiments (Heuer et al., 2021; Myrick & Cech, 2000; Nikora et al., 2003; Quintella et al., 2010; Santos et al., 2007). The underpinning idea is that these fish are likely to under-perform also in the swimming trial (Van Den Thillart et al., 2004). In our experiment, contrary to expectations, fish actively swimming at the end of habituation displayed lower swimming performance compared to fish resting on the grid. Importantly, 20 out of 21 (95.24%) of these fish were also swimming during the transition time, therefore spending energy reserves already before the initiation of the swimming test (McKenzie, 2011; Vezza et al., 2020). Since such a transition time is unavoidable in forced swimming tests, our results suggest that this might cause an underestimation of time-to-fatigue. This is especially relevant when experiments are performed using velocities within the burst range, where the transition to test period ratio is relatively large. Volitional swimming tests, where the fish chooses its own velocity would be a way around this problem (Castro-Santos, 2005; Castro-Santos et al., 2013; Colavecchia et al., 1998; Haro et al., 2004).

Other times, orientation but not swimming is used as an inclusion criterion in swimming trials, allowing fish to rest on the grid during habituation as long as it faces the flow (Myrick & Cech, 2000). Among the fish resting on the grid, however, no difference in proportion of successful test or swimming performance was found between fish laterally impinged or fish resting on the grid facing the flow. This is somewhat surprising, given that being laterally impinged seems a highly unnatural behaviour, indicating a stressed condition (Tudorache et al., 2010a), that however, still allowed fish to conserve energy to be used during the test period (Liao, 2007).

Giving external physical stimulation to encourage fish to swim is commonly used in forced swimming tests in flumes and swim chambers. In our study, fish resting on the downstream grid were tapped from the downstream side of the grid to motivate them to start swimming. Comparing fish swimming voluntarily in response to the flow (no tap) with fish that swam after having been tapped at the start of the testing velocity showed that the former outperformed the latter. Motivation to swim could potentially influence swimming performance (Castro-Santos, 2005; Goerig & Castro-Santos, 2017). For example, fish tested in protocols where they voluntarily enter the swimming arena and are allowed to choose their own swimming velocity have been observed to perform better than conspecific in forced swimming trials (Peake & Farrell, 2004; Tudorache et al., 2010a; Videler, 1993). Our results highlight the role of motivation in fish swimming, and also, again, suggest that volitional swimming tests may increase the precision of our estimates of swimming capability (Castro-Santos et al., 2013; Colavecchia et al., 1998; Peake, 2008a).

Fish swimming performance varies not only due to the different testing methodologies adopted but also due to the intrinsic variation in fish ability, behaviour, and motivation (Goerig & Castro-Santos, 2017; Jones et al., 2020). In our experiments, only one fish species belonging to a specific age and size group was tested at a specific

flow velocity and temperature. This poses a limitation to the generalisation of our results towards other species and sizes swimming at different velocities and temperatures. For example, would fish swimming performance at lower velocity, in the prolonged or sustained swimming activity levels, encompassing aerobic processes, react in the same way in relation to habituation time? Also, as this experiment also alludes to, swimming performance is the product of capability and behaviour. Volitional swimming test protocol, where fish choose to swim or not, could avoid the potential pitfalls of forced performance tests and may improve our assessments of fish actual swimming capability (Colavecchia et al., 1998; Haro et al., 2004; Peake, 2008b). In addition, while 5 min habituation period may be enough for a small-sized fish, the results of this study may not hold true for larger fish as they may require longer times to recuperate from fish handling stress prior to the testing since fish body size is known to scale with its total anaerobic capacity (Karlsson-Drangsholt et al., 2018; Casselberry et al., 2023; Goolish, 1989; Somero & Childress, 1980), prompting similar experiments on larger fish. Given that the results of fish performance studies are used for the fishways design and management of fisheries (Enders et al., 2017; Knapp et al., 2019), it is imperative to investigate the effect of habituation time on fish swimming abilities and behaviour for different species, sizes, and swimming activity levels, prompting for similar experiments.

The present paper highlights the importance of in-flume habituation time in forced performance tests. While extremely short habituation times need to be avoided, findings suggest that, in burst swimming performance tests, a 5 min habituation time may be sufficient, or at least as effective as 20 min habituation time, at least for small-sized fish. Furthermore, the study also highlights potential impacts of fish behaviour – and researcher choices - on performance estimates, underlining that fish swimming performance is context dependent. This underlines the subjectivity of fish swimming performance estimates, and calls for a unifying methodology.

## References

Aedo, J. R., Otto, K. R., Rader, R. B., Hotchkiss, R. H., & Belk, M. C. (2021). Size Matters, but Species Do Not: No Evidence for Species-Specific Swimming Performance in Co-Occurring Great Basin Stream Fishes. *Water*, 13(18), 2570. <https://doi.org/10.3390/w13182570>

Arnekleiv, J. V., Urke, H. A., Kristensen, T., Halleraker, J. H., & Flodmark, L. E. W. (2004). Recovery of wild, juvenile brown trout from stress of flow reduction, electrofishing, handling and transfer from river to an indoor simulated stream channel. *Journal of Fish Biology*, 64(2), 541–552. <https://doi.org/10.1111/j.0022-1112.2004.00320.x>

Barton, B. A., & Schreck, C. B. (1987). Metabolic Cost of Acute Physical Stress in Juvenile Steelhead. *Transactions of the American Fisheries Society*, 116(2), 257–263. [https://doi.org/10.1577/1548-8659\(1987\)116<257:MCOAPS>2.0.CO;2](https://doi.org/10.1577/1548-8659(1987)116<257:MCOAPS>2.0.CO;2)

Beamish, F. W. H. (1978). *Fish Physiology* (W. S. Hoar & D. J. Randall, Eds.; 1st ed., Vol. 7). Academic Press, London.

Black, E. C. (1957). Alterations in the Blood Level of Lactic Acid in Certain Salmonoid Fishes Following Muscular Activity: I. Kamloops Trout, *Salmo gairdneri*. *Journal of the Fisheries Research Board of Canada*, 14(2), 117–134. <https://doi.org/10.1139/f57-004>

Brett, J. R. (1964). The Respiratory Metabolism and Swimming Performance of Young Sockeye Salmon. *Journal of the Fisheries Research Board of Canada*, 21(5), 1183–1226. <https://doi.org/10.1139/f64-103>

Brett, J. R. (1967). Swimming Performance of Sockeye Salmon (*Oncorhynchus nerka*) in relation to Fatigue Time and Temperature. *Journal of the Fisheries Research Board of Canada*, 24(8), 1731–1741. <https://doi.org/10.1139/f67-142>

Casselberry, G. A., Drake, J. C., Perlot, N., Cooke, S. J., Danylchuk, A. J., & Lennox, R. J. (2023). Allometric Scaling of Anaerobic Capacity Estimated from a Unique Field-Based Data Set of Fish Swimming. *Physiological and Biochemical Zoology*, 96(1), 17–29. <https://doi.org/10.1086/722134>

Castro-Santos, T. (2005). Optimal swim speeds for traversing velocity barriers: An analysis of volitional high-speed swimming behavior of migratory fishes. *Journal of Experimental Biology*, 208(3), 421–432. <https://doi.org/10.1242/jeb.01380>

Castro-Santos, T. R. (2002). *Swimming performance of upstream migrant fishes: New methods, new perspectives* [University of Massachusetts Amherst]. <https://scholarworks.umass.edu/dissertations/AAI3056208>

Castro-Santos, T., Sanz-Ronda, F. J., & Ruiz-Legazpi, J. (2013). Breaking the speed

limit—Comparative sprinting performance of brook trout ( *Salvelinus fontinalis* ) and brown trout ( *Salmo trutta* ). *Canadian Journal of Fisheries and Aquatic Sciences*, 70(2), 280–293. <https://doi.org/10.1139/cjfas-2012-0186>

Colavecchia, M., Katopodis, C., Goosney, R., Scruton, D. A., & McKinley, R. S. (1998). Measurement of burst swimming performance in wild Atlantic salmon (*Salmo salar* L.) using digital telemetry. *Regulated Rivers: Research & Management*, 14(1), 41–51. [https://doi.org/10.1002/\(SICI\)1099-1646\(199801/02\)14:1<41::AID-RRR475>3.0.CO;2-8](https://doi.org/10.1002/(SICI)1099-1646(199801/02)14:1<41::AID-RRR475>3.0.CO;2-8)

Deslauriers, D., & Kieffer, J. D. (2011). The influence of flume length and group size on swimming performance in shortnose sturgeon *Acipenser brevirostrum*. *Journal of Fish Biology*, 79(5), 1146–1155. <https://doi.org/10.1111/j.1095-8649.2011.03094.x>

Deslauriers, D., & Kieffer, J. D. (2012). Swimming performance and behaviour of young-of-the-year shortnose sturgeon ( *Acipenser brevirostrum* ) under fixed and increased velocity swimming tests. *Canadian Journal of Zoology*, 90(3), 345–351. <https://doi.org/10.1139/z2012-004>

Domenici, P., & Blake, R. (1997). The kinematics and performance of fish fast-start swimming. *Journal of Experimental Biology*, 200(8), 1165–1178. <https://doi.org/10.1242/jeb.200.8.1165>

Enders, E. C., Castro-Santos, T., & Lacey, R. W. J. (2017). The effects of horizontally and vertically oriented baffles on flow structure and ascent performance of upstream-migrating fish. *Journal of Ecohydraulics*, 2(1), 38–52. <https://doi.org/10.1080/24705357.2017.1288555>

Farrell, A. P., Johansen, J. A., Steffensen, J. F., Moyes, C. D., West, T. G., & Suarez, R. K. (1990). Effects of exercise training and coronary ablation on swimming performance, heart size, and cardiac enzymes in rainbow trout, *Oncorhynchus mykiss*. *Canadian Journal of Zoology*, 68(6), 1174–1179. <https://doi.org/10.1139/z90-174>

Farrell, A. P., Lee, C. G., Tierney, K., Hodaly, A., Clutterham, S., Healey, M., Hinch, S., & Lotto, A. (2003). Field-based measurements of oxygen uptake and swimming performance with adult Pacific salmon using a mobile respirometer swim tunnel: a mobile respirometer for pacific salmon. *Journal of Fish Biology*, 62(1), 64–84. <https://doi.org/10.1046/j.1095-8649.2003.00010.x>

Fortini, N. (2016). *Nuovo atlante dei pesci delle acque interne italiane: Guida completa ai pesci, ciclostomi, crostacei decapodi di acque dolci e salmastre*. Canterano, Aracne Ed.

Goerig, E., & Castro-Santos, T. (2017). Is motivation important to brook trout passage through culverts? *Canadian Journal of Fisheries and Aquatic Sciences*, 74(6), 885–893. <https://doi.org/10.1139/cjfas-2016-0237>

Goolish, E. M. (1989). The Scaling of Aerobic and Anaerobic Muscle Power in Rainbow Trout (*Salmo Gairdneri*). *Journal of Experimental Biology*, 147(1), 493–505. <https://doi.org/10.1242/jeb.147.1.493>

Hammer, C. (1995). Fatigue and exercise tests with fish. *Comparative Biochemistry and Physiology Part A: Physiology*, 112(1), 1–20. [https://doi.org/10.1016/0300-9629\(95\)00060-K](https://doi.org/10.1016/0300-9629(95)00060-K)

Haro, A., Castro-Santos, T., Noreika, J., & Odeh, M. (2004). Swimming performance of upstream migrant fishes in open-channel flow: A new approach to predicting passage through velocity barriers. *Canadian Journal of Fisheries and Aquatic Sciences*, 61(9), 1590–1601. <https://doi.org/10.1139/f04-093>

Heuer, R. M., Stieglitz, J. D., Pasparakis, C., Enochs, I. C., Benetti, D. D., & Grosell, M. (2021). The Effects of Temperature Acclimation on Swimming Performance in the Pelagic Mahi-Mahi (*Coryphaena hippurus*). *Frontiers in Marine Science*, 8, 654276. <https://doi.org/10.3389/fmars.2021.654276>

Hvas, M., & Oppedal, F. (2019). Influence of experimental set-up and methodology for measurements of metabolic rates and critical swimming speed in Atlantic salmon *Salmo salar*. *Journal of Fish Biology*, jfb.14087. <https://doi.org/10.1111/jfb.14087>

Jones, D. R., Kiceniuk, J. W., & Bamford, O. S. (1974). Evaluation of the Swimming Performance of Several Fish Species from the Mackenzie River. *Journal of the Fisheries Research Board of Canada*, 31(10), 1641–1647. <https://doi.org/10.1139/f74-206>

Jones, P. E., Svendsen, J. C., Börger, L., Champneys, T., Consuegra, S., Jones, J. A. H., & Garcia De Leaniz, C. (2020). One size does not fit all: Inter- and intraspecific variation in the swimming performance of contrasting freshwater fish. *Conservation Physiology*, 8(1), coaa126. <https://doi.org/10.1093/conphys/coaa126>

Karlsson-Drangsholt, A., Svalheim, R. A., Aas-Hansen, Ø., Olsen, S.-H., Midling, K., Breen, M., Grimstbø, E., & Johnsen, H. K. (2018). Recovery from exhaustive swimming and its effect on fillet quality in haddock (*Melanogrammus aeglefinus*). *Fisheries Research*, 197, 96–104. <https://doi.org/10.1016/j.fishres.2017.09.006>

Katopodis, C. (1992). Introduction to fishway design. *Freshwater Institute, Central and Arctic Region Department of Fisheries and Oceans, Manitoba, Canada*.

Katopodis, C., Cai, L., & Johnson, D. (2019). Sturgeon survival: The role of swimming performance and fish passage research. *Fisheries Research*, 212, 162–171. <https://doi.org/10.1016/j.fishres.2018.12.027>

Katopodis, C., & Gervais, R. (2012). Ecohydraulic analysis of fish fatigue data. *River Research and Applications*, 28(4), 444–456. <https://doi.org/10.1002/rra.1566>

Katopodis, C., & Gervais, R. (2016). Fish swimming performance database and analyses.



*DFO Can. Sci. Advis. Sec. Res. Doc. 2016/002*, vi + 550p.

Knapp, M., Montgomery, J., Whittaker, C., Franklin, P., Baker, C., & Friedrich, H. (2019). Fish passage hydrodynamics: Insights into overcoming migration challenges for small-bodied fish. *Journal of Ecohydraulics*, 4(1), 43–55.

<https://doi.org/10.1080/24705357.2019.1604091>

Liao, J. C. (2007). A review of fish swimming mechanics and behaviour in altered flows. *Philosophical Transactions of the Royal Society B: Biological Sciences*, 362(1487), 1973.

<https://doi.org/10.1098/rstb.2007.2082>

Louison, M. J., Stein, J. A., & Suski, C. D. (2019). The role of social network behavior, swimming performance, and fish size in the determination of angling vulnerability in bluegill. *Behavioral Ecology and Sociobiology*, 73(10), 139.

<https://doi.org/10.1007/s00265-019-2754-0>

Lupandin, A. I. (2005). Effect of Flow Turbulence on Swimming Speed of Fish. *Biology Bulletin*, 32(5), 461–466.

<https://doi.org/10.1007/s10525-005-0125-z>

McFarlane, W. J., & McDonald, D. G. (2002). Relating Intramuscular Fuel Use to Endurance in Juvenile Rainbow Trout. *Physiological and Biochemical Zoology*, 75(3), 250–259.

<https://doi.org/10.1086/341815>

McKenzie, D. J. (2011). *The energetics of Fish Swimming* (pp. 1075–1080). Amsterdam: Elsevier Inc.

Mu, Cao, Gong, Baiyin, & Li. (2019). A Classification Method for Fish Swimming Behaviors under Incremental Water Velocity for Fishway Hydraulic Design. *Water*, 11(10), 2131.

<https://doi.org/10.3390/w11102131>

Myrick, C. A., & Cech, J. J. (2000). Swimming Performances of Four California Stream Fishes: Temperature Effects. *Environmental Biology of Fishes*, 58(3), 289–295.

<https://doi.org/10.1023/A:1007649931414>

Nikora, V. I., Aberle, J., Biggs, B. J. F., Jowett, I. G., & Sykes, J. R. E. (2003). Effects of fish size, time-to-fatigue and turbulence on swimming performance: A case study of *Galaxias maculatus* : swimming performance of inanga. *Journal of Fish Biology*, 63(6), 1365–1382.

<https://doi.org/10.1111/j.1095-8649.2003.00241.x>

Olla, B. L., Davis, M. W., & Schreck, C. B. (1992). Notes: Comparison of Predator Avoidance Capabilities with Corticosteroid Levels Induced by Stress in Juvenile Coho Salmon. *Transactions of the American Fisheries Society*, 121(4), 544–547.

[https://doi.org/10.1577/1548-8659\(1992\)121<0544:NCOPAC>2.3.CO;2](https://doi.org/10.1577/1548-8659(1992)121<0544:NCOPAC>2.3.CO;2)

Palstra, A. P., Kals, J., Böhm, T., Bastiaansen, J. W. M., & Komen, H. (2020). Swimming Performance and Oxygen Consumption as Non-lethal Indicators of Production Traits in Atlantic Salmon and Gilthead Seabream. *Frontiers in Physiology*, 11, 759.

<https://doi.org/10.3389/fphys.2020.00759>

Peake, S. J. (2008a). Behavior and passage performance of northern pike, walleyes, and white suckers in an experimental raceway. *North American Journal of Fisheries Management*, 28(1), 321–327.

Peake, S. J. (2008b). Gait transition speed as an alternate measure of maximum aerobic capacity in fishes. *Journal of Fish Biology*, 72(3), 645–655. <https://doi.org/10.1111/j.1095-8649.2007.01753.x>

Peake, S. J., & Farrell, A. P. (2004). Locomotory behaviour and post-exercise physiology in relation to swimming speed, gait transition and metabolism in free-swimming smallmouth bass (*Micropterus dolomieu*). *Journal of Experimental Biology*, 207(9), 1563–1575. <https://doi.org/10.1242/jeb.00927>

Peake, S., McKinley, R. S., & Scruton, D. A. (1997). Swimming performance of various freshwater Newfoundland salmonids relative to habitat selection and fishway design. *Journal of Fish Biology*, 51(4), 710–723. <https://doi.org/10.1111/j.1095-8649.1997.tb01993.x>

Penghan, L.-Y., Pang, X., & Fu, S.-J. (2016). The effects of starvation on fast-start escape and constant acceleration swimming performance in rose bitterling (*Rhodeus ocellatus*) at two acclimation temperatures. *Fish Physiology and Biochemistry*, 42(3), 909–918. <https://doi.org/10.1007/s10695-015-0184-0>

Pickering, A. D., Pottinger, T. G., & Christie, P. (1982). Recovery of the brown trout, *Salmo trutta* L., from acute handling stress: A time-course study. *Journal of Fish Biology*, 20(2), 229–244. <https://doi.org/10.1111/j.1095-8649.1982.tb03923.x>

Plew, D. R., Nikora, V. I., Larned, S. T., Sykes, J. R. E., & Cooper, G. G. (2007). Fish swimming speed variability at constant flow: *Galaxias maculatus*. *New Zealand Journal of Marine and Freshwater Research*, 41(2), 185–195. <https://doi.org/10.1080/00288330709509907>

Quintella, B. R., Mateus, C. S., Costa, J. L., Domingos, I., & Almeida, P. R. (2010). Critical swimming speed of yellow- and silver-phase European eel (*Anguilla anguilla*, L.): Critical swimming speed of yellow- and silver-phase European eel. *Journal of Applied Ichthyology*, 26(3), 432–435. <https://doi.org/10.1111/j.1439-0426.2010.01457.x>

Romão, F., Quintella, B. R., Pereira, T. J., & Almeida, P. R. (2012). Swimming performance of two Iberian cyprinids: The Tagus nase *Pseudochondrostoma polylepis* (Steindachner, 1864) and the bordallo *Squalius carolitertii* (Doadrio, 1988): Critical swimming speed of two Iberian cyprinids. *Journal of Applied Ichthyology*, 28(1), 26–30. <https://doi.org/10.1111/j.1439-0426.2011.01882.x>

Santos, H. de A. e, Pompeu, P. dos S., & Martinez, C. B. (2007). Swimming performance

of the migratory Neotropical fish *Leporinus reinhardtii* (Characiformes: Anostomidae). *Neotropical Ichthyology*, 5(2), 139–146. <https://doi.org/10.1590/S1679-62252007000200007>

Schiavon, A., Comoglio, C., Candioto, A., Hölker, F., Ashraf, M. U., & Nyqvist, D. (2023). Survival and swimming performance of a small-sized Cypriniformes (*Telestes muticellus*) tagged with passive integrated transponders. *Journal of Limnology*, 82.2129 <https://doi.org/10.4081/jlimnol.2023.2129>

Schreck, C. B., & Tort, L. (2016). The Concept of Stress in Fish. In *Fish Physiology; Academic Press: Cambridge, MA, USA*; (Vol. 35, pp. 1–34). Elsevier. <https://doi.org/10.1016/B978-0-12-802728-8.00001-1>

Shiau, J., Watson, J. R., Cramp, R. L., Gordos, M. A., & Franklin, C. E. (2020). Interactions between water depth, velocity and body size on fish swimming performance: Implications for culvert hydrodynamics. *Ecological Engineering*, 156, 105987. <https://doi.org/10.1016/j.ecoleng.2020.105987>

Silva, A. T., Katopodis, C., Santos, J. M., Ferreira, M. T., & Pinheiro, A. N. (2012). Cyprinid swimming behaviour in response to turbulent flow. *Ecological Engineering*, 44, 314–328. <https://doi.org/10.1016/j.ecoleng.2012.04.015>

Silva, A. T., Santos, J. M., Ferreira, M. T., Pinheiro, A. N., & Katopodis, C. (2011). Effects of water velocity and turbulence on the behaviour of Iberian barbel (*Luciobarbus bocagei*, Steindachner 1864) in an experimental pool-type fishway: IBERIAN BARBEL'S RESPONSE TO VELOCITY AND TURBULENCE. *River Research and Applications*, 27(3), 360–373. <https://doi.org/10.1002/rra.1363>

Silva, S. S., Alexandre, C. M., Quintella, B. R., & de Almeida, P. R. (2021). Seasonal environmental variability drives the swimming performance of a resident Iberian fish. *Ecology of Freshwater Fish*, 30(3), 366–374. <https://doi.org/10.1111/eff.12587>

Somero, G. N., & Childress, J. J. (1980). A Violation of the Metabolism-Size Scaling Paradigm: Activities of Glycolytic Enzymes in Muscle Increase in Larger-Size Fish. *Physiological Zoology*, 53(3), 322–337. <https://doi.org/10.1086/physzool.53.3.30155794>

Stevens, E. D. (1979). The effect of temperature on tail beat frequency of fish swimming at constant velocity. *Canadian Journal of Zoology*, 57(8), 1628–1635. <https://doi.org/10.1139/z79-214>

Tritico, H. M., & Cotel, A. J. (2010). The effects of turbulent eddies on the stability and critical swimming speed of creek chub (*Semotilus atromaculatus*). *Journal of Experimental Biology*, 213(13), 2284–2293. <https://doi.org/10.1242/jeb.041806>

Tudorache, C., O'Keefe, R. A., & Benfey, T. J. (2010a). Flume length and post-exercise impingement affect anaerobic metabolism in brook charr *Salvelinus fontinalis*. *Journal of*

*Fish Biology*, 76(3), 729–733. <https://doi.org/10.1111/j.1095-8649.2009.02513.x>

Tudorache, C., O’Keefe, R. A., & Benfey, T. J. (2010b). The effect of temperature and ammonia exposure on swimming performance of brook charr (*Salvelinus fontinalis*). *Comparative Biochemistry and Physiology Part A: Molecular & Integrative Physiology*, 156(4), 523–528. <https://doi.org/10.1016/j.cbpa.2010.04.010>

Tudorache, C., Viaene, P., Blust, R., Vereecken, H., & De Boeck, G. (2008). A comparison of swimming capacity and energy use in seven European freshwater fish species. *Ecology of Freshwater Fish*, 17(2), 284–291. <https://doi.org/10.1111/j.1600-0633.2007.00280.x>

Tudorache, C., Viaenen, P., Blust, R., & De Boeck, G. (2007). Longer flumes increase critical swimming speeds by increasing burst-glide swimming duration in carp *Cyprinus carpio*, L. *Journal of Fish Biology*, 71(6), 1630–1638. <https://doi.org/10.1111/j.1095-8649.2007.01620.x>

Van Den Thillart, G., Van Ginneken, V., Korner, F., Heijmans, R., Van Der Linden, R., & Gluvers, A. (2004). Endurance swimming of European eel. *Journal of Fish Biology*, 65(2), 312–318. <https://doi.org/10.1111/j.0022-1112.2004.00447.x>

Veza, P., Libardoni, F., Manes, C., Tsuzaki, T., Bertoldi, W., & Kemp, P. S. (2020). Rethinking swimming performance tests for bottom-dwelling fish: The case of European glass eel (*Anguilla anguilla*). *Scientific Reports*, 10(1), 16416. <https://doi.org/10.1038/s41598-020-72957-w>

Videler, J. J. (1993). *Fish Swimming*. Springer Netherlands. <https://doi.org/10.1007/978-94-011-1580-3>

Watson, J. R., Goodrich, H. R., Cramp, R. L., Gordos, M. A., Yan, Y., Ward, P. J., & Franklin, C. E. (2019). *Swimming performance traits of twenty-one Australian fish species: A fish passage management tool for use in modified freshwater systems* bioRxiv, 961898. Zoology. <https://doi.org/10.1101/861898>

Webb, P. W., KostECKI, P. T., & Stevens, E. D. (1984). The Effect of Size and Swimming Speed on Locomotor Kinematics of Rainbow Trout. *Journal of Experimental Biology*, 109(1), 77–95. <https://doi.org/10.1242/jeb.109.1.77>

## **Chapter 4**

# **Decoding Burst Swimming Performance: A Scaling Perspective on Time-to-Fatigue**

## 4.1 Abstract

Fatigue curves quantify fish swimming performance, providing information about the time ( $T_f$ ) fish can swim against a steady flow-velocity ( $U_f$ ) before fatiguing. Such curves represent a key tool for many applications in ecological engineering, especially for fish pass design and management. Despite years of research, though, our current ability to model fatigue curves still lacks theoretical foundations and relies primarily on fitting empirical data, as obtained from time-consuming and costly experiments. In the present paper, we address this shortcoming by proposing a theoretical analysis that builds upon concepts of fish hydrodynamics to derive scaling laws linking statistical properties of  $T_f$  to velocities  $U_f$ , pertaining to the so-called burst range. Theoretical arguments, in the present study, suggest that the proposed scaling laws may hold true for all fish species and sizes. A new experimental database obtained from over 800 trials and five small-sized Cypriniformes support theoretical predictions satisfactorily and calls for further experiments on more fish species and sizes to confirm their general validity.

## 4.2 Introduction

Fish swimming performance has drawn a lot of interest in recent decades owing to its importance for fish migration, habitat selection, and predator-prey interactions (Castro-Santos, 2002; Domenici & Blake, 1997; Katopodis & Gervais, 2012; Peake et al., 1997; Tudorache et al., 2008; Watson et al., 2019). From an applied perspective, fish swimming performance estimates are used extensively in the design of fishways allowing for the passage of fish through dams, weirs, culverts, and other anthropogenic barriers (Barbarossa et al., 2020; Belletti et al., 2020; Katopodis, 1992). Other important applications include the design of sustainable fishing methods (Castro-Santos et al., 2022) and the optimisation of practices in aquaculture industry (Hvas et al., 2021).

Two well-established experimental protocols are commonly used to characterise fish swimming performance: critical velocity and fixed velocity tests (Beamish, 1978; Brett, 1964; Hammer, 1995). Both tests are typically conducted in either a swim chamber or an open channel flume, where fish swims until fatiguing. Fatigue is typically defined as the state of exhaustion where fish rests at the downstream end of the test section and is not able to swim despite external motivation (Aedo et al., 2021; Ashraf et al., 2024b; Tudorache et al., 2010). In the critical velocity test, a fish is forced to swim against a flow velocity  $U_f$  which is progressively increased at fixed time intervals  $\Delta t$ , until the fish fatigues. The velocity and time at which fatigue occurs are then used to compute the so-called critical velocity  $U_{crit}$  (Brett, 1964; Farrell & Steffensen, 1987; Gregory & Wood, 1999). Fixed velocity tests, on the other hand, consist of repeated swimming trials under a range of fixed velocities. Each trial results in a time-to-fatigue  $T_f$  – the time a fish can resist swimming against the defined steady flow velocity ( $U_f$ ). By repeating trials for different values of  $U_f$ , a scatter plot of  $T_f$  (dependent variable) vs  $U_f$  (independent variable) can be produced. A predetermined model is then fitted to the data to obtain a so-called *fatigue- or endurance-curve* (Katopodis & Gervais, 2016). Fixed velocity tests are more informative than critical velocity tests as they allow for the assessment of fish endurance over a range of flow velocities and associated swimming activity levels (Nikora et al., 2003). Three of such levels are believed to exist and hereafter are referred to as: sustained, prolonged, and burst swimming (Beamish, 1978; Hammer, 1995; Webb, 1975). Sustained swimming occurs at velocities whereby fish swim using red muscles and aerobic processes. Utilising somatic energy reserves, fish can theoretically maintain sustained swimming indefinitely (Beamish, 1978; Videler, 1993). Prolonged swimming is driven by both red and white muscles, and hence by both aerobic and anaerobic processes. In burst swimming, fish use primarily white muscles and anaerobic processes. Both prolonged and burst swimming are limited by anaerobic energy reserves and therefore subject to exhaustion. By convention, it is assumed that fish can endure prolonged swimming for up to 200 minutes, while burst swimming is usually associated with  $T_f \lesssim 20$  seconds (Beamish, 1978; Katopodis, 1992). Actual  $T_f$  thresholds between burst and prolonged swimming, however, are known to vary with species, size and even amongst similar individuals, so much so burst swimming has been often associated with  $T_f$  of the order of

1 minute or more in the literature (Castro-Santos, 2005; Nikora et al., 2003; Videler & Wardle, 1991).

Our current ability to model fatigue curves is primarily based on empirical mathematical relations between  $T_f$  and  $U_f$ , which sometimes are supported by dimensional analysis (Katopodis & Gervais, 2012, 2016; Nikora et al., 2003). Burst and prolonged swimming are commonly associated with fatigue curves following either a log-linear or a power law (Brett, 1964; Castro-Santos, 2005; Castro-Santos et al., 2013; Haro et al., 2004; Katopodis & Gervais, 2012; Nikora et al., 2003; Videler, 1993; Videler & Wardle, 1991). A theoretical argument in support of either of these laws, however, has never been provided. In their review paper, Katopodis & Gervais (2012) collected and analysed a large dataset of fatigue curves, and employed a power law model to elucidate relations between  $T_f$  and  $U_f$  classified by grouping different fish species displaying a similar morphology or swimming kinematics. Nevertheless, the conceptual framework underpinning such relations remains undefined and rooted mostly on empirical grounds. Furthermore, an assessment of the available database by Katopodis & Gervais (2012) highlighted that majority of the published fatigue-curve data is limited to the prolonged activity. Instead, comparatively little efforts have been made to characterise the burst swimming activity (Haro et al., 2004) despite white muscles constituting the bulk of fish musculature, and burst swimming being key to dictate predator-prey interactions and for overcoming velocity barriers (Burnett et al., 2014; Nyqvist et al., 2023; Taylor & McPhail, 1985; Videler, 1993), the latter directly relates to the design of fish passage systems (Katopodis, 1992; Peake et al., 1997; Silva et al., 2018).

Swimming performance, as estimated in fixed velocity experiments, is characterised by an enormous and unexplored variability where fish species, size and water temperature are often pointed out as key drivers<sup>1</sup> (Hammill et al., 2004; Jones et al., 2020; Videler, 1993; Wardle, 1975). A large variability has also been reported for conspecifics of the same size in response to different fitness and/or motivation (Goerig & Castro-Santos, 2017; Hvas et al., 2021; Jones et al., 2020). Therefore, considering a fixed velocity experiment where many fish of the same size and species are tested over a range of flow velocities at constant water temperature, it is reasonable to expect that experimental data will qualitatively spread around mean values of  $T_f$  (Figure 4.1). For each tested velocity,  $T_f$  will display a variability that can be described by a probability function  $p(T_f)$ . Typically, a fatigue curve is obtained by fitting the entire cloud of experimental data with a predetermined mathematical law (red line in Figure 4.1). This, however, only provides information about the general trend of the data but does not provide any clue about  $p(T_f)$  and how it varies with  $U_f$ .

---

<sup>1</sup> Note that life-stage, sex, experience, health status, and nutrition have also been seen to cause variation in fish swimming performance, see Beamish et al., 1989; Jain et al., 1998; Li et al., 2017; Penghan et al., 2016; Quintella et al., 2010; Reidy et al., 2000.



The aim of this paper is to present and validate a theoretical framework allowing for the statistical description of  $T_f$  vs  $U_f$  data in the burst range. Towards this end, the following objectives are set:

- i) to present a theoretical framework based on simple concepts of fish hydrodynamics that can statistically describe the relation between  $T_f$  and  $U_f$ , showing that  $\bar{T}_f$  (where  $\bar{T}_f$  is the mean value of  $T_f$ ) and central moments of  $p(T_f)$  (which indeed help defining  $p(T_f)$ ) vary with  $U_f$  following power laws with well constrained and, in principle, universal exponents.
- ii) to test theoretical predictions in a series of fixed velocity tests using five small-sized Cypriniformes.

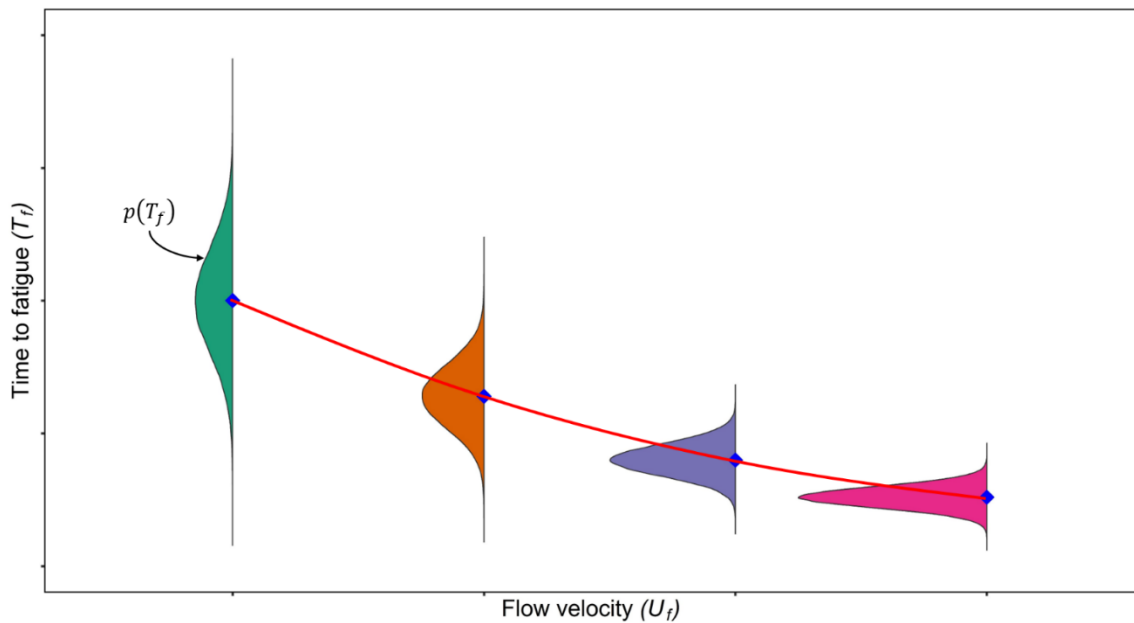


Figure 4.1 Illustration of the relationship between fish time-to-fatigue ( $T_f$ ) and flow velocity ( $U_f$ ). For each test flow velocity value,  $p(T_f)$  is the probability density function of related time-to-fatigue. Blue diamonds mark the mean time-to-fatigues at a given test flow velocity. Red curve is the best fitted line to the entire cloud of data points, referred to as fatigue- or endurance-curve.

### 4.3 Theoretical framework

In what follows, section 4.3.1 reviews the formulations for fish drag proposed in the literature, while section 4.3.2 derive the sought scaling relations using energetic principles.

#### 4.3.1 Fish drag

The drag force experienced by a fish while swimming can be parameterised as (Videler, 1993):

$$F_D \sim \rho C_D L S U_r^2 \quad [4.1]$$

where  $F_D$  is the average drag force, the symbol " $\sim$ " stands for *scales as*,  $\rho$  is the density of water,  $C_D$  is fish drag coefficient,  $L$  is total fish length (Figure A.1 in Appendix A),  $S$  is fish body depth,  $U_r$  is the relative fish-water velocity, assumed to be identical to the flow velocity in performance tests (Nikora et al., 2003; Plew et al., 2007). The estimation of  $C_D$  for swimming fish has been a matter of debate for a long time and no shared consensus has been reached (Anderson et al., 2001; Lighthill, 1960, 1969, 1970, 1971; Webb, 1975). At high Reynolds numbers ( $Re_L = LU_r/\vartheta$ , where  $\vartheta$  is the kinematic viscosity of water), which are typical for fish swimming at burst velocities, pressure drag is believed to dominate over friction drag (Gazzola et al., 2014; Saadat et al., 2017) so that  $C_D$  can be considered as a constant. As a result,  $F_D$  is estimated as:

$$F_D \sim \rho C_D L S U_r^2 \sim \rho L S U_r^2 = (\rho L S) U_r^2 = \Gamma_1 U_r^2 \quad [4.2]$$

where  $\Gamma_1 = \rho L S$  is a function that is herein introduced to lump the effects of parameters pertaining to fish size (i.e.  $L$  and  $S$ ) and fluid properties (i.e.  $\rho$ ).

The above formulation is however questionable as it completely ignores skin friction effects (and hence the dependence of  $C_D$  on  $Re_L$ ) which some researchers argue to be significant, even at high Reynolds numbers (Anderson et al., 2001; Eloy, 2012). While we do not intend to contribute to the debate about the nature of drag in swimming fish, in Appendix A we demonstrate that even when skin friction effects are accounted for and considered the main source of drag,  $F_D$  can be generally parameterised as

$$F_D \sim \Gamma_j U_r^\beta \quad [4.3]$$

where  $\Gamma_{j=1-3}$  ( $\Gamma_2$  and  $\Gamma_3$  are defined in Appendix A) depend on water properties ( $\rho$  and  $\nu$ ) and fish size, shape, and tail beat amplitude (i.e.  $S$ ,  $L$ , and  $A$ ), and the scaling exponent  $\beta$  remains well constrained between 1.73 and 2.0. This range of also accounts for combined effects of skin friction and body undulations on  $C_D$ .

### 4.3.2 Energetic considerations and scaling laws

The power (energy per unit time) expended by a fish while swimming can be estimated as  $P \sim F_D U_r = \Gamma_j U_r^{\beta+1}$ . Therefore, the total energy spent by an  $i^{\text{th}}$  fish ( $E_i$ ) during a fixed velocity test can be obtained by integrating power ( $P$ ) over time, between zero (i.e. the beginning of the test) and the measured time-to-fatigue ( $T_{fi}$ ) as

$$E_i \sim \Gamma_j U_r^{\beta+1} T_{fi}. \quad [4.4]$$

When swimming is dominated by anaerobic processes, as in the burst range, fatigue occurs when white-fibre muscles burn the available anaerobic reserves down to a critical limit which can be related to  $E_i$  (via a conversion factor similar to an efficiency coefficient) (Beamish, 1978; Hammer, 1995; Videler, 1993) and assumed independent of  $U_r$ . Such a critical limit clearly varies extensively among individuals (Jones et al., 2020; Kolok, 1992; Marras et al., 2010) and cannot be predicted from first principles but it can be described statistically. Towards this end, firstly it should be noted that, considering a population of fish of the same species and size and swimming at a constant water temperature,  $\Gamma_j$  in Eq. 4.4, depends only on fish size, shape, and tail beat amplitude ( $L$ ,  $S$ , and  $A$ ), and water properties ( $\rho$  and  $\nu$ ), and hence can be considered constant. Secondly, if averaging is taken over a representative sample of the chosen population of fish, the resulting mean energy  $\bar{E}$ , can be also considered as constant. Therefore, averaging both sides of Eq. 4.4 leads to  $\bar{E} \sim U_r^{\beta+1} \bar{T}_f \approx \text{constant}$ , which in turn means that  $\bar{T}_f$  scales as:

$$\bar{T}_f \sim U_r^{-(\beta+1)}. \quad [4.5]$$

Using analogous arguments as above, it is possible to derive the scaling of central moments of any order as follows.

First, considering the  $i^{\text{th}}$  fish

$$(E_i - \bar{E}) \sim U_r^{\beta+1} (T_{fi} - \bar{T}). \quad [4.6]$$

Hence, defining  $E'_i = E_i - \bar{E}$  and  $T'_{fi} = T_{fi} - \bar{T}$ , Eq. 4.6 is rewritten as

$$E'_i \sim U_r^{\beta+1} T'_{fi}. \quad [4.7]$$

By elevating both sides of Eq. 4.7 to a power  $k$  and then applying the averaging operator, Eq. 4.7 transforms into

$$\overline{E'^k} \sim U_r^{k(\beta+1)} \overline{T_f'^k}. \quad [4.8]$$

As per  $\bar{E}$ , also  $\overline{E'^k}$  can be considered a statistical trait of a fish population that is constant (and therefore independent of  $U_r$ ), hence

$$\overline{T_f'^k} \sim U_r^{-k(\beta+1)}. \quad [4.9]$$

Eq. 4.9 provides the scaling for central moments  $\overline{T_f'^k}$ , as sought.

## 4.4 Materials and Methods

The study was performed with permission from the Protection of Flora and Fauna Department of the Metropolitan City of Turin (authorization D.D. n.4457 of 29 October 2020) and the Fauna and Ichthyofauna Technical Office of the Alessandria Province (authorization n.1570 of 19 January 2023), under the provisions of art.2 of the national Decree n.26/2014 (implementation of Dir. 2010/63/EU).

### 4.4.1 Fish

Experiments were conducted on five freshwater fish species (Table 4.1): Italian riffle dace (*Telestes muticellus*), common minnow (*Phoxinus phoxinus*), European bitterling (*Rhodeus amarus*), North Italian roach (*Leucos aula*), and common bleak (*Alburnus alburnella*). These small-sized riverine Cypriniformes were selected because they are all common within their geographic range (Freyhof & Kottelat, 2007), are classified as least concerned in the IUCN red lists (IUCN, 2023), and were expected to display interspecific variation in swimming abilities. Mean fish length ranged between 4.87-6.04 cm, with a standard deviation no larger than 0.70 cm for the five fish species (see Table 4.1 for details). *T. muticellus* and *P. phoxinus* were tested in May-June 2022 and were captured from the Noce stream near Pinerolo, Italy (44°56'17.9"N 7°23'09.1"E) on 20<sup>th</sup> May 2022 and 11<sup>th</sup> June 2022, respectively, using electrofishing. Fish were transferred to the hatchery facility located in Porte di Pinerolo and were housed in two spring-fed flow-through holding tanks divided into six compartments. *R. amarus*, *L. aula*, and *A. alburnella* were tested in Jan-Feb 2023. They were captured from the Orba stream in the Province of Alessandria, Italy (44°45'46.7"N 8°40'15.6"E) using electrofishing. *R. amarus* were electrofished on 17<sup>th</sup> January 2023, whereas *L. aula* and *A. alburnella* were caught on 30<sup>th</sup> January 2023. These fish were brought to the Alessandria Province hatchery in Predosa, Italy and were kept in spring-fed flow-through holding tanks. All fish were allowed to habituate to hatchery conditions for 3-7 days before the experimental trials.

A HOBO MX-2022 logger was used to record temperature in the holding tanks at 10 minutes intervals. Temperatures were  $13.3 \pm 0.4$  °C (mean  $\pm$  standard deviation (sd)) in 2022 and  $12.3 \pm 0.7$  °C for the experiments in 2023. All fish were fed commercial aquaria fish pellets (Tetra TabiMin) and were starved at least 24 hours before testing to ensure a post-absorptive state (Penghan et al., 2016; Schneider et al., 2019). Throughout the experiments, fish appeared to be in good health.

### 4.4.2. Experimental protocol

Experiments were conducted in an open channel recirculating flume with a width of 30 cm and a fixed water depth at any given test flow velocity. The water depth was slightly different for different velocities and ranged from 7 to 9 cm. The swimming arena (flume length) was 60 cm in 2022 and 80 cm in 2023 and delimited by a flow straightener in the

upstream direction and a fine meshed grid in the downstream direction. In a previous study, we demonstrated that such small differences in the length of the swimming arena had no appreciable effect on time-to-fatigue for fish swimming in burst activity level (Ashraf et al. 2024b). Trials were recorded from underneath and from the side of the flume using two Sony AX43 handycams with a resolution of 1920x1080 pixels at 50 frames per second. A pump allowed water recirculation and the flow rate was manually adjusted using the inverter (DGFIT MT 12) installed with the pump. The flow rate was measured using an AquaTrans™ AT600 flow metre sensor. During trials, water temperature in the system was maintained within a narrow range of 1°C using a chiller unit (TECO TK-2000). The difference between the water temperature in the flume and the holding tanks was kept at less than 1°C to avoid any confounding effects of temperature change on swimming performance (Tudorache et al., 2010b; Vezza et al., 2020).

All fish were tested individually using a fixed velocity testing protocol. Preliminary tests were conducted on each species to determine which flow velocities could be related to burst swimming (Castro-Santos, 2005). Such tests indicated that flow velocities greater than either 55 cm s<sup>-1</sup> (European bitterling, common bleak, North Italian roach, and Italian riffle dace) or 60 cm s<sup>-1</sup> (common minnow) resulted in fish simply being unable to swim, hence leading to a large number of unsuccessful trials (a trial where  $T_f$  data is not available). Moreover, it was observed that velocities lower than 40 cm s<sup>-1</sup> (Italian riffle dace), 45 cm s<sup>-1</sup> (European bitterling, common bleak, North Italian roach) and 50 cm s<sup>-1</sup> (common minnow) resulted in average times-to-fatigue  $\bar{T}_f$  significantly exceeding the commonly accepted threshold, in burst swimming, of 20 seconds. Therefore, fish were tested over a limited range of flow velocities. *T. muticellus* were tested at four flow velocities  $U_f = 40, 45, 50,$  and  $55 \text{ cm s}^{-1}$ . *P. phoxinus* were tested at three  $U_f = 50, 55,$  and  $60 \text{ cm s}^{-1}$ . The remaining three species, *R. amarus*, *R. aula*, and *A. alborella*, were tested at  $U_f = 45, 50,$  and  $55 \text{ cm s}^{-1}$ . A single fish was tested per trial at a fixed flow velocity, and no fish was tested more than once. At the beginning of each trial, the fish was habituated for 5 mins at 5 cm s<sup>-1</sup> (Ashraf et al., 2024a; Schiavon et al., 2023). The flow rate was then increased manually to achieve the testing flow velocity. Fish were allowed to swim at testing velocity until fatigued. Fatigue was defined as fish resting at the downstream grid and not responding to tapping (Aedo et al., 2021; Heuer et al., 2021; Tudorache et al., 2010a; Videler & Wardle, 1991). A fish was tapped no more than three times during an experimental trial. At the end of the trial, the fish was sedated in clove oil (Aroma Labs, Kalamazoo, MI, USA; approximately 0.2 ml clove oil/litre water), and fork length [cm], mass [g], width [cm], and height [cm] were measured.

#### 4.4.3 Data analysis

In order to test the validity of the scaling relations proposed in section 4.3.2, it was assumed that the mean relative velocity between fish and water  $U_r$  could be well approximated by the bulk flow velocity  $U_f$  (Nikora et al., 2003). Experimental data were then used to test the validity of the scaling laws for time-to-fatigue mean ( $\bar{T}_f$ ; Eq. 4.5) and variance ( $\overline{T_f'^2}$ ; Eq. 4.9). The test was limited to the second-order central moment ( $k=2$ ),

since the estimation of higher orders would have required an enormous amount of data, not available from the above experimental protocol (Appendix D).

As outlined in section 4.3.2, statistical properties of  $T_f$  must be obtained from data pertaining to a population of fish from the same species, having the same size and swimming at constant temperature. For all fish species, the experimental data was well in line with the constant water temperature requirement (in all trials the water temperature varied over a narrow range of maximum  $\pm 1^\circ\text{C}$ ). However, variations in fish size were significant. For example, the fork length  $L_f$  ( $L_f$  is taken as a proxy for fish size, see Appendix C, showing allometric relations) varied within the range  $\pm 10.3\text{-}38.8\%$ . Hence, following Katopodis & Gervais (2012) data were reorganised in subsamples where variations in  $L_f$  never exceeded  $\pm 10\%$  (Appendix B presents detailed explanation on subsampling procedure).

For all fish species and for each subsampled group separately (Appendix B), time-to-fatigue mean ( $\bar{T}_f$ ) and variance ( $\overline{T_f'^2}$ ) were calculated for each tested flow velocity  $U_f$ . Linear regression was then carried out on log-transformed values of  $\bar{T}_f$  vs  $U_f$ , and  $\overline{T_f'^2}$  vs  $U_f$  to empirically estimate the exponent  $\beta$  in the proposed scaling relations (Eq. 4.5 and Eq. 4.9 with  $k=2$ ). Results from the regression analysis were deemed acceptable if the null hypothesis of zero slope could be rejected with a 5% significance level (i.e. p-value  $< 0.05$ ) using Fisher's test, otherwise they were discarded.

Since time-to-fatigue data exhibits widespread variability (Aedo et al., 2021; Deslauriers, 2011; Katopodis & Gervais, 2016), estimates of  $\bar{T}_f$  and  $\overline{T_f'^2}$  might be subjected to significant errors unless many data points are available. Moreover, from a statistical standpoint, linear regression in logarithmic coordinates improves when performed over a wide range of velocities in log scale, namely for large values of  $\ln(U_M/U_m)$ , where  $U_M$  and  $U_m$  are the maximum and minimum tested velocities. Small number of data points and low values of  $\ln(U_M/U_m)$  may lead to poor estimates of the scaling exponent ( $\beta$ ), even if the regression analysis results in high values of  $R^2$  and p-values  $< 0.05$ . Therefore, a reliability index ( $ReI$ ) was defined and used to compare the reliability of  $\beta$  estimates. Following an approach similar to Jerde et al. (2019), the  $ReI$  is defined as

$$ReI = p \ln\left(\frac{U_M}{U_m}\right), \quad [4.10]$$

where  $p$  is the total number of individual data points used for the regression analysis. Eq. 4.10 serves as a useful metric to assess the reliability of  $\beta$  estimates obtained from data sets of varying quality, regarding the number of samples and range of test flow velocities. Since  $ReI$  is essentially an index that quantifies the confidence that can be put in the regression of each curve, it is expected that the higher the  $ReI$  the more likely  $\beta$  should fall into the theoretically predicted range.

For all fish species, the distribution of time-to-fatigue data  $p(T_f)$  at all test flow velocities was estimated using Kernel Density Estimation (KDE), a non-parametric method to estimate the Probability Density Function (PDF). This was done to explore whether a working model for  $p(T_f)$  could be identified from the available data.

All statistical analyses were run using R version 4.2.2 (R Foundation for Statistical Computing, Vienna, Austria. URL <https://www.R-project.org>). Package *dplyr* was used for data management (<https://CRAN.R-project.org/package=dplyr>), package *ggplot2* was used for plotting (<https://CRAN.R-project.org/package=ggplot2>), package *boot* was used for bootstrap resampling procedure, and package *confintr* was used to calculate the confidence intervals (<https://cran.r-project.org/web/packages/confintr/index.html>).

## 4.5 Experimental results

A total of 850 fish were tested for the five fish species. 626 fish (74%) resulted in successful trials where time-to-fatigue was recorded (Table 4.1).

Table 4.1 Summary of experimental data for five tested Cypriniformes fish species reporting scientific names, the total number of test fish, the number of successful fish trials  $n$ , test flow velocity  $U_f$  values, fish fork length  $L_f$ , test water temperature  $T$ , and wet fish mass  $m$ .

Species	Total test fish	Tested $U_f$ [cm/s]	Successful trials ( $n$ )	Min	Max	Mean $\pm$ sd		
				$L_f$ [cm]	$L_f$ [cm]	$L_f$ [cm]	$T$ [°C]	$m$ [g]
<i>Telestes muticellus</i>	202	40	45	4	6.6	4.87 $\pm$ 0.46	13.4 $\pm$ 0.23	1.56 $\pm$ 0.49
		45	45					
		50	45					
		55	45					
<i>Phoxinus phoxinus</i>	225	50	54	3.7	6.8	4.90 $\pm$ 0.70	16.2 $\pm$ 0.31	2.05 $\pm$ 0.95
		55	54					
		60	54					
<i>Rhodeus amarus</i>	148	45	30	5.4	6.7	6.04 $\pm$ 0.34	11.7 $\pm$ 0.34	3.13 $\pm$ 0.59
		50	30					
		55	30					
<i>Leucos aula</i>	160	45	35	4.6	6	5.24 $\pm$ 0.36	12.7 $\pm$ 0.35	1.85 $\pm$ 0.45
		50	38					
		55	39					
<i>Alburnus albonella</i>	115	45	26	4.5	6	5.04 $\pm$ 0.38	11.4 $\pm$ 0.67	1.16 $\pm$ 0.31
		50	34					
		55	22					

For all the five fish species  $T_f$  values show a very large variability at all test flow velocities (Figure 4.2). Mean values of  $T_f$  are below 20 seconds except for common minnow and Italian riffle dace as recorded for  $U_f = 40 \text{ cm s}^{-1}$  and  $50 \text{ cm s}^{-1}$ , respectively (Figure 4.2). Even in these cases, mean values of  $T_f$  never exceeded 32 seconds. This means that great majority of fish were likely tested at burst swimming velocities or very close to. Note that individual values of  $T_f$  can be instead very large (in some cases exceeding 80 seconds), meaning that some trials may have occurred under (partly) aerobic swimming conditions.



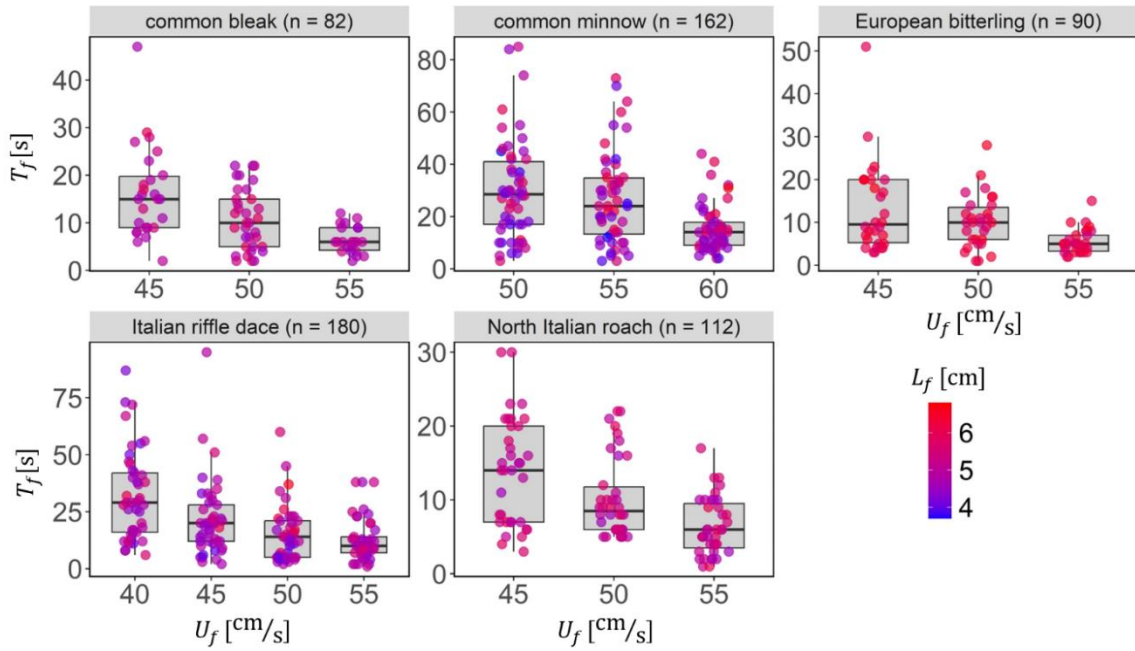


Figure 4.2 Box plot of all experimentally collected time-to-fatigue ( $T_f$ ) data, without subsampling, for all five fish species superimposed with jitter plot with varying colour intensity based on fish fork length ( $L_f$ ). The solid horizontal black line inside the boxplot marks the median  $T_f$  against a test flow velocity  $U_f$ . The bounding box defines the Interquartile Range (IQR), containing 50% of time-to-fatigue data. The whiskers mark  $Q1 - 1.5 \cdot IQR$  (bottom end) and  $Q3 + 1.5 \cdot IQR$  (top end), where  $Q1$  and  $Q3$  are the 25<sup>th</sup> and 75<sup>th</sup> percentiles, respectively.

Despite the large number of tests that were carried out, the Kernel Density Estimation (KDE) of time-to-fatigue data for the subsampled groups does not follow a consistent shape, showing in some cases multimodal while in others unimodal distributions, hence making the identification of a working model for  $p(T_f)$  rather difficult. Nonetheless, it is noteworthy to note that the variability in  $T_f$  diminishes with increasing  $U_f$ , as theoretically predicted (Equation 4.9,  $k = 2$ ). This can be appreciated from Figure 4.3, which shows the KDE related to subsampled groups characterised by the highest reliability index ( $ReI$ ). Similar conclusions can be drawn from results obtained analysing other subsampled datasets with lower  $ReI$ .

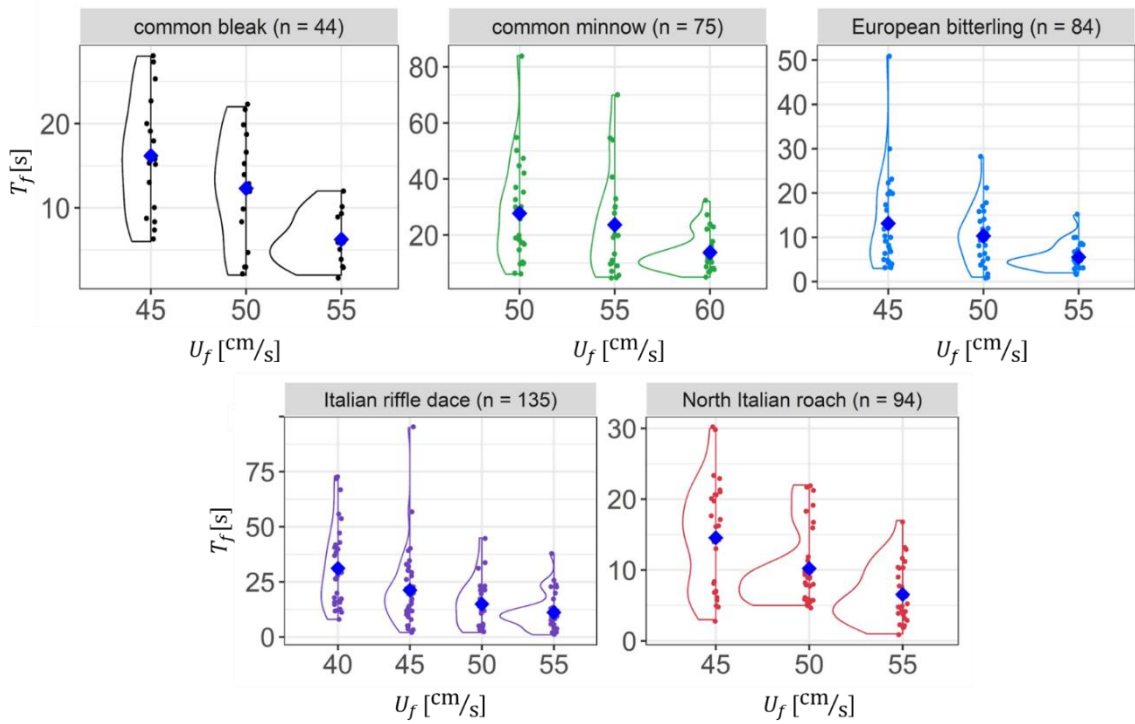


Figure 4.3 Kernel Density Estimation (KDE) of time-to-fatigue ( $T_f$ ) against flow velocity  $U_f$  for the best fit subsampled group (with the highest reliability index value) for the five fish species. Blue diamonds mark the mean time-to-fatigue  $\bar{T}_f$  at each tested flow velocity.

When plotted in logarithmic coordinates data pertaining to  $\bar{T}_f$  vs  $U_f$  and  $\overline{T_f^2}$  vs  $U_f$  plots, follow straight lines with slopes (which represent the exponent of the power law in linear coordinates) that are in reasonably good agreement with theoretical predictions. This is confirmed by Figure 4.4, which reports, as an example, results taken from the subsampled group with the highest *Rel*.

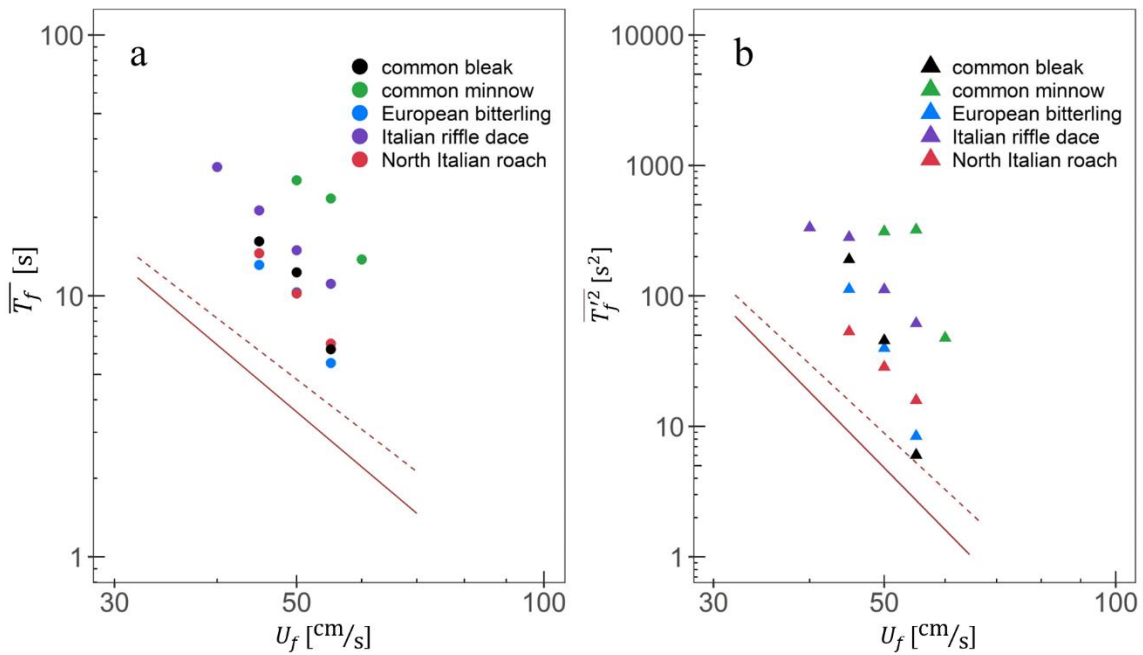


Figure 4.4 Data for time-to-fatigue mean  $\bar{T}_f$  (panel (a)) and variance  $\overline{T}_f'^2$  (panel (b)) versus flow velocity  $U_f$  for the subsampled group with the highest Reliability Index ( $ReI$ ) value. Different colours correspond to different fish species as specified in the legend. Dashed and solid grey lines have slope values calculated from the lower and upper limit of  $\beta$  i.e. 1.73 and 2.0, respectively, and are plotted to guide reader's eye serving as a benchmark for slope comparison with experimental data (Note: the two lines are not empirically fitted fatigue curves). In plot (a), the dashed grey line has a slope of  $-(\beta + 1) = -2.73$ , whereas the solid grey line has a slope of  $-3$ . Similarly, in plot (b), the dashed grey line has a slope of  $-(\beta + 1) = -5.46$ , whereas the solid grey line has a slope of  $-6$ .

A more comprehensive view of the results is provided by Figure 4.5, which reports the estimates of the scaling exponent ( $\beta$ ) obtained from the linear regression analysis of  $\ln(\bar{T}_f)$  vs  $\ln(U_f)$  (panel a) and  $\ln(\overline{T}_f'^2)$  vs  $\ln(U_f)$  (panel b) for all fish species and subsampled groups. For all subsampled groups, there was no effect of fish length on empirical data fitting. The majority of subsampled groups showed a non-significant relationship between time-to-fatigue and flow velocity, likely due to insufficient data, and were consequently omitted from the results (Appendix B). For subsamples with significant regression outcomes, results indicate that empirical estimates of  $\beta$  closely match the theoretically predicted range (yellow band in Figure 4.5) for Italian riffle dace (panel a) and both Italian riffle dace and North Italian roach (panel b), respectively. Interestingly, data points pertaining to low values of  $ReI$  generally display a larger mismatch with theoretical predictions and overall, such a mismatch gradually diminishes with increasing values of  $ReI$ .

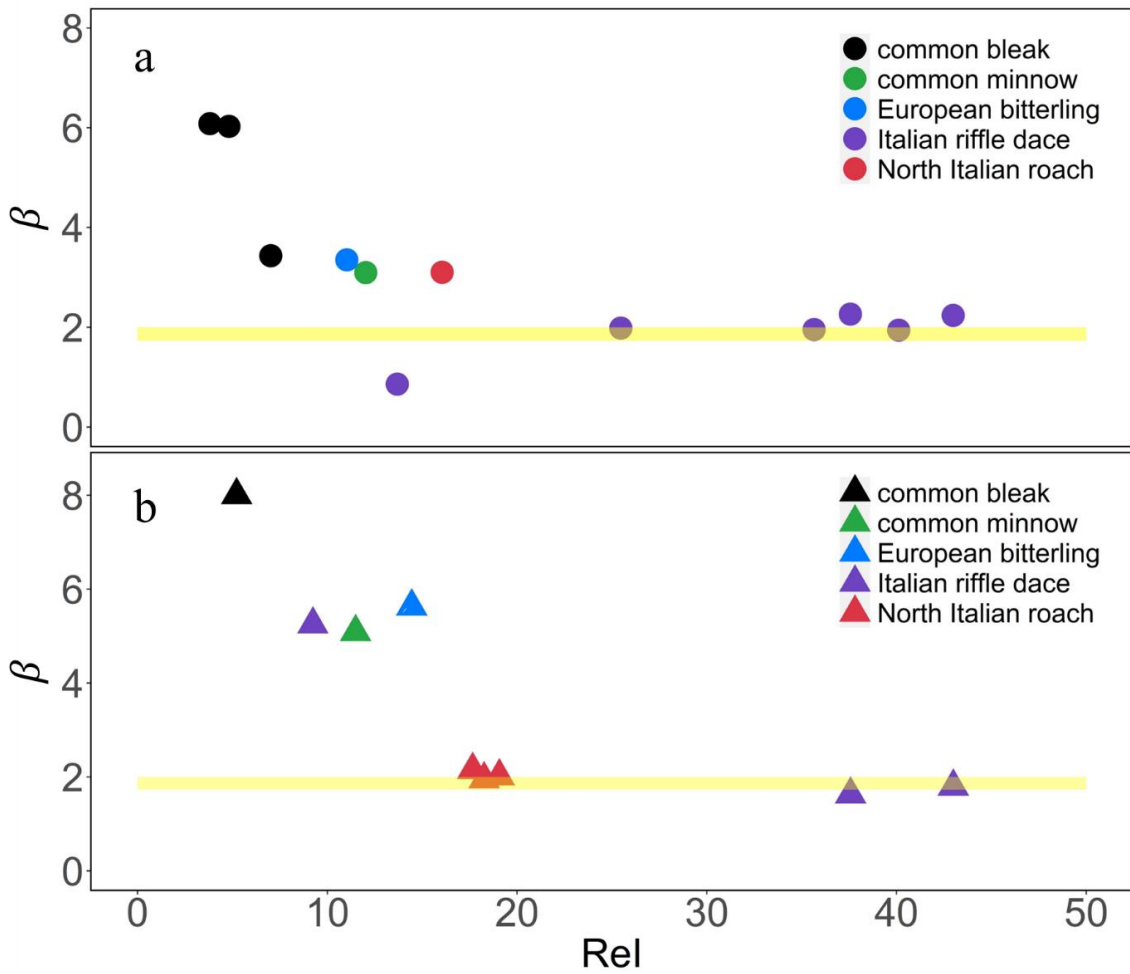


Figure 4.5 Empirical estimates of scaling exponent  $\beta$  obtained from the linear regression analysis between (a)  $\ln(\bar{T}_f)$  and  $\ln(U_f)$  and (b)  $\ln(\bar{T}_f^2)$  and  $\ln(U_f)$  plotted against reliability index (Rel), as defined in Eq. 4.14. The yellow band is the theoretically predicted range of scaling exponent  $\beta$ , i.e. [1-73-2.0]. Each different colour corresponds to a different fish species as specified in the legend. The repeated data points with the same colour indicate the  $\beta$  values obtained from the fitting of more than one subsampled group related to one single fish species.

## 4.6 Discussion

This paper presents a theoretical approach that predicts scaling laws linking statistical properties of time-to-fatigue  $T_f$  to the mean relative velocity between water and fish, here estimated as  $U_f$ . In particular, theory predicts that  $\bar{T}_f \sim U_r^{-(\beta+1)}$  and  $\overline{T_f'^k} \sim U_r^{-k(\beta+1)}$ , and arguments based on state of the art fish-drag hydrodynamics, indicate that the scaling exponent  $\beta$  is constrained between 1.73 and 2.00; the overbar-symbol refers to an averaging operator associated with a population of fish of the same species and size, and swimming in water at a given temperature and velocity  $U_f$ ; the prime symbol identifies variations of  $T_f$  around the mean  $\bar{T}_f$  while  $k$  is the moment order and can be any integer greater than one. Dedicated fixed velocity experiments were conducted on five Cypriniformes, and time-to-fatigue data obtained were used to test the proposed scaling relations for time-to-fatigue mean  $\bar{T}_f$  and variance  $\overline{T_f'^2}$ , by comparing theoretically predicted values of  $\beta$  with those estimated from empirical data. Data indicates that empirical estimates of the scaling exponent  $\beta$  agree well with theoretical predictions for Italian riffle dace (as estimated from  $\bar{T}_f$  data) or Italian riffle dace and North Italian roach (as estimated from  $\overline{T_f'^2}$  data). Overall, deviations from theoretical predictions tend to reduce noticeably with increasing the Reliability Index (*Rel*; Figure 4.5). This encouragingly supports the validity of the proposed scaling laws, however, it is also true that the trend is only clearly noticeable for Italian riffle dace, for which data span a large range of *Rel*. Since data for the other four species do not cover the same span (in some cases only one data point is available), there is also a possibility that the extent of the deviations may be species-specific.

It is noteworthy to observe that, at low values of *Rel*, deviations are not uniformly distributed around the theoretically predicted range but biased towards higher values (i.e. mostly larger than 2). This could be explained as follows. The proposed scaling laws apply to fish swimming in the burst range, i.e. in purely anaerobic conditions but, as mentioned in the results section, it is possible that some fish employed both anaerobic and aerobic processes during the trials. Clearly, the probability that individual fish swim using aerobic process reduces with increasing  $U_f$ , meaning that  $T_f$ -outliers (i.e. large values of  $T_f$  caused by aerobic swimming) affect estimates of  $\bar{T}_f$  and  $\overline{T_f'^2}$  more in the lower range of  $U_f$  than in the higher. Since these outliers contribute to increase both  $\bar{T}_f$  and  $\overline{T_f'^2}$ , they also contribute to enhance the steepness of  $\bar{T}_f$  and  $\overline{T_f'^2}$  vs  $U_f$  curves, and hence the values of  $\beta$  estimated from the regression analysis.

The theoretical results reported here, can have important practical implications. Firstly, they offer advantages for experimental research aiming at quantifying fatigue in fish. In this respect, note that equations 4.5 and 4.9 can be rewritten, in more general form as

$$\bar{T}_f = \alpha_1 U_r^{-(\beta+1)} \quad [4.11]$$

$$\overline{T_f^k} = \alpha_k U_r^{-k(\beta+1)}, \quad [4.12]$$

where  $\alpha_1$  and  $\alpha_k$  are scaling functions which depend mainly on fish species, size, and water temperature and  $\beta$ , as discussed, is a well-constrained parameter dictated by theory. This means that, in future studies, it will be possible to explore the statistical behaviour of  $T_f$  at only one velocity  $U_f$  to retrieve the scaling functions  $\alpha_1$  and  $\alpha_k$ , hence significantly reducing experimental efforts devoted to the investigation of endurance in burst swimming. Given the enormous biodiversity reported for fish worldwide and the overwhelming variability in swimming performance associated to it, this result is particularly relevant. Secondly, equation 4.11 represents a useful tool for fishways' design and management as it allows to derive the maximum distance a fish can swim before becoming fatigued (Castro-Santos, 2005; Katopodis, 1992; Katopodis & Gervais, 2012, 2016). Recalling the work by Castro-Santos (2005) and Katopodis (1992), the maximum distance a fish can swim before fatiguing can be defined as  $D_s = U_g \overline{T_f} = (U_r - U_f) \overline{T_f}$ , where  $U_g = U_r - U_f$  is the fish ground speed. Employing Eq. 4.11 for  $\overline{T_f}$  leads to a function  $D_s(U_r)$  that displays a maximum  $D_{smax}$  at an optimal relative velocity  $U_{ropt} = U_f (1 + \frac{1}{\beta})$  and hence an optimal ground speed

$$U_{gopt} = \frac{U_f}{\beta}. \quad [4.13]$$

Eq. 4.13 indicates that, in the burst swimming range, the maximum distance that a fish can travel, is reached at swimming ground speeds of about half of the water flow velocity (recall  $\beta \approx 2$ ). This is clearly true only if fish are fit enough to reach such velocity. If not, the maximum distance is reached at the maximum ground speed they are capable to swim at.

At optimal velocity, the maximum swimming distance can be estimated as

$$D_{smax} = \frac{\alpha}{\beta} U_f^{-\beta} \left(1 + \frac{1}{\beta}\right)^{-\beta-1}, \quad [4.14]$$

which represents a very important design parameter being the maximum allowed length for a fish passage system (Castro-Santos, 2005; Katopodis, 1992; Nikora et al., 2003).

Lastly, we propose that Eq. 4.14 might offer some biomimicry-inspired insights for the control of underwater robotics, which are now being employed for a plethora of applications (Cui et al., 2023). Analogously to a fish swimming anaerobically, an underwater robot stops moving (i.e. reaches fatigue) when running out of the energy provided by a battery. Since the theoretical analysis presented in sections 4.3.1 and 4.3.2 is applicable to any fully submerged solid body that is self-propelled by limited energy resources, Eq. 4.13, which is a direct consequence of this analysis, indicates that an underwater robot can maximise cruising distances when swimming at ground speeds that are half of the opposing fluid velocity. Note that underwater robots cannot be charged during operations, therefore these insights offer a simple strategy to optimise energy

consumption in opposing moving waters, as often required in freshwater and marine environments (Li et al., 2023).

In conclusion, the main outcome of the present paper is a set of theoretically derived scaling laws linking statistical properties of  $T_f$  to  $U_r$  for burst swimming fish. These laws are relevant for applications in fishways' design and to develop bioinspired underwater-robot control. Results from a new and large experimental dataset of five fish species support the proposed theory, while calling for more experiments from a wider range of fish species and sizes to be carried out, to further establish the general applicability of the proposed scaling laws.

## References

- Aedo, J. R., Otto, K. R., Rader, R. B., Hotchkiss, R. H., & Belk, M. C. (2021). Size Matters, but Species Do Not: No Evidence for Species-Specific Swimming Performance in Co-Occurring Great Basin Stream Fishes. *Water*, 13(18), 2570. <https://doi.org/10.3390/w13182570>
- Anderson, E. J., McGillis, W. R., & Grosenbaugh, M. A. (2001). The boundary layer of swimming fish. *Journal of Experimental Biology*, 22.
- Ashraf, M. U., Nyqvist, D., Comoglio, C., & Manes, C. (2024a). The effect of in-flume habituation time and fish behaviour on estimated swimming performance. *Journal of Ecohydraulics*. <https://doi.org/10.1080/24705357.2024.2306411>
- Ashraf, M. U., Nyqvist, D., Comoglio, C., Mozzi, G., Domenici, P., Marion, A., & Manes, C. (2024b). Fish Swimming Performance: Effect of Flume Length and Different Fatigue Definitions. In M. B. Kalinowska, M. M. Mrokowska, & P. M. Rowiński (Eds.), *Advances in Hydraulic Research* (pp. 1–11). Springer Nature Switzerland. [https://doi.org/10.1007/978-3-031-56093-4\\_1](https://doi.org/10.1007/978-3-031-56093-4_1)
- Bainbridge, R. (1958). The Speed of Swimming of Fish as Related to Size and to the Frequency and Amplitude of the Tail Beat. *Journal of Experimental Biology*, 35(1), 109–133. <https://doi.org/10.1242/jeb.35.1.109>
- Bainbridge, R. (1960). Speed and Stamina in Three Fish. *Journal of Experimental Biology*, 37(1), 129–153. <https://doi.org/10.1242/jeb.37.1.129>
- Barbarossa, V., Schmitt, R. J. P., Huijbregts, M. A. J., Zarfl, C., King, H., & Schipper, A. M. (2020). Impacts of current and future large dams on the geographic range connectivity of freshwater fish worldwide. *Proceedings of the National Academy of Sciences*, 117(7), 3648–3655. <https://doi.org/10.1073/pnas.1912776117>
- Beamish, F. W. H. (1978). *Fish Physiology* (W. S. Hoar & D. J. Randall, Eds.; 1st ed., Vol. 7). Academic Press, London.
- Beamish, F. W. H., Howlett, J. C., & Medland, T. E. (1989). Impact of Diet on Metabolism and Swimming Performance in Juvenile Lake Trout, *Salvelinus namaycush*. *Canadian Journal of Fisheries and Aquatic Sciences*, 46(3), 384–388. <https://doi.org/10.1139/f89-050>
- Belletti, B., Garcia De Leaniz, C., Jones, J., Bizzi, S., Börger, L., Segura, G., Castelletti, A., Van De Bund, W., Aarestrup, K., Barry, J., Belka, K., Berkhuisen, A., Birnie-Gauvin, K., Bussetini, M., Carolli, M., Consuegra, S., Dopico, E., Feierfeil, T., Fernández, S., ... Zalewski, M. (2020). More than one million barriers fragment Europe's rivers. *Nature*, 588(7838), 436–441. <https://doi.org/10.1038/s41586-020-3005-2>
- Brett, J. R. (1964). The Respiratory Metabolism and Swimming Performance of Young Sockeye Salmon. *Journal of the Fisheries Research Board of Canada*, 21(5), 1183–1226. <https://doi.org/10.1139/f64-103>



Burnett, N. J., Hinch, S. G., Braun, D. C., Casselman, M. T., Middleton, C. T., Wilson, S. M., & Cooke, S. J. (2014). Burst Swimming in Areas of High Flow: Delayed Consequences of Anaerobiosis in Wild Adult Sockeye Salmon. *Physiological and Biochemical Zoology*, 87(5), 587–598. <https://doi.org/10.1086/677219>

Castro-Santos, T. (2002). Swimming performance of upstream migrant fishes: New methods, new perspectives [University of Massachusetts Amherst]. <https://scholarworks.umass.edu/dissertations/AAI3056208/>

Castro-Santos, T. (2005). Optimal swim speeds for traversing velocity barriers: An analysis of volitional high-speed swimming behavior of migratory fishes. *Journal of Experimental Biology*, 208(3), 421–432. <https://doi.org/10.1242/jeb.01380>

Castro-Santos, T., Goerig, E., He, P., & Lauder, G. V. (2022). Applied aspects of locomotion and biomechanics. In *Fish Physiology* (Vol. 39, pp. 91–140). Elsevier. <https://doi.org/10.1016/bs.fp.2022.04.003>

Castro-Santos, T., Sanz-Ronda, F. J., & Ruiz-Legazpi, J. (2013). Breaking the speed limit—Comparative sprinting performance of brook trout ( *Salvelinus fontinalis* ) and brown trout ( *Salmo trutta* ). *Canadian Journal of Fisheries and Aquatic Sciences*, 70(2), 280–293. <https://doi.org/10.1139/cjfas-2012-0186>

Cui, Z., Li, L., Wang, Y., Zhong, Z., & Li, J. (2023). Review of research and control technology of underwater bionic robots. *Intelligent Marine Technology and Systems*, 1(1), 7. <https://doi.org/10.1007/s44295-023-00010-3>

Deslauriers, D. (2011). Factors influencing swimming performance and behaviour of the shortnose sturgeon (*Acipenser brevirostrum*). University of New Brunswick, Saint John.

Domenici, P., & Blake, R. (1997). The kinematics and performance of fish fast-start swimming. *Journal of Experimental Biology*, 200(8), 1165–1178. <https://doi.org/10.1242/jeb.200.8.1165>

Eloy, C. (2012). Optimal Strouhal number for swimming animals. *Journal of Fluids and Structures*, 30, 205–218. <https://doi.org/10.1016/j.jfluidstructs.2012.02.008>

Farrell, A. P., & Steffensen, J. F. (1987). An analysis of the energetic cost of the branchial and cardiac pumps during sustained swimming in trout. *Fish Physiology and Biochemistry*, 4.

Freyhof, J., & Kottelat, M. (2007). Handbook of European freshwater fishes. <https://portals.iucn.org/library/node/9068>

Gazzola, M., Argentina, M., & Mahadevan, L. (2014). Scaling macroscopic aquatic locomotion. *Nature Physics*, 10(10), 758–761. <https://doi.org/10.1038/nphys3078>

Goerig, E., & Castro-Santos, T. (2017). Is motivation important to brook trout passage through culverts? *Canadian Journal of Fisheries and Aquatic Sciences*, 74(6), 885–893. <https://doi.org/10.1139/cjfas-2016-0237>

Gregory, T. R., & Wood, C. M. (1999). The Effects of Chronic Plasma Cortisol Elevation on the Feeding Behaviour, Growth, Competitive Ability, and Swimming Performance of Juvenile Rainbow Trout. *Physiological and Biochemical Zoology*, 72(3), 286–295. <https://doi.org/10.1086/316673>

Hammer, C. (1995). Fatigue and exercise tests with fish. *Comparative Biochemistry and Physiology Part A: Physiology*, 112(1), 1–20. [https://doi.org/10.1016/0300-9629\(95\)00060-K](https://doi.org/10.1016/0300-9629(95)00060-K)

Hammill, E., Wilson, R. S., & Johnston, I. A. (2004). Sustained swimming performance and muscle structure are altered by thermal acclimation in male mosquitofish. *Journal of Thermal Biology*, 29(4–5), 251–257. <https://doi.org/10.1016/j.jtherbio.2004.04.002>

Haro, A., Castro-Santos, T., Noreika, J., & Odeh, M. (2004). Swimming performance of upstream migrant fishes in open-channel flow: A new approach to predicting passage through velocity barriers. *Canadian Journal of Fisheries and Aquatic Sciences*, 61(9), 1590–1601. <https://doi.org/10.1139/f04-093>

Heuer, R. M., Stieglitz, J. D., Pasparakis, C., Enochs, I. C., Benetti, D. D., & Grosell, M. (2021). The Effects of Temperature Acclimation on Swimming Performance in the Pelagic Mahi-Mahi (*Coryphaena hippurus*). *Frontiers in Marine Science*, 8, 654276. <https://doi.org/10.3389/fmars.2021.654276>

Hvas, M., Folkedal, O., & Oppedal, F. (2021). Fish welfare in offshore salmon aquaculture. *Reviews in Aquaculture*, 13(2), 836–852. <https://doi.org/10.1111/raq.12501>

IUCN. 2023. The IUCN Red List of Threatened Species. Version 2023-1. <https://www.iucnredlist.org>.

Jain, K. E., Birtwell, I. K., & Farrell, A. P. (1998). Repeat swimming performance of mature sockeye salmon following a brief recovery period: A proposed measure of fish health and water quality. *Canadian Journal of Zoology*, 76(8), 1488–1496. <https://doi.org/10.1139/z98-079>

Jerde, C. L., Kraskura, E. J., Eliason, E. J., Csik, S. R., Stier, A. C., & Taper, M. L. (2019). Strong Evidence for an Intraspecific Metabolic Scaling Coefficient Near 0.89 in Fish. *Frontiers in Physiology*, 10.

Jones, P. E., Svendsen, J. C., Börger, L., Champneys, T., Consuegra, S., Jones, J. A. H., & Garcia De Leaniz, C. (2020). One size does not fit all: Inter- and intraspecific variation in the swimming performance of contrasting freshwater fish. *Conservation Physiology*, 8(1), coaa126. <https://doi.org/10.1093/conphys/coaa126>

Katopodis, C. (1992). Introduction to fishway design. Freshwater Institute, Central and Arctic Region Department of Fisheries and Oceans, Manitoba, Canada.

Katopodis, C., & Gervais, R. (2012). Ecohydraulic analysis of fish fatigue data. *River Research and Applications*, 28(4), 444–456. <https://doi.org/10.1002/rra.1566>

Katopodis, C., & Gervais, R. (2016). Fish swimming performance database and analyses. DFO Can. Sci. Advis. Sec. Res. Doc. 2016/002, vi + 550p.

Kolok, A. S. (1992). The Swimming Performances of Individual Largemouth Bass ( *Micropterus Salmoides* ) Are Repeatable. *Journal of Experimental Biology*, 170(1), 265–270. <https://doi.org/10.1242/jeb.170.1.265>

Li, J., Lin, X., Xu, Z., & Sun, J. (2017). Differences in swimming ability and its response to starvation among male and female *Gambusia affinis*. *Biology Open*, bio.022822. <https://doi.org/10.1242/bio.022822>

Li, X., & Yu, S. (2023). Comparison of biological swarm intelligence algorithms for AUVs for three-dimensional path planning in ocean currents' conditions. *Journal of Marine Science and Technology*, 28(4), 832–843. <https://doi.org/10.1007/s00773-023-00960-7>

Lighthill, M. J. (1960). Note on the swimming of slender fish. *Journal of Fluid Mechanics*, 9(2), 305–317. <https://doi.org/10.1017/S0022112060001110>

Lighthill, M. J. (1969). Hydromechanics of Aquatic Animal Propulsion. *Annual Review of Fluid Mechanics*, 1(1), 413–446. <https://doi.org/10.1146/annurev.fl.01.010169.002213>

Lighthill, M. J. (1970). Aquatic animal propulsion of high hydromechanical efficiency. *Journal of Fluid Mechanics*, 44(02), 265. <https://doi.org/10.1017/S0022112070001830>

Lighthill, M. J. (1971). Large-amplitude elongated-body theory of fish locomotion. *Proceedings of the Royal Society of London. Series B. Biological Sciences*, 179(1055), 125–138. <https://doi.org/10.1098/rspb.1971.0085>

Marras, S., Claireaux, G., McKenzie, D. J., & Nelson, J. A. (2010). Individual variation and repeatability in aerobic and anaerobic swimming performance of European sea bass, *Dicentrarchus labrax*. *Journal of Experimental Biology*, 213(1), 26–32. <https://doi.org/10.1242/jeb.032136>

Nikora, V. I., Aberle, J., Biggs, B. J. F., Jowett, I. G., & Sykes, J. R. E. (2003). Effects of fish size, time-to-fatigue and turbulence on swimming performance: A case study of *Galaxias maculatus* : SWIMMING PERFORMANCE OF INANGA. *Journal of Fish Biology*, 63(6), 1365–1382. <https://doi.org/10.1111/j.1095-8649.2003.00241.x>

Nyqvist, D., Schiavon, A., Candiotta, A., Mozzi, G., Eggers, F., & Comoglio, C. (2023). PIT -tagging Italian spined loach ( *COBITIS BILINEATA* ): Methodology, survival and behavioural effects. *Journal of Fish Biology*, 102(3), 575–580. <https://doi.org/10.1111/jfb.15289>

Peake, S., McKinley, R. S., & Scruton, D. A. (1997). Swimming performance of various freshwater Newfoundland salmonids relative to habitat selection and fishway design. *Journal of Fish Biology*, 51(4), 710–723. <https://doi.org/10.1111/j.1095-8649.1997.tb01993.x>

Penghan, L.-Y., Pang, X., & Fu, S.-J. (2016). The effects of starvation on fast-start escape and constant acceleration swimming performance in rose bitterling (*Rhodeus ocellatus*) at two acclimation temperatures. *Fish Physiology and Biochemistry*, 42(3), 909–918. <https://doi.org/10.1007/s10695-015-0184-0>

Plew, D. R., Nikora, V. I., Larned, S. T., Sykes, J. R. E., & Cooper, G. G. (2007). Fish swimming speed variability at constant flow: *Galaxias maculatus*. *New Zealand Journal of Marine and Freshwater Research*, 41(2), 185–195. <https://doi.org/10.1080/00288330709509907>

Quintella, B. R., Mateus, C. S., Costa, J. L., Domingos, I., & Almeida, P. R. (2010). Critical swimming speed of yellow- and silver-phase European eel (*Anguilla anguilla*, L.): Critical swimming speed of yellow- and silver-phase European eel. *Journal of Applied Ichthyology*, 26(3), 432–435. <https://doi.org/10.1111/j.1439-0426.2010.01457.x>

Reidy, S. P., Kerr, S. R., & Nelson, J. A. (2000). Aerobic and Anaerobic Swimming Performance of Individual Atlantic Cod. *Journal of Experimental Biology*, 203(2), 347–357. <https://doi.org/10.1242/jeb.203.2.347>

Saadat, M., Fish, F. E., Domel, A. G., Di Santo, V., Lauder, G. V., & Haj-Hariri, H. (2017). On the rules for aquatic locomotion. *Physical Review Fluids*, 2(8), 083102. <https://doi.org/10.1103/PhysRevFluids.2.083102>

Schiavon, A., Comoglio, C., Candiotta, A., Hölker, F., Ashraf, M. U., & Nyqvist, D. (2023). Survival and swimming performance of a small-sized Cypriniformes (*Telestes muticellus*) tagged with passive integrated transponders. *Journal of Limnology*, 82. <https://doi.org/10.4081/jlimnol.2023.2129>

Schneider, E. V., Hasler, C. T., & Suski, C. D. (2019). Swimming performance of a freshwater fish during exposure to high carbon dioxide. *Environmental Science and Pollution Research*, 26(4), 3447–3454. <https://doi.org/10.1007/s11356-018-3849-2>

Silva, A. T., Lucas, M. C., Castro-Santos, T., Katopodis, C., Baumgartner, L. J., Thiem, J. D., Aarestrup, K., Pompeu, P. S., O'Brien, G. C., Braun, D. C., Burnett, N. J., Zhu, D. Z., Fjeldstad, H.-P., Forseth, T., Rajaratnam, N., Williams, J. G., & Cooke, S. J. (2018). The future of fish passage science, engineering, and practice. *Fish and Fisheries*, 19(2), 340–362. <https://doi.org/10.1111/faf.12258>

Taylor, E. B., & McPhail, J. D. (1985). Burst Swimming and Size-Related Predation of Newly Emerged Coho Salmon *Oncorhynchus kisutch*. *Transactions of the American Fisheries Society*, 114(4), 546–551. [https://doi.org/10.1577/1548-8659\(1985\)114<546:BSASPO>2.0.CO;2](https://doi.org/10.1577/1548-8659(1985)114<546:BSASPO>2.0.CO;2)

Tudorache, C., O'Keefe, R. A., & Benfey, T. J. (2010a). Flume length and post-exercise impingement affect anaerobic metabolism in brook charr *Salvelinus fontinalis*. *Journal of Fish Biology*, 76(3), 729–733. <https://doi.org/10.1111/j.1095-8649.2009.02513.x>

Tudorache, C., O'Keefe, R. A., & Benfey, T. J. (2010b). The effect of temperature and ammonia exposure on swimming performance of brook charr (*Salvelinus fontinalis*).

Comparative Biochemistry and Physiology Part A: Molecular & Integrative Physiology, 156(4), 523–528. <https://doi.org/10.1016/j.cbpa.2010.04.010>

Tudorache, C., Viaene, P., Blust, R., Vereecken, H., & De Boeck, G. (2008). A comparison of swimming capacity and energy use in seven European freshwater fish species. *Ecology of Freshwater Fish*, 17(2), 284–291. <https://doi.org/10.1111/j.1600-0633.2007.00280.x>

Veza, P., Libardoni, F., Manes, C., Tsuzaki, T., Bertoldi, W., & Kemp, P. S. (2020). Rethinking swimming performance tests for bottom-dwelling fish: The case of European glass eel (*Anguilla anguilla*). *Scientific Reports*, 10(1), 16416. <https://doi.org/10.1038/s41598-020-72957-w>

Videler, J. J. (1993). *Fish Swimming*. Springer Netherlands. <https://doi.org/10.1007/978-94-011-1580-3>

Videler, J. J., & Wardle, C. S. (1991). Fish swimming stride by stride: Speed limits and endurance. *Reviews in Fish Biology and Fisheries*, 1(1), 23–40. <https://doi.org/10.1007/BF00042660>

Wardle, C. S. (1975). Limit of fish swimming speed. *Nature*, 255(5511), 725–727. <https://doi.org/10.1038/255725a0>

Watson, J., Goodrich, H., Cramp, R., Gordos, M., Yan, Y., Ward, P., & Franklin, C. (2019). Swimming performance traits of twenty-one Australian fish species: A fish passage management tool for use in modified freshwater systems. <https://doi.org/10.1101/861898>

Webb, P. (1975). Hydrodynamics and energetics of fish propulsion. *Bulletin of the fisheries Research Board of Canada* 190, 1-156.

## **Chapter 5**

### **Exploring Fish-Velocity Statistics in Burst Swimming Activity Level**

## 5.1 Abstract

Intermittent swimming, also referred to as burst-and-coast behaviour, is a commonly employed type of locomotion observed in various fish species. Several studies have linked this behaviour with specific advantages, including reduced energy expenditure, stabilised visual field, and enhanced sensing ability. However, these studies are limited to stationary or slow-moving water conditions, and little is known about the unsteady swimming patterns that fish may adopt, if any, in rapidly moving waters. Moreover, although fluctuations in fish velocity are associated with increased energy expenditure and are considered an additional component of swimming performance, very few studies have focused on examining these variations to date. In the present study, we address these knowledge gaps by exploring swimming velocity of juvenile Italian riffle dace (*Telestes muticellus*) at four different flow velocities ( $U_f$ ), in burst swimming range. In particular, we study the maximum fish velocity ( $U_{max}$ ) and fluctuations in fish velocity at constant  $U_f$ . The results suggest that both  $U_{max}$  and fluctuations in fish velocity increase with increasing  $U_f$  up to a certain threshold, beyond which they plateau. Additionally, power spectra analysis of fish velocity signal uncovered periodic swimming patterns characterised by a sharp peak at a frequency of 1 Hz, attributed to fish reaction time. Also, a consistent slope in the power spectra of fish velocity is observed, which remained independent of flow velocity and unexplained.

## 5.2 Introduction

Fish swimming performance has important implications for activities such as feeding, growth, migration, habitat selection, predator-prey interaction, competition, and survival (Beamish, 1978; Videler, 1993). Various attributes of fish swimming performance such as swimming velocities, energy expenditure, time-to-fatigue, and manoeuvrability are interlinked and in turn define the fish's ability to thrive in nature (Domenici & Kapoor, 2010; Videler, 1993).

Increasing velocity and fixed velocity tests are two most commonly used testing methodologies to estimate different metrics of fish swimming performance (Beamish, 1978; Brett, 1964; Hammer, 1995). In increasing velocity tests, the flow velocity  $U_f$  is increased progressively at fixed time interval  $\Delta t$  until the fish fatigues to compute the so-called critical velocity  $U_{crit}$ . In fixed velocity tests, instead, a fish is forced to swim at a steady flow velocity  $U_f$  until fatigued (Beamish, 1978; Hammer, 1995). Time-to-fatigue  $T_f$  is measured as a performance indicator in fixed velocity tests defining three activity levels: sustained, prolonged, and burst swimming (Hammer, 1995). In sustained swimming, fish employ only red muscles and aerobic processes and therefore, theoretically, can swim indefinitely. Prolonged swimming is simultaneously powered by red and white muscles, eventually leading to fatigue. Lastly, burst swimming activities rely entirely on white muscles and anaerobic processes resulting in fish fatigue within a few tens of seconds.

For numerous fish species, the ability to swim in short, rapid bursts is not only essential for their ongoing health, but also for their very survival (Beamish, 1978). This is particularly true for those species that need to navigate rapidly flowing rivers during their migration. Their successful journey may ultimately depend on their ability to perform burst swimming (Beamish, 1978; Burnett et al., 2014). While average burst or peak swimming velocities are often reported and are useful indicators of burst performance, they fail to provide information about variability in burst swimming velocities (Plew et al., 2007). The fluctuations in fish velocity, particularly in burst swimming velocities, could significantly influence the energy needed to resist or cross fast flowing water stream over a certain duration (Burnett et al., 2014; Taylor & McPhail, 1985). In burst swimming, Reynolds number is typically of the order  $10^3$  and the power required by fish to overcome drag can be considered, as a first approximation, proportional to the velocity cubed, (Vogel, 1994), suggesting that the effects of even a small increase in velocity can have a significant effect in terms of energy expenditure.

Intermittent swimming, also commonly referred to as burst-and-coast, behaviour is frequently observed in various fish species consisting of cyclic bursts of forward movements followed by a coasting or gliding phase in which the body is kept straight and motionless however still moving in the forward direction (Videler, 1993; Videler & Weihs, 1982). Several studies have shown that, in comparison to continuous swimming, a burst-and-coast swimming pattern can reduce energy expenditure and enable fish to



cover a certain forward distance even during the coasting periods (Ribak et al., 2005; Videler & Weihs, 1982; Weihs, 1974). However this holds true only when the water flow velocity is very low or zero (Müller et al., 2000) because fish can exploit their inertia and move forward even without tail beating. It is logical to assume that when the fish is exposed to very high flow velocities (as when trying to overcome velocity barriers during migration) the propulsion generated by the fish's undulating body would not permit it to glide forward on its own inertia. Instead, the swift current will carry the fish downstream, leading to a (potential) reduction in the distance gained during the bursting phase. Therefore, burst-and-coast swimming makes little sense in fast flowing waters as far as optimising travel distances are concerned.

In the last few decades, significant efforts have been made to understand intermittent fish swimming motion using analytical (Videler & Weihs, 1982; Weihs, 1974), experimental (Floryan et al., 2017; Wu et al., 2007), and numerical studies (Chung, 2009). While most published literature agrees that one of the primary reasons fish employ intermittent swimming motion is to save energy, other studies attribute enhancement in sensory capabilities as the primary function of burst-coast swimming. In their study on tetra fish (*Hemigrammus bleheri*), I. Ashraf et al (2021) coupled experimental data, at flow velocities of 0.36-3 BL/s, with numerical simulations and found that the fish could theoretically expend less mechanical energy swimming continuously than intermittently. They suggested that the main benefit of intermittent swimming may not be energy conservation but rather stabilizing the visual field and improving sensing abilities as also highlighted in several other research works (Mogdans, 2019; Teyke, 1985; Windsor et al., 2008).

Despite the significant progress made in studying fish burst-and-coast and unsteady swimming behaviour (Blake, 1983; Müller et al., 2000; Tudorache et al., 2007), this wealth of knowledge is limited to the case of standing or slowly moving water and little is known about unsteady swimming patterns that fish adopts (if any) in rapidly moving waters. To bridge this knowledge gap, this paper aims to explore whether fish use any swimming patterns in fast moving water where they cannot benefit from a burst-and-coast behaviour to either minimise energy expenditure, stabilise the visual field, or enhance their sensory abilities. To accomplish this goal, we analyse the experimentally collected fish swimming velocity data in burst swimming activity level to investigate:

- i) the maximum fish velocity ( $U_{max}$ ) and its relation with flow velocity ( $U_f$ )
- ii) the variability of fish velocity ( $U_r$ ) for fish swimming continuously at constant  $U_f$
- iii) whether the  $U_r$  time series signal exhibits any periodicities (i.e. recurrent patterns such as burst-and-coast) at different flow velocities.

Systematic experiments were conducted using a fixed velocity testing protocol on *Telestes muticellus*, a small-sized riverine cyprinid (Freyhof & Kottelat, 2007).

## 5.3 Materials and Methods

### 5.3.1 Fish

Juvenile *Telestes muticellus* with an average fork length of 4.8 cm (standard deviation,  $sd \pm 0.4$  cm) and average mass of 1.4 g ( $sd \pm 0.3$  g) were captured using electrofishing from the Noce stream near Pinerolo, Italy (44°56'17.9 "N 7°23'09.1"E) and tested in May 2022. Fish were transferred to a hatchery facility in Porte di Pinerolo and were kept in spring-fed flow through holding tanks. All fish were habituated for 4 days before experimental trials.

A HOBO MX-2202 logger was used to record water temperature in the holding tanks at 10 minute intervals. Average recorded water temperature was 13.3 °C ( $sd \pm 0.4$  °C). All fish were fed daily using commercial aquaria fish pellets (Tetra TabiMin) and were starved at least 24 hours before testing to ensure post-absorptive state (Penghan et al., 2016). Throughout the experiments, no fish mortality was observed and fish appeared to be in good health.

### 5.3.2 Experimental protocol

An open channel recirculating hydraulic flume with a total flume length of 280 cm and a cross sectional area of 900 cm<sup>2</sup> (30 cm by 30 cm) was used to carry out experiments. For detailed description of the flume, please refer to Ashraf et al (2024). The swimming arena (flume length) was 60 cm and delimited by a flow straightener in the upstream direction and a fined meshed grid in the downstream direction. Swimming trials were recorded using two Sony AX43 handycams with a resolution of 1920x1080 pixels at 50 frames per second. The difference between the water temperature in the flume and the holding tanks was kept at less than 1°C to avoid any confounding effects of temperature change on swimming performance (Tudorache et al., 2010b; Vezza et al., 2020).

A total of 40 fish were tested using fixed velocity testing protocol. One fish was tested per trial and no fish was tested more than once. All fish were tested at burst swimming velocities, defined by flow velocities ( $U_f$ ) resulting in mean time-to-fatigue ( $\bar{T}_f$ ) no higher than 15 to 50 seconds (Beamish, 1978; Haro et al., 2004; Videler, 1993). Average cross-sectional flow velocities were computed by dividing the volume flow rate ( $Q$ ) by the test cross-sectional flume area ( $X$ ) as  $U_f = Q/X$ . The four test flow velocities (40, 45, 50, and 55 cms<sup>-1</sup> with 10 fish each) were selected based on preliminary trials resulting in  $\bar{T}_f$  well within the typical fatigue times associated with burst swimming activity level. At the beginning of each trial, fish were habituated for 5 min at 5 cms<sup>-1</sup> (Ashraf et al., 2024). The flow rate was increased manually following the habituation period to achieve the desired  $U_f$  value. Fish were allowed to swim at test flow velocity until fatigued. Fatigue was defined as fish resting on the downstream grid and not responding to tapping (Aedo et al., 2021; Heuer et al., 2021; Tudorache et al., 2010a; Videler & Wardle, 1991). A fish was tapped no more than three times. At the end of each

trial, fish were sedated in clove oil (Aroma Labs, Kalamazoo, MI, USA; approximately 0.2 ml clove oil / litre water), and measured for fork length [cm] and mass [g]. The study was performed in accordance with the Protection of Flora and Fauna Department of the Metropolitan City of Turin (authorization D.D. n.4457 of 29 October 2020).

### 5.3.3 Data analysis

#### 5.3.3.1 Computational Fluid Dynamics (CFD)

Flow velocities experienced by fish in forced performance tests are assumed to be identical to the average cross-sectional velocities (Nikora et al., 2003; Vezza et al., 2020). However it is well known that in channel flows or swim tunnels, the velocity fields are not uniform. For instance, lower velocities are present in the near-wall regions due to the presence of so-called boundary layers (Çengel & Cimbala, 2006). It is often reported that fish prefer to swim near the walls and corners of the channel during performance tests, presumably taking advantage of areas with slower velocities to conserve energy (Kern et al., 2018; Kerr et al., 2016; Newbold & Kemp, 2015; Vezza et al., 2020). Therefore, relying solely on averaged cross-sectional velocities, without accounting for flow field variations, may lead to an overestimation of the flow velocities experienced by fish, affecting the overall results. From hereafter, flow velocity and average cross sectional flow velocity are used as interchangeable terms and denoted by  $U_f$ .

Therefore, Computational Fluid Dynamics (CFD) models, using ANSYS Fluent (Canonsburg, Pennsylvania, USA) software, were used to provide a detailed description of the flow field variations in the test section of the flume for all four  $U_f$  values. This allowed to effectively represent the flow velocities experienced by fish in near-wall regions (i.e. bottom and side walls of the flume) and hence an accurate estimation of fish swimming velocities. Modelled flow velocities  $\vec{Z}(\bar{u}, \bar{v}, \bar{w})$ , where  $\bar{u}$ ,  $\bar{v}$ , and  $\bar{w}$  are the longitudinal, lateral, and vertical velocity components (overbar denotes time-averaging), were numerically computed at each node of the defined grid using hexahedral cells which subdivided the entire flow domain into finite elements. To accurately capture the flow velocities in boundary layers, so-called *inflation layers*—layers of cells with progressively increasing height—were employed in near-wall regions, producing a finer mesh near walls and a coarser mesh far from the walls. The selected mesh size reduced the computational effort as much as possible while producing outputs that were observed to be mesh-independent from dedicated tests. A k-epsilon ( $k$ - $\epsilon$ ) turbulence closure model was used where the value of turbulent kinetic energy ( $k$ ) was estimated from direct measurements of velocity fluctuations measured 5 cm from the upstream grid using Laser Doppler Anemometry (LDA by Dantec Dynamics). The order of magnitude of the turbulent dissipation rate  $\epsilon$  was estimated as  $\epsilon = U_f^3/l_{ms}$ , where  $U_f$  is the average cross-sectional flow velocity and  $l_{ms}$  is the upstream grid mesh size (6 mm) as the characteristic velocity and length scales, respectively (Vezza et al., 2020).

A mass flow inlet boundary condition was used at the inlet, as the volume discharge entering the flow domain was known. The free surface was modelled as a free slip plane and the outlet was set to an outflow boundary condition. The bottom and side walls were set as hydrodynamically smooth walls with no-slip condition.

### 5.3.3.2 LDA measurements and validation of CFD data

For all flow velocity treatments, single-point longitudinal flow velocities ( $u$ ) were measured using Laser Doppler Anemometry (LDA). Measurements were taken at four cross-sections located at a distance of 5, 15, 30 and 55 cm from the upstream grid and in the centre of each cross-section along a vertical column at two points: 0.5 and 5 cm (Figure 5.1). At each point (P1-P8; Figure 5.1), 500,000 measurements were taken at an average sampling frequency of no less than 800 Hz. Figure 5.2 shows a comparison between simulated and measured mean flow velocities with LDA for the treatment with  $U_f$  of 50  $\text{cm s}^{-1}$ . The agreement is very good, hence providing confidence that the simulated flow fields are representative of experimental conditions.

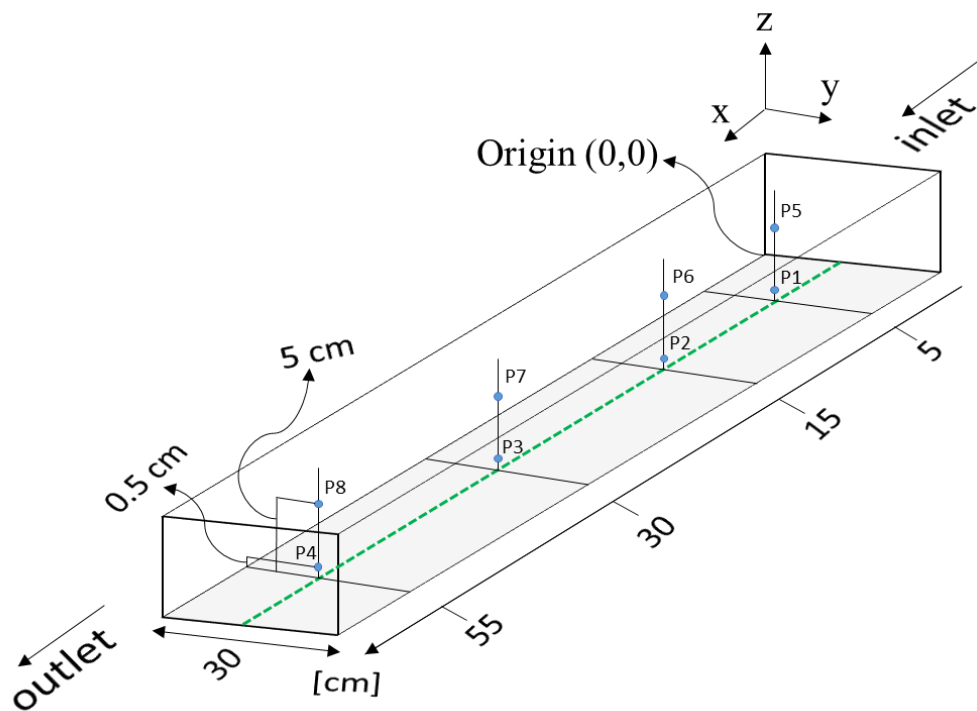


Figure 5.1 Sketch of the open channel flume with location of the points where longitudinal flow velocity measurement were carried out using LDA. The middle of the flume width is marked with a dashed green line. Points P1 to P4 are located at an elevation of 0.5 cm, while points P5 to P8 are located at an elevation of 5 cm from the bottom of the flume.

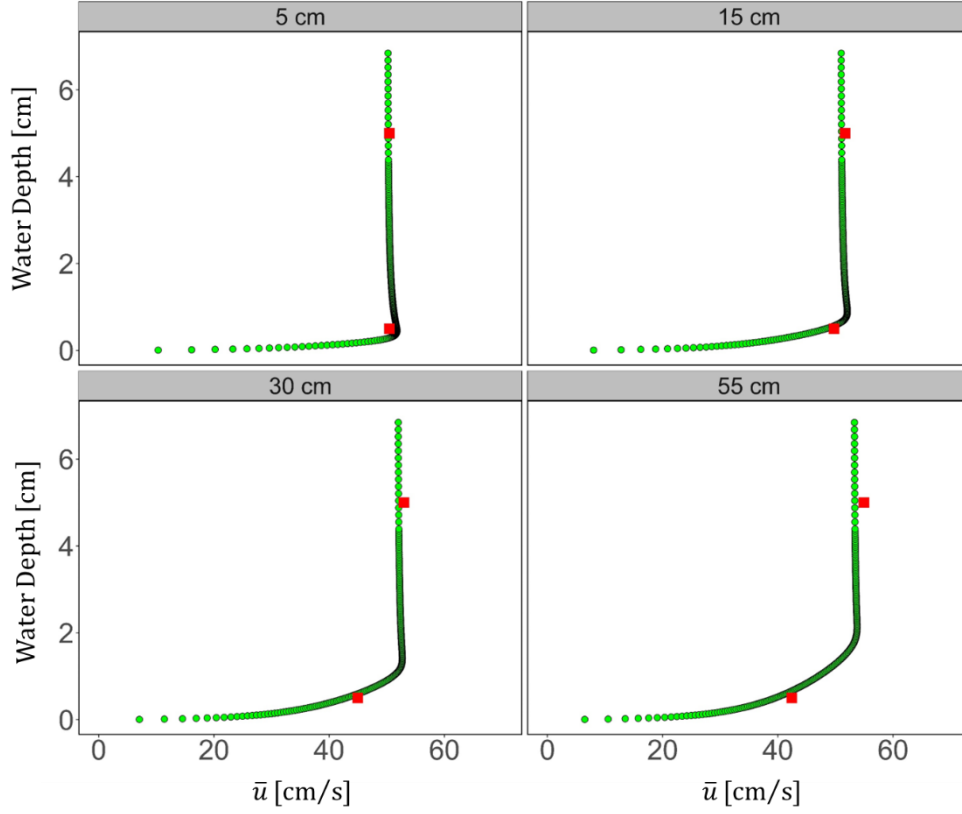


Figure 5.2 Validation of CFD simulated flow velocity data against LDA measurements for a treatment with an averaged cross-sectional flow velocity of  $50 \text{ cm s}^{-1}$ . Mean vertical flow velocity profiles were extracted from CFD data corresponding to the mid cross section of the simulated domain and at four cross sections located at 5, 15, 30, and 55 cm from the inlet. Red squares represent the mean of empirically measured longitudinal flow velocity values obtained using LDA.

### 5.3.3.3 Fish trajectories and swimming velocities

Fish swimming trajectories were reconstructed following the detection of fish's head position in each frame of the recorded video using a deep learning approach with a convolutional neural network (CNN) (Redmon et al., 2016). A detailed description of the tracking methodology is available in Mozzi et al (2024). The fish swam mostly near the bottom wall of the flume (Mozzi et al., 2024), therefore video footage was analysed in the horizontal plane only to obtain fish position over the longitudinal (i.e. aligned with the flow direction, and hereafter referred to as X) and lateral (hereafter referred to as Y) coordinate, whose origin was located at the bottom-left corner from the inlet (see Figure 5.1). For each video frame, two dimensional ground distance was calculated as  $D_{gi} = \sqrt{(X_i - X_{i-1})^2 + (Y_i - Y_{i-1})^2}$ , where  $i$  is the video frame of interest. For each video frame, fish ground velocity ( $U_g$ ) was computed by dividing  $D_g$  by the time interval between two consecutive video frames (0.02 seconds). It should be noted that  $D_g$  and  $U_g$  for the first video frame were set to zero.

Flow velocity data was extracted from CFD simulations for a two dimensional plane located 0.5 cm above the bottom wall. This depth aligns with the average swimming depth of fish, as observed from experiments. Fish-water relative velocity ( $U_r$ ) was determined for each video frame by adding the fish ground velocity ( $U_g$ ) to the

longitudinal flow velocity ( $\bar{u}$ ) value as obtained from CFD. Based on fish's position (X, Y),  $\bar{u}$  from CFD was estimated using bilinear interpolation based on surrounding velocity values at neighbouring nodes within a hexahedral mesh grid. The maximum swimming velocity ( $U_{max}$ ) reached by each individual fish was plotted using boxplots and compared across all flow velocity treatments using the Kruskal-Wallis test. To determine which of the four  $U_{max}$  differed significantly amongst different treatments, a post-hoc Dunn test was used. Moreover, at each  $U_f$  treatment, fish-water relative velocity ( $U_r$ ) distribution was plotted and the mean, standard deviation, skewness, and kurtosis were computed. Hereafter, the term “fish-water relative velocity” will be referred to simply as “fish velocity”, for the sake of clarity and simplicity.

#### 5.3.3.4 Power Spectral Density

Power Spectral Density (PSD) analysis was performed to interpret fish velocity time series signal in the frequency domain. This analysis was carried out separately for both longitudinal fish velocity ( $U_{rx}$ ) and lateral fish velocity ( $U_{ry}$ ) signals. In Matlab, the so-called Welch method was used to compute the PSD of each individual fish velocity signal using one single window (containing all values of fish velocity) resulting in two output vectors:  $S$  (PSD estimates) and  $f$  (frequencies). PSD for each treatment was then computed by averaging the PSD estimates of 10 individual fish using the binning method. According to the Nyquist theorem, the spectrum of fish velocity time series was resolved only up to 25 Hz (i.e. half the sampling frequency of 50 Hz as defined by the recorded video footage frame rate).

Similarly, PSD analysis was carried out on flow velocity data obtained empirically using LDA. In this case, the data was first resampled to obtain a fixed time interval of 1 ms for all measured flow velocities before computing the spectra. Number of windows in Welch method were set to 50 as it resulted in a robust and reasonably smooth spectrum.

For both flow and fish velocities, the frequency vector ( $f$ ) from the PSD was multiplied by the PSD estimates ( $S$ ) to create premultiplied spectra (a plot of  $S*f$  vs  $f$ ), plotted in log-linear coordinates. This is justified by the fact that premultiplied spectra are more effective than spectra to identify peaks associated with dominant modes in the signal (see e.g. Manes et al 2011)

## 5.4 Results

The distribution of mean longitudinal flow velocities  $\bar{u}$  was relatively uniform across the channel at various cross sections, with the exception of the areas close to the side and bottom walls, where the presence of a boundary layer caused  $\bar{u}$  to be significantly lower than in the central region (Figure 5.3). The thickness of the boundary layer increased with increasing downstream distance from the upstream grid, as shown in Figure 5.4, which displays a longitudinal cross section at the centre of the flume width (15 cm from either side wall) with velocity contours for treatment with an average cross-sectional flow velocity ( $U_f$ ) of  $50 \text{ cm s}^{-1}$ .

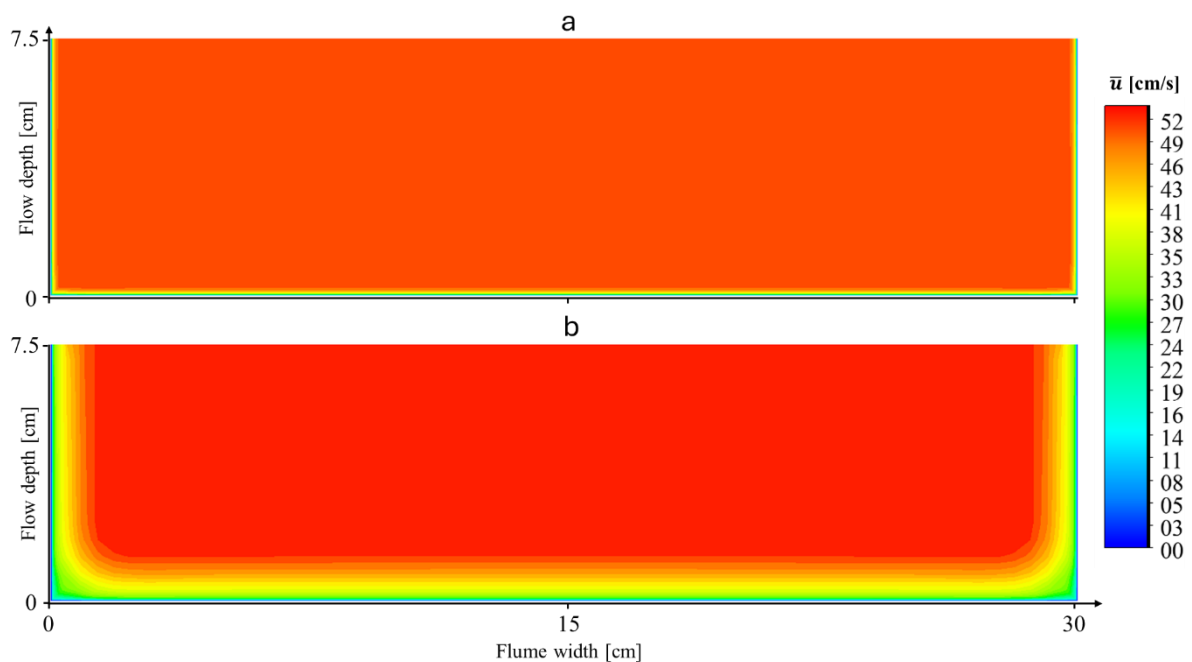


Figure 5.3 Lateral cross sections of the flow domain showing the time averaged flow velocity  $\bar{u}$  obtained from CFD simulations for treatment with  $U_f = 50 \text{ cm s}^{-1}$ . The cross sections are located at a distance of (a) 5 cm and (b) 55 cm from the upstream grid.

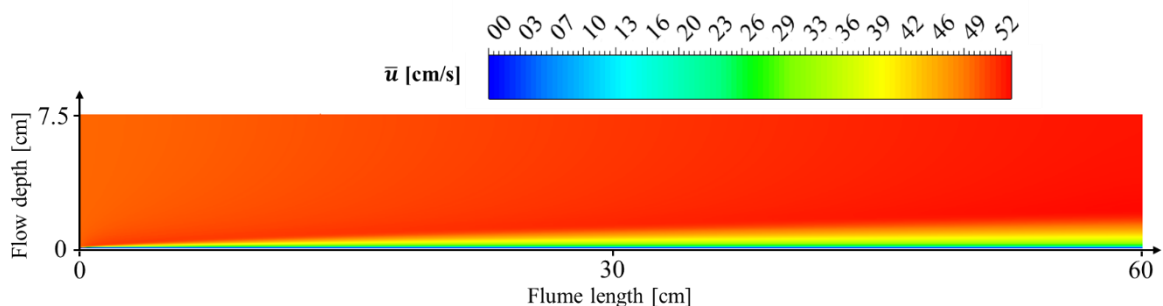


Figure 5.4 Longitudinal cross section, in the middle of flume width, showing the development of boundary layer along the bottom flume wall for the longitudinal flow velocity magnitude obtained using the CFD  $k-\epsilon$  model.

The maximum fish velocity ( $U_{max}$ ) of *T. muticellus* recorded in the experiments was  $129 \text{ cm s}^{-1}$  (24.8 BL/s) at the highest average cross-sectional flow velocity of  $55 \text{ cm s}^{-1}$

<sup>1</sup> (Figure 5.5). The average of the highest  $U_r$  measured for each fish was  $91.3 \text{ cm/s}^{-1}$  (19 BL/s).

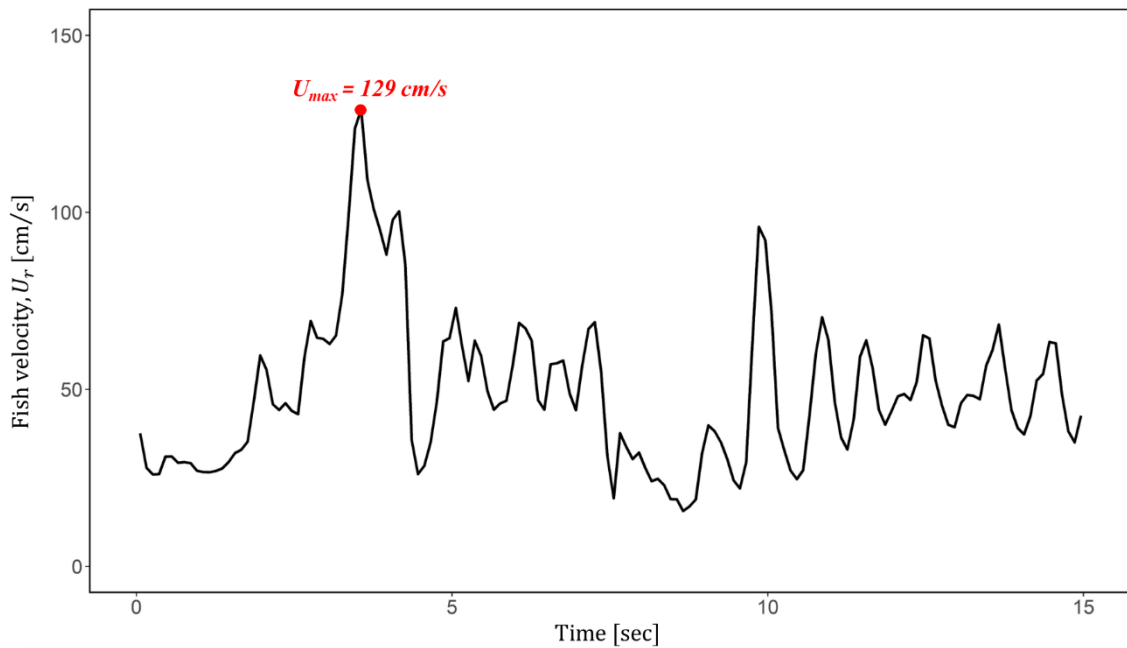


Figure 5.5 Fish velocity ( $U_r$ ) time-series signal for fish swimming against an average cross-sectional flow velocity of  $55 \text{ cm/s}^{-1}$ . The maximum fish velocity ( $U_{max}$ ) is highlighted by red dot.

The maximum fish swimming velocity ( $U_{max}$ ) increased with an increasing mean  $U_f$  (Kruskal-Wallis test,  $p < 0.05$ ; Figure 5.6). However, post hoc test revealed that this was only true for the  $U_{max}$  comparison at flow velocities of 40 and 50  $\text{cm/s}^{-1}$  (Dunn test,  $p < 0.05$ ). All other treatment groups resulted in non-significant differences for  $U_{max}$ .



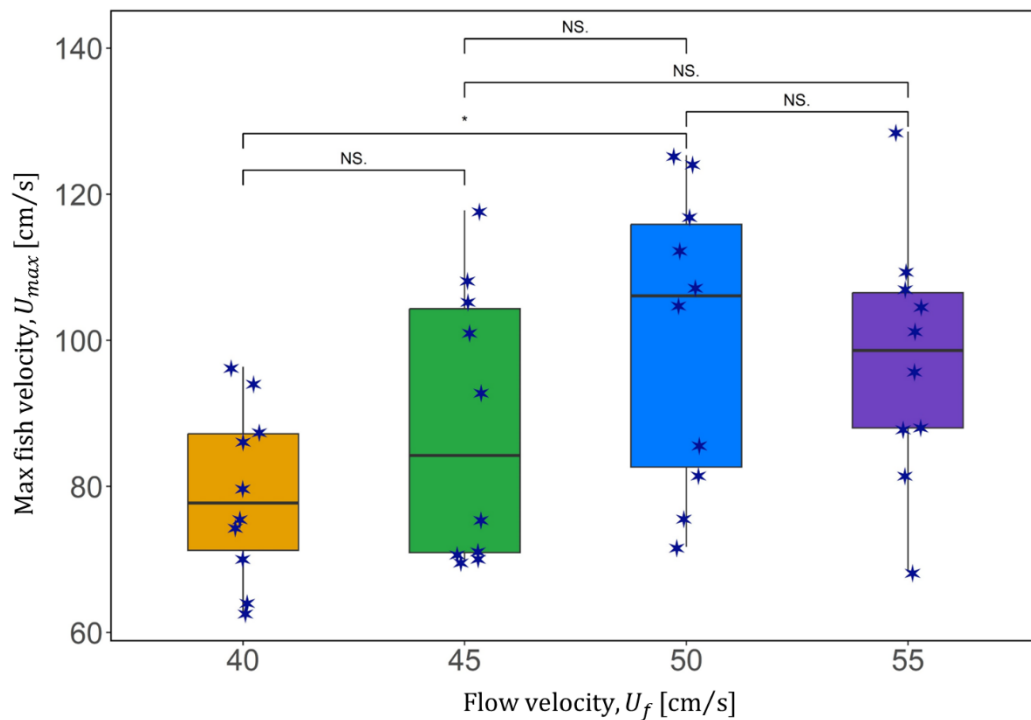


Figure 5.6 Boxplot of maximum fish swimming velocity  $U_{max}$  ( $n = 10$ ) for all average cross-sectional flow velocity treatments. The bounding box defines the Interquartile range (IQR) whereas the solid black horizontal line inside the bounding box is the median of  $U_{max}$ . The vertical solid black lines mark  $Q1 - 1.5 \cdot IQR$  (bottom end) and  $Q3 + 1.5 \cdot IQR$  (top end), where  $Q1$  and  $Q3$  are the 25<sup>th</sup> and 75<sup>th</sup> percentiles of  $U_{max}$ , respectively. The asterisk symbol indicates which groups have significant differences, while NS stands for non-significant

In comparing distributions of fish velocity ( $U_r$ ), the results from individual fish were combined based on flow velocity ( $U_f$ ). Frequency distributions of  $U_r$  were positively skewed and with high kurtosis values compared to normal distribution (Figure 5.7). For all treatments, mean fish velocities were always lower than the averaged cross-sectional flow velocities. The variability of  $U_r$  was quantified by its standard deviation, which increased from  $8.08 \text{ cms}^{-1}$  to  $11.72 \text{ cms}^{-1}$  as the  $U_f$  increased from  $40 \text{ cms}^{-1}$  to  $50 \text{ cms}^{-1}$ . At the highest  $U_f$  of  $55 \text{ cms}^{-1}$ , standard deviation was  $11.23 \text{ cms}^{-1}$ , slightly lower than at  $50 \text{ cms}^{-1}$  (Figure 5.7). The skewness and kurtosis of the fish velocity distributions did not show any clear trend with  $U_f$ .

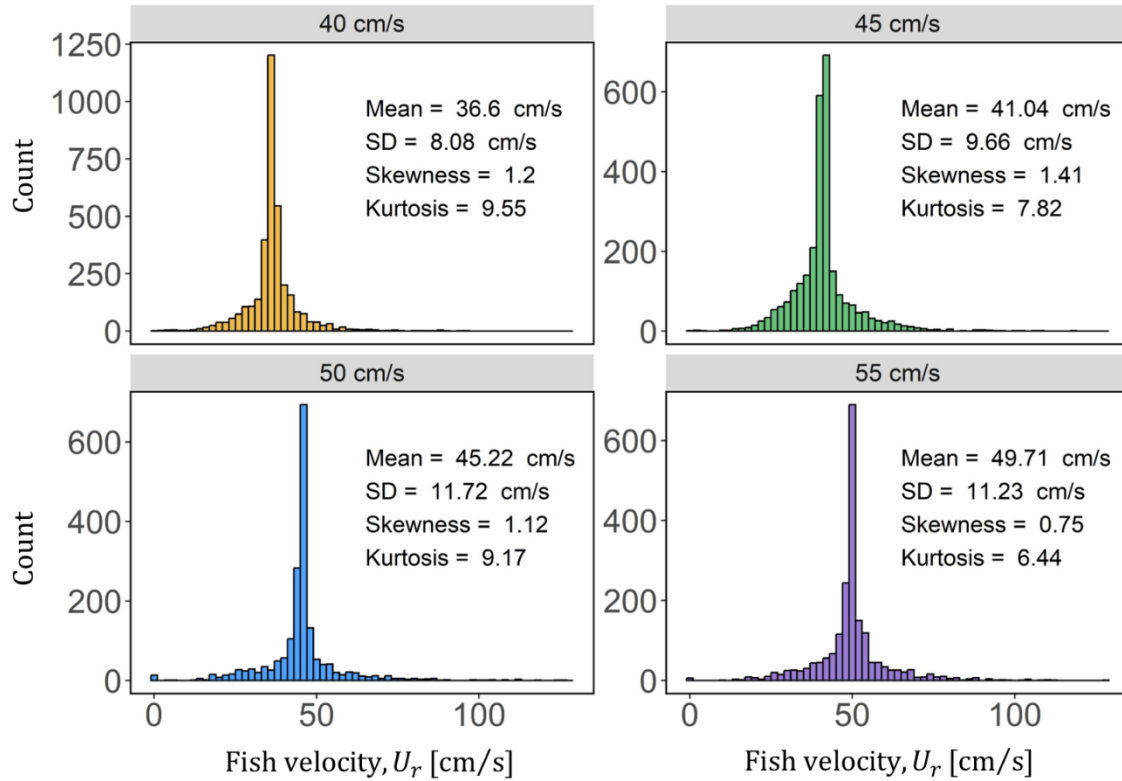


Figure 5.7 Frequency distributions of fish velocity ( $U_r$ ) at four mean flow velocity treatments.

The power spectra derived from the longitudinal fish velocity ( $U_{rx}$ ) and lateral fish velocity ( $U_{ry}$ ) time series across all  $U_f$  values are shown in Figure 5.8 in premultiplied form. Notably, irrespective of the  $U_f$ , the  $U_{rx}$  spectra exhibit a prominent peak and a consistent slope. The peak emerges at a characteristic frequency of approximately 1 Hz highlighting a dominant periodicity in the longitudinal fish velocity (Figure 5.8(b)). This periodicity is also observed in  $U_{ry}$ , at the same characteristic frequency of 1 Hz, although not consistently across all treatments. Specifically, for  $U_{ry}$ , spectra peaks are visible for flow velocities of 45 and 55  $\text{cm s}^{-1}$ , while for the other two flow velocities, they appear more diffused (Figure 5.8(d)). Nevertheless, for both  $U_{rx}$  and  $U_{ry}$ , the frequency corresponding to spectral peaks show no clear dependence on flow velocity.

The power spectra computed from velocity measurements obtained from LDA, are displayed in Figure 5.9. Spectra were computed from measurements taken at four distinct locations: P1, P2, P3, and P4 as shown in Figure 5.1. Figure 5.9 indicates that power spectral peaks at these locations are contained within a frequency range 5-30 Hz, hence significantly higher than those observed for spectra of fish velocity. Note that the frequencies associated with spectral peaks in Figure 5.9 are associated with the eddies time-scales that contribute the most to the variance of the turbulent signal.

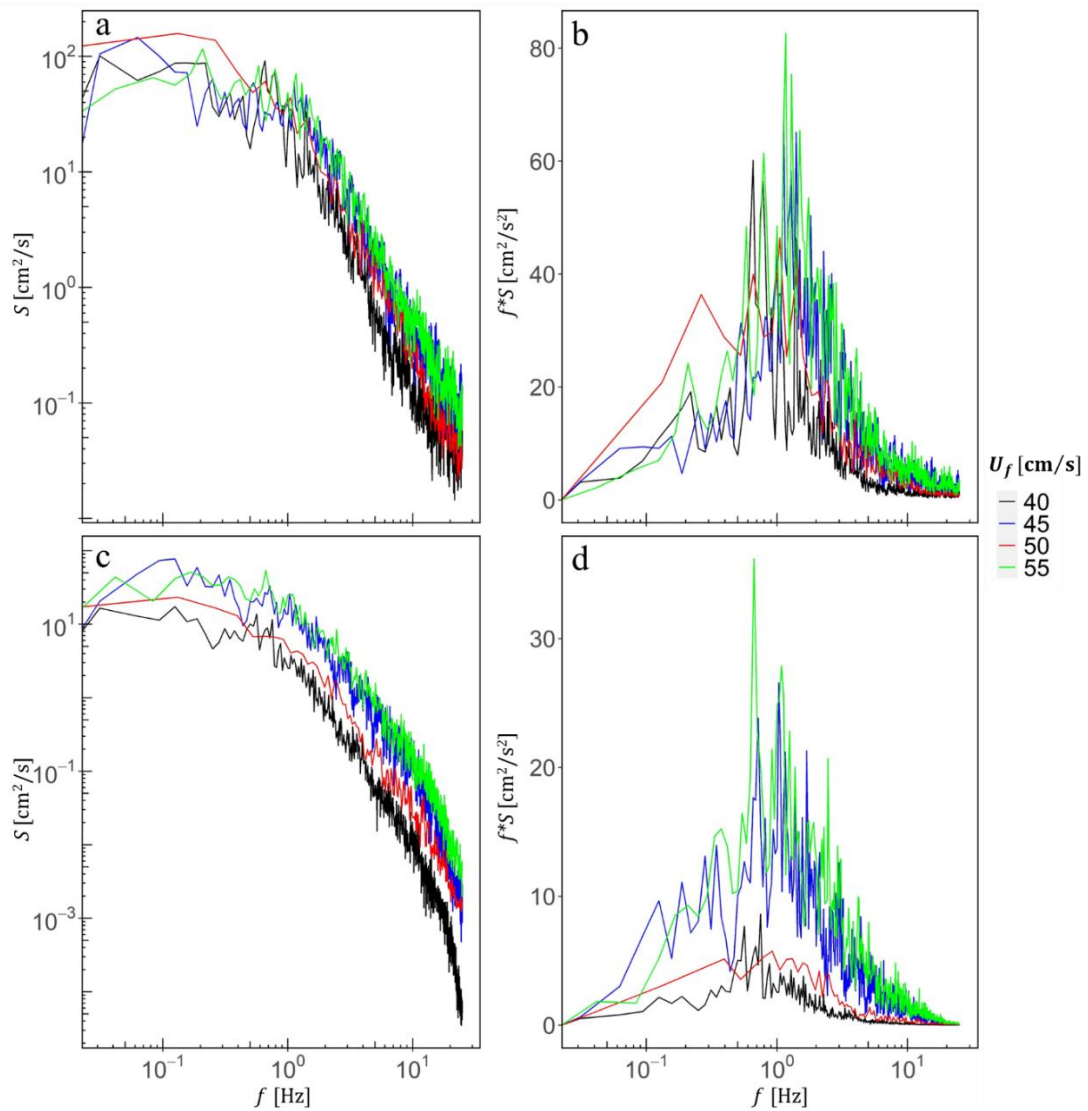


Figure 5.8 Power Spectra of longitudinal (panel (a) and (b)) and lateral (panel (c) and (d)) fish velocity time series at four  $U_f$  values. Panel (a) & (c) shows spectra plotted against frequency vector whereas panel (b) & (d) shows spectra plotted in premultiplied form. Data from different flow velocities is shown with different line colours as specified in the legend.

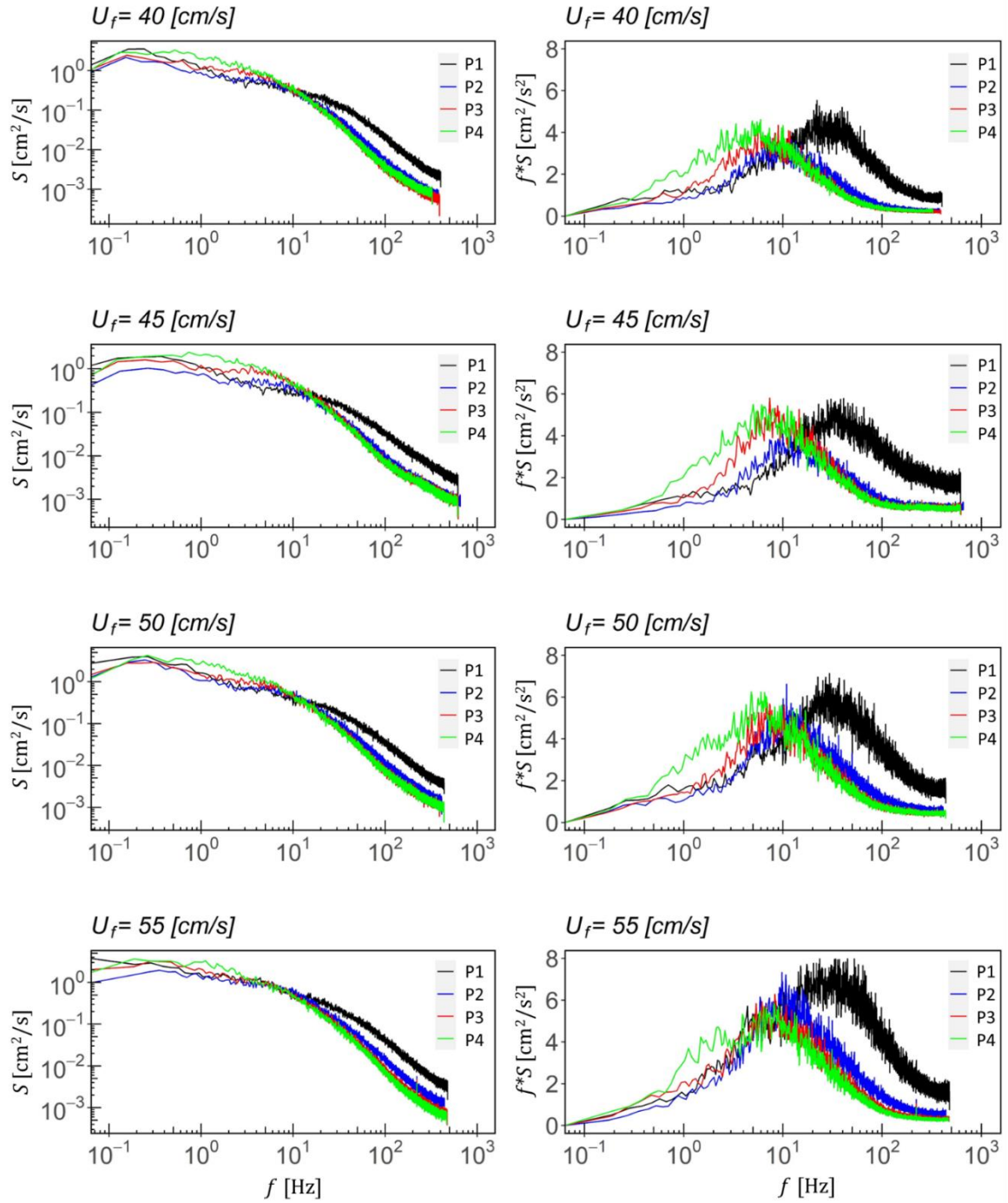


Figure 5.9 Plots of power spectra and its premultiplied form for time-averaged single-point longitudinal flow velocity ( $\bar{u}$ ) measurements, as obtained from the LDA, at four locations in the flow domain (P1, P2, P3, and P4) for all  $U_f$  treatments.

## 5.5 Discussion

An increase in flow velocity ( $U_f$ ), from 40  $\text{cm s}^{-1}$  to 55  $\text{cm s}^{-1}$ , resulted in higher maximum fish swimming velocity ( $U_{max}$ ) and increased variability in fish swimming velocity ( $U_r$ ). Maximum fish velocity has significant ecological importance as it has been shown that the ability of a fish to accelerate rapidly helps in avoiding predation (Domenici & Kapoor, 2010; Walker et al., 2005). The maximum fish velocities presented here for *T. muticellus* are likely an underestimation of their true maximum swimming abilities. This is because our experiment were designed to investigate time-to-fatigue and not maximum swimming velocities, which is often done by adopting different experimental procedures (e.g. by startling fish) (Domenici et al., 2004; Harper & Blake, 1991; Roche et al., 2023). Results from the present study show that  $U_{max}$  increased with increasing  $U_f$ ; however, they seemed to plateau at the highest tested flow velocities of 50 and 55  $\text{cm s}^{-1}$ . This can be explained in two ways. Firstly, it is plausible that fish may have simply reached their peak swimming velocities, making it physically impractical to achieve even higher  $U_r$  values. Secondly, fish behaviour may also be a factor, as beyond a critical maximum flow velocity, fish may decide not to expend the energy required to achieve even higher swimming velocities, thus swimming at a capped  $U_{max}$ .

As with  $U_{max}$ , the variation around the mean fish velocity increased with increasing  $U_f$  and appeared to reach a maximum at  $U_f$  of 50  $\text{cm s}^{-1}$ . These results agree with the findings of Plew et al (2007) who also observed increased variations in swimming velocity of *Galaxias maculatus* with increasing flow velocity, suggesting that the variations in  $U_r$  caused by flow velocity are not species-specific. These variations may be attributed to increased stress levels experienced by fish (resulting in erratic stress-driven accelerations) when exposed to progressively increasing high flow velocities. At the highest  $U_f$  of 55  $\text{cm s}^{-1}$ , though, the variation in  $U_r$  remained approximately the same as at 50  $\text{cm s}^{-1}$ . This can be most likely explained as a tradeoff between energy-saving strategies and stress induced behaviour. In other words, when hydrodynamic conditions become very challenging, fish can no longer afford a stress-induced erratic behaviour associated with large velocity variations (i.e. sprints) and hence major energy-consuming events.

Power spectra of  $U_r$  revealed a sharp peak at a characteristic frequency of 1 Hz for all flow velocity treatments. This shows clear periodicity in fish velocity time series, leading us to the following question: why do fish prefer to regulate their swimming velocity at a specific frequency? The 1 Hz frequency corresponds to a characteristic time-scale of 1 second, indicating that fish velocity undergoes periodic changes over this interval. To explore the reasons behind this periodicity, several hypotheses were postulated. Initially, it was hypothesised that periodic fluctuations in fish velocity may be due to fish response to flow turbulence. Analysis of single-point longitudinal flow velocity measurements, obtained from LDA, indicate that the dominant frequency of turbulence was one order of magnitude higher than that observed in the fish velocity spectra, suggesting that the turnover time scale associated with large-scale eddies is significantly

smaller than the 1-second characteristic time scale of fish velocity signal. Thus, it is improbable that the observed 1-second periodicity can be attributed to turbulence effects.

Fish tail beat frequency (TBF) serves as a proxy for a range of physiological and behavioural parameters, such as energy consumption, swimming efficiency, and locomotor performance (Bainbridge, 1958; Eloy, 2012; Hunter & Zweifel, 1971; Steinhausen et al., 2005). Therefore, as a second working hypothesis, TBF data was analysed (though not presented in the paper) to explore whether the 1-second characteristic time scale observed in fish velocity signals is driven by tail beat oscillations. While the maximum measured tail beat frequency was 25 Hz, fish never displayed TBF lower than 6 Hz. This equates to a time scale approximately one order of magnitude smaller than the characteristic 1-second time scale observed in fish velocity signals, suggesting that periodic fluctuations in fish swimming velocity are also not driven by tail beat frequency. Another time scale that could potentially explain the observed periodicity in fish velocity signal is the duration required for fish to experience the flow passing its body. For initial assessment, this could be estimated as fish length divided by mean flow velocity. In our experiments, this time-scale ranges from 0.09-0.12 seconds, also an order of magnitude smaller than the dominant time scale observed in fish velocity signal.

Fish are known to utilise their surrounding flow field or the induced flow field of a neighbour to reduce their physical exertion (Harvey et al., 2022). It is also known that fish exhibit a time lag in their response to any activity that happens in their vicinity (Webb, 2004). Wang et al (2016) studied the upstream passage through culverts on Silver perch (*Bidyanus bidyanus*) and Duboulay's Rainbowfish (*Melanotaenia duboulayi*) and reported that fish velocity auto-correlation time scale characterised a typical reaction time of the fish. Mozzi (2024) investigated the response times of *Telestes muticellus* swimming in groups, revealing that peaks of cross-correlation functions in the longitudinal direction occurred at lags ranging from 0.47 to 0.54 seconds, while those in the lateral direction ranged from 0.28 to 0.73 seconds. Similarly, Sakamoto et al (1976) studied the similarities of movement and response time lag among individuals in a school. They reported that approximately 20% of combinations showed a 0.5-second response time—coinciding with the latent period of fish swimming motion. In our experiment, the 1-second periodic fluctuations in fish velocity indicate cyclic alterations, wherein fish oscillate between forward and backward motions within this timeframe, resulting in directional changes occurring twice. Assuming a fish reaction time of approximately 0.5 seconds, this implies directional shifts (either forward or backward) occurring every half-second, matching with the characteristic timescale observed in the fish velocity signal.

The consistent shape of the spectra across various flow velocities, along with the presence of a distinct peak, suggests an underlying fish behaviour, when swimming in fast flowing streams. We have posited a working hypothesis attributing the observed periodicity in fish velocity at 1 Hz to fish reaction time. However, the reason why the slope of the power spectra appears to be so consistent, independent of flow velocity, is still unclear, highlighting the necessity for further research studies to address this knowledge gap.

## References

- Aedo, J. R., Otto, K. R., Rader, R. B., Hotchkiss, R. H., & Belk, M. C. (2021). Size Matters, but Species Do Not: No Evidence for Species-Specific Swimming Performance in Co-Occurring Great Basin Stream Fishes. *Water*, 13(18), 2570. <https://doi.org/10.3390/w13182570>
- Ashraf, I., Van Wassenbergh, S., & Verma, S. (2021). Burst-and-coast swimming is not always energetically beneficial in fish (*Hemigrammus bleheri*). *Bioinspiration & Biomimetics*, 16(1), 016002. <https://doi.org/10.1088/1748-3190/abb521>
- Ashraf, M. U., Nyqvist, D., & Comoglio, C. (2024). The effect of in-flume habituation time and fish behaviour on estimated swimming performance. *Journal of Ecohydraulics*. <https://doi.org/10.1080/24705357.2024.2306411>
- Bainbridge, R. (1958). The Speed of Swimming of Fish as Related to Size and to the Frequency and Amplitude of the Tail Beat. *Journal of Experimental Biology*, 35(1), 109–133. <https://doi.org/10.1242/jeb.35.1.109>
- Beamish, F. W. H. (1978). *Fish Physiology* (W. S. Hoar & D. J. Randall, Eds.; 1st ed., Vol. 7). Academic Press, London.
- Blake, R. W. (1983). Functional design and burst-and-coast swimming in fishes. *Canadian Journal of Zoology*, 61(11), 2491–2494. <https://doi.org/10.1139/z83-330>
- Brett, J. R. (1964). The Respiratory Metabolism and Swimming Performance of Young Sockeye Salmon. *Journal of the Fisheries Research Board of Canada*, 21(5), 1183–1226. <https://doi.org/10.1139/f64-103>
- Burnett, N. J., Hinch, S. G., Braun, D. C., Casselman, M. T., Middleton, C. T., Wilson, S. M., & Cooke, S. J. (2014). Burst Swimming in Areas of High Flow: Delayed Consequences of Anaerobiosis in Wild Adult Sockeye Salmon. *Physiological and Biochemical Zoology*, 87(5), 587–598. <https://doi.org/10.1086/677219>
- Çengel, Y. A., & Cimbala, J. M. (2006). *Fluid mechanics: Fundamentals and applications*. McGraw-Hill Higher Education.
- Chrétien, E., Boisclair, D., Cooke, S. J., & Killen, S. S. (2021). Social Group Size and Shelter Availability Influence Individual Metabolic Traits in a Social Fish. *Integrative Organismal Biology*, 3(1), obab032. <https://doi.org/10.1093/iob/obab032>
- Chung, M.-H. (2009). On burst-and-coast swimming performance in fish-like locomotion. *Bioinspiration & Biomimetics*, 4(3), 036001. <https://doi.org/10.1088/1748-3182/4/3/036001>
- Domenici, P., & Kapoor, B. G. (Eds.). (2010). *Fish locomotion: An eco-ethological perspective*. Science Publishers.
- Domenici, P., Standen, E. M., & Levine, R. P. (2004). Escape manoeuvres in the spiny dogfish (*Squalus acanthias*). *Journal of Experimental Biology*, 207(13), 2339–2349. <https://doi.org/10.1242/jeb.01015>



- Eloy, C. (2012). Optimal Strouhal number for swimming animals. *Journal of Fluids and Structures*, 30, 205–218. <https://doi.org/10.1016/j.jfluidstructs.2012.02.008>
- Floryan, D., Van Buren, T., & Smits, A. J. (2017). Forces and energetics of intermittent swimming. *Acta Mechanica Sinica*, 33(4), 725–732. <https://doi.org/10.1007/s10409-017-0694-3>
- Freyhof, J., & Kottelat, M. (2007). *Handbook of European freshwater fishes*. <https://portals.iucn.org/library/node/9068>
- Hammer, C. (1995). Fatigue and exercise tests with fish. *Comparative Biochemistry and Physiology Part A: Physiology*, 112(1), 1–20. [https://doi.org/10.1016/0300-9629\(95\)00060-K](https://doi.org/10.1016/0300-9629(95)00060-K)
- Haro, A., Castro-Santos, T., Noreika, J., & Odeh, M. (2004). Swimming performance of upstream migrant fishes in open-channel flow: A new approach to predicting passage through velocity barriers. *Canadian Journal of Fisheries and Aquatic Sciences*, 61(9), 1590–1601. <https://doi.org/10.1139/f04-093>
- Harper, D. G., & Blake, R. W. (1991). Prey Capture and the Fast-Start Performance of Northern Pike *Esox Lucius*. *Journal of Experimental Biology*, 155(1), 175–192. <https://doi.org/10.1242/jeb.155.1.175>
- Harvey, S. T., Muhawenimana, V., Müller, S., Wilson, C. A. M. E., & Denissenko, P. (2022). An inertial mechanism behind dynamic station holding by fish swinging in a vortex street. *Scientific Reports*, 12(1), 12660. <https://doi.org/10.1038/s41598-022-16181-8>
- Heuer, R. M., Stieglitz, J. D., Pasparakis, C., Enochs, I. C., Benetti, D. D., & Grosell, M. (2021). The Effects of Temperature Acclimation on Swimming Performance in the Pelagic Mahi-Mahi (*Coryphaena hippurus*). *Frontiers in Marine Science*, 8, 654276. <https://doi.org/10.3389/fmars.2021.654276>
- Hunter, J. R., & Zweifel, J. R. (1971). SWIMMING SPEED, TAIL BEAT FREQUENCY, TAIL BEAT AMPLITUDE, AND SIZE IN JACK MACKEREL, *Trachurus symmetricus*, AND OTHER FISHES. *Fishery Bulletin*, 69(2).
- Kern, P., Cramp, R. L., Gordos, M. A., Watson, J. R., & Franklin, C. E. (2018). Measuring  $U_{crit}$  and endurance: Equipment choice influences estimates of fish swimming performance. *Journal of Fish Biology*, 92(1), 237–247. <https://doi.org/10.1111/jfb.13514>
- Kerr, J. R., Manes, C., & Kemp, P. S. (2016). Assessing hydrodynamic space use of brown trout, *Salmo trutta*, in a complex flow environment: A return to first principles. *Journal of Experimental Biology*, jeb.134775. <https://doi.org/10.1242/jeb.134775>
- Manes, C., Poggi, D., Ridolfi, L. (2011). Turbulent boundary layers over permeable walls: scaling and near-wall structure. *Journal of Fluid Mechanics*, 687:141-170. doi:10.1017/jfm.2011.329
- Mogdans, J. (2019). Sensory ecology of the fish lateral-line system: Morphological and physiological adaptations for the perception of hydrodynamic stimuli. *Journal of Fish Biology*, 95(1), 53–72. <https://doi.org/10.1111/jfb.13966>



Mozzi, G. (2024). Fish collective behaviour in flowing waters (Doctoral dissertation). Politecnico di Torino, Italy.

Müller, U. K., Stamhuis, E. J., & Videler, J. J. (2000). Hydrodynamics of Unsteady Fish Swimming and the Effects of Body Size: Comparing the Flow Fields of Fish Larvae and Adults. *Journal of Experimental Biology*, 203(2), 193–206. <https://doi.org/10.1242/jeb.203.2.193>

Newbold, L. R., & Kemp, P. S. (2015). Influence of corrugated boundary hydrodynamics on the swimming performance and behaviour of juvenile common carp ( *Cyprinus carpio* ). *Ecological Engineering*, 82, 112–120. <https://doi.org/10.1016/j.ecoleng.2015.04.027>

Nikora, V. I., Aberle, J., Biggs, B. J. F., Jowett, I. G., & Sykes, J. R. E. (2003). Effects of fish size, time-to-fatigue and turbulence on swimming performance: A case study of *Galaxias maculatus* : swimming performance of inanga. *Journal of Fish Biology*, 63(6), 1365–1382. <https://doi.org/10.1111/j.1095-8649.2003.00241.x>

Penghan, L.-Y., Pang, X., & Fu, S.-J. (2016). The effects of starvation on fast-start escape and constant acceleration swimming performance in rose bitterling (*Rhodeus ocellatus*) at two acclimation temperatures. *Fish Physiology and Biochemistry*, 42(3), 909–918. <https://doi.org/10.1007/s10695-015-0184-0>

Plew, D. R., Nikora, V. I., Larned, S. T., Sykes, J. R. E., & Cooper, G. G. (2007). Fish swimming speed variability at constant flow: *Galaxias maculatus*. *New Zealand Journal of Marine and Freshwater Research*, 41(2), 185–195. <https://doi.org/10.1080/00288330709509907>

Redmon, J., Divvala, S., Girshick, R., & Farhadi, A. (2016). You Only Look Once: Unified, Real-Time Object Detection. *2016 IEEE Conference on Computer Vision and Pattern Recognition (CVPR)*, 779–788. <https://doi.org/10.1109/CVPR.2016.91>

Ribak, G., Weihs, D., & Arad, Z. (2005). Submerged swimming of the great cormorant *Phalacrocorax carbo sinensis* is a variant of the burst-and-glide gait. *Journal of Experimental Biology*, 208(20), 3835–3849. <https://doi.org/10.1242/jeb.01856>

Roche, D. G., Tytell, E. D., & Domenici, P. (2023). Kinematics and behaviour in fish escape responses: Guidelines for conducting, analysing and reporting experiments. *Journal of Experimental Biology*, 226(14), jeb245686. <https://doi.org/10.1242/jeb.245686>

Schumann, S., Mozzi, G., Piva, E., Devigili, A., Negrato, E., Marion, A., Bertotto, D., & Santovito, G. (2023). Social buffering of oxidative stress and cortisol in an endemic cyprinid fish. *Scientific Reports*, 13(1), 20579. <https://doi.org/10.1038/s41598-023-47926-8>

Steinhausen, M. F., Steffensen, J. F., & Andersen, N. G. (2005). Tail beat frequency as a predictor of swimming speed and oxygen consumption of saithe (*Pollachius virens*) and whiting (*Merlangius merlangus*) during forced swimming. *Marine Biology*, 148(1), 197–204. <https://doi.org/10.1007/s00227-005-0055-9>

Taylor, E. B., & McPhail, J. D. (1985). Variation in Burst and Prolonged Swimming Performance Among British Columbia Populations of Coho Salmon, *Oncorhynchus kisutch*. *Canadian Journal of Fisheries and Aquatic Sciences*, 42(12), 2029–2033.

<https://doi.org/10.1139/f85-250>

Teyke, T. (1985). Collision with and avoidance of obstacles by blind cave fish *Anoptichthys jordani* (Characidae). *Journal of Comparative Physiology A*, 157(6), 837–843. <https://doi.org/10.1007/BF01350081>

Tudorache, C., O’Keefe, R. A., & Benfey, T. J. (2010a). Flume length and post-exercise impingement affect anaerobic metabolism in brook charr *Salvelinus fontinalis*. *Journal of Fish Biology*, 76(3), 729–733. <https://doi.org/10.1111/j.1095-8649.2009.02513.x>

Tudorache, C., O’Keefe, R. A., & Benfey, T. J. (2010b). The effect of temperature and ammonia exposure on swimming performance of brook charr (*Salvelinus fontinalis*). *Comparative Biochemistry and Physiology Part A: Molecular & Integrative Physiology*, 156(4), 523–528. <https://doi.org/10.1016/j.cbpa.2010.04.010>

Tudorache, C., Viaenen, P., Blust, R., & De Boeck, G. (2007). Longer flumes increase critical swimming speeds by increasing burst-glide swimming duration in carp *Cyprinus carpio*, L. *Journal of Fish Biology*, 71(6), 1630–1638. <https://doi.org/10.1111/j.1095-8649.2007.01620.x>

Veza, P., Libardoni, F., Manes, C., Tsuzaki, T., Bertoldi, W., & Kemp, P. S. (2020). Rethinking swimming performance tests for bottom-dwelling fish: The case of European glass eel (*Anguilla anguilla*). *Scientific Reports*, 10(1), 16416. <https://doi.org/10.1038/s41598-020-72957-w>

Videler, J. J. (1993). *Fish Swimming*. Springer Netherlands. <https://doi.org/10.1007/978-94-011-1580-3>

Videler, J. J., & Wardle, C. S. (1991). Fish swimming stride by stride: Speed limits and endurance. *Reviews in Fish Biology and Fisheries*, 1(1), 23–40. <https://doi.org/10.1007/BF00042660>

Videler, J., & Weihs, D. (1982). Energetic advantages of burst-and-coast swimming of fish at high speeds. *The Journal of Experimental Biology*, 97, 169–178.

Vogel, S. (1994). *Life in Moving Fluids: The Physical Biology of Flow - Revised and Expanded Second Edition*. Princeton University Press. <https://doi.org/10.2307/j.ctvzsmfc6>

Walker, J. A., Ghalambor, C. K., Griset, O. L., McKENNEY, D., & Reznick, D. N. (2005). Do faster starts increase the probability of evading predators? *Functional Ecology*, 19(5), 808–815. <https://doi.org/10.1111/j.1365-2435.2005.01033.x>

Wang, H., Chanson, H., Kern, P., & Franklin, C. (2016). Culvert Hydrodynamics to enhance Upstream Fish Passage: Fish Response to Turbulence. *20th Australasian Fluid Mechanics Conference*.

Webb, P. W. (2004). Response latencies to postural disturbances in three species of teleostean fishes. *Journal of Experimental Biology*, 207(6), 955–961. <https://doi.org/10.1242/jeb.00854>

Weihs, D. (1974). Energetic advantages of burst swimming of fish. *Journal of Theoretical*

*Biology*, 48(1), 215–229. [https://doi.org/10.1016/0022-5193\(74\)90192-1](https://doi.org/10.1016/0022-5193(74)90192-1)

Windsor, S. P., Tan, D., & Montgomery, J. C. (2008). Swimming kinematics and hydrodynamic imaging in the blind Mexican cave fish ( *Astyanax fasciatus* ). *Journal of Experimental Biology*, 211(18), 2950–2959. <https://doi.org/10.1242/jeb.020453>

Wu, G., Yang, Y., & Zeng, L. (2007). Kinematics, hydrodynamics and energetic advantages of burst-and-coast swimming of koi carps ( *Cyprinus carpio koi* ). *Journal of Experimental Biology*, 210(12), 2181–2191. <https://doi.org/10.1242/jeb.001842>

# **Chapter 6**

## **Conclusions**

The present thesis work contributes to advancements in fish swimming performance studies from three perspectives. Firstly, it fills some methodological knowledge gaps that exist in currently employed testing protocols for studying fish swimming performance. Secondly, it presents a novel theoretical approach for assessing fish fatigue curves in burst swimming activity level. Lastly, it advances our understanding of fish swimming in fast-moving waters highlighting consistent swimming patterns/behaviours.

The results from Chapters 2 and 3 emphasise that fish swimming performance estimates are sensitive to the choice of testing protocols and fish behaviour during trials. The findings suggest that various factors such as fatigue definition, flume length, and habituation time affect fish swimming performance in fatigue tests. However, it is important to note that these findings are based only on two fish species of similar age and size groups, tested under specific flow velocities and temperature conditions. While this limitation restricts the generalisation of our findings to other cases, it underscores the significance of such studies as a foundational step towards establishing a unified methodology. In recent years, efforts have been made to establish guidelines for conducting, analysing, and reporting experiments studying fish escape response and metabolic rates (Killen et al., 2021; Roche et al., 2023). This is encouraging and in future, similar efforts should be devoted to developing protocol guidelines for studying other metrics of fish swimming performance such as time-to-fatigue.

Chapter 4 advances our understanding of the relationship between time-to-fatigue and fish velocity by presenting a theoretical framework based on concepts of fish hydrodynamics. To test the validity of proposed scaling laws, significant efforts were invested in collecting a diverse and rich experimental database however, practical limitations such as time constraints, fish availability, and the capacity of our flume setup restricted the extent of our findings. Given that our limited database from five Cypriniformes species showed results in line with the theoretical predictions, the author encourages other researchers to carry out more experiments on various fish species and sizes to confirm the general validity of proposed scaling laws. If established, this could significantly reduce experimental efforts currently devoted to investigating fish swimming performance in burst swimming activity level. Furthermore, generally speaking, theoretical approaches should be developed and used to help identify and assess appropriate models predicting swimming performance. For example, there is a potential to develop similar scaling laws linking statistical properties of time-to-fatigue and fish velocity in the prolonged swimming range, where fish use both aerobic and anaerobic metabolism.

Chapter 5 presents a unique exploration of fish velocity in fast-moving waters, an area of study that has been almost unexplored until now. Results from the spectral analysis of fish velocity offer insights about fish behaviour in burst swimming velocities. While the authors propose a hypothesis linking the observed peak in fish velocity spectra to fish reaction time, the consistent slope of the power spectra, regardless of flow velocity, requires further investigation. Future studies involving different fish species and sizes are needed to determine if the observed 1 Hz characteristic frequency in fish velocity signal

is species- and/or size-specific.

To sum up, the author believes that although research on fish swimming performance has advanced significantly over the past few decades, there is still much to learn about fish behaviour and swimming performance. Enhanced knowledge of fish swimming abilities and behaviour is crucial for informed decision-making, particularly in areas like fishway design and maintenance.

## References

Killen, S. S., Christensen, E. A. F., Cortese, D., Závorka, L., Norin, T., Cotgrove, L., Crespel, A., Munson, A., Nati, J. J. H., Papatheodoulou, M., & McKenzie, D. J. (2021). Guidelines for reporting methods to estimate metabolic rates by aquatic intermittent-flow respirometry. *Journal of Experimental Biology*, 224(18), jeb242522. <https://doi.org/10.1242/jeb.242522>

Roche, D. G., Tytell, E. D., & Domenici, P. (2023). Kinematics and behaviour in fish escape responses: Guidelines for conducting, analysing and reporting experiments. *Journal of Experimental Biology*, 226(14), jeb245686. <https://doi.org/10.1242/jeb.245686>

# **Appendix A-E**



## Appendix A

In this Appendix, we derive the scaling laws linking  $F_D$  to the relative fish-water velocity  $U_r$  assuming skin friction being the dominant source of fish drag. Firstly we consider skin friction effects assuming fish as a rigid body. We then relax this hypothesis and explore the combined effects of skin friction and undulating fish body.

### *Skin friction effects assuming fish as a rigid body*

Using the rigid body approximation, the literature proposes that the drag coefficient of a fish  $C_D$  can be taken as dependent on the Reynolds number ( $Re_L$ ) (Webb, 1975). Dependence of  $C_D$  on  $Re_L$  can be estimated following classical smooth wall boundary layer theory, which suggests that  $C_D \sim Re_L^e$ , where  $Re_L = \frac{U_r L}{\nu}$  is the fish Reynolds number,  $\nu$  is the water kinematic viscosity, and  $e$  is a scaling exponent, whose value is  $e = -\frac{1}{2}$  if the boundary layer over the fish is predominantly laminar and  $e = -\frac{1}{5}$ , if turbulent (Schlichting & Gersten, 2017). Turbulent boundary layer conditions are believed to occur for  $Re_L \gtrsim 10^3$  (Anderson et al., 2001), where all available experimental data on fish swimming performance are found. In what follows, therefore, only turbulent boundary layer conditions will be considered. Hence, at these conditions  $F_D$  can be estimated as:

$$F_D \sim \rho C_D L S U_r^2 \sim \rho \left( \frac{U_r L}{\nu} \right)^{-1/5} L S U_r^2 = (\rho L^{4/5} S \nu^{1/5}) U_r^{9/5} = \Gamma_2 U_r^{9/5} \quad [A1]$$

where  $\Gamma_2 = \rho L^{4/5} S \nu^{1/5}$  is a function that is herein introduced to lump the effects of parameters pertaining to fish size (i.e.  $L$  and  $S$ ) and fluid properties (i.e.  $\rho$  and  $\nu$ ).

### *Combined skin friction and undulating body effects*

The effects of fish body undulations can be considered using the so-called Bone-Lighthill boundary-layer thinning hypothesis. From Ehrenstein et al. (2014) and Ehrenstein and Eloy (2013), the drag force per unit depth ( $F_{DS}$ ) of a laminar boundary layer developing over an undulating flat plate is estimated as:

$$F_{DS} \sim \mu U_r Re_s^{1/2} \sqrt{St} \sim \mu U_r \frac{U_r^{1/2} S^{1/2}}{\nu^{1/2}} \frac{L^{1/2}}{L^{1/2}} \sqrt{St} \sim \mu U_r Re_L^{1/2} \sqrt{\frac{S}{L}} \sqrt{St} \quad [A2]$$

where  $\mu$  is water dynamic viscosity,  $Re_s = \frac{U_r S}{\nu}$  and  $Re_L = \frac{U_r L}{\nu}$  are fish Reynolds numbers defined using fish depth ( $S$ ) and fish length ( $L$ ) as characteristic lengths, respectively,  $\nu$  is the water kinematic viscosity, and  $St = V/U_r$  is the fish Strouhal number with  $V = fA$  being the transverse velocity of fish body undulations,  $f$  is the tail beat frequency, and  $A$  is the half-peak tail beat amplitude.

Further simple algebra leads to define  $F_{DS}$  as follows

$$F_{DS} \sim \mu U_r Re_L^2 \sqrt{\frac{s}{L}} \sqrt{St} \sim \rho \nu U_r \frac{U_r^2 L^{\frac{1}{2}}}{v^{\frac{1}{2}}} \sqrt{\frac{s}{L}} \sqrt{St} \sim \rho \frac{\nu^{\frac{1}{2}}}{U_r^{\frac{1}{2}} L^{\frac{1}{2}}} L U_r^2 \sqrt{\frac{s}{L}} \sqrt{St} \sim \rho C_D L U_r^2 \sqrt{\frac{s}{L}} \sqrt{St} \quad [A3]$$

where  $C_D \sim Re_L^{-1}$ , as suggested by Blasius (1908), and  $C_{DU} \sim C_D \sqrt{\frac{s}{L}} \sqrt{St}$  is the drag coefficient of an undulating fish-like body. Although the above equation was initially derived for laminar boundary layer conditions, we argue it can also be applied to turbulent boundary layers as the physical effect of undulation is similar for both cases.

To derive a scaling relation between  $F_D$  and  $U_r$ , like Eq. 4.2 and A1, it is now necessary to find a relation between  $St$  and  $Re_L$ . To achieve this, building upon the approach proposed by Gazzola et al. (2014), we argue that the average thrust per unit depth of fish  $F_{tx}$  results from the sum of many linear accelerations leading to inertial type forces  $F_t$  that can be parameterised as  $F_t \sim ma$ , where  $m$  is the mass of displaced fluid per unit fish depth during a tail beat and can be scaled as  $m \sim \rho AL$  (see Figure A1),  $A$  is the half-peak tail beat amplitude, and  $L$  is the total fish length. The resulting fluid acceleration scales as  $a \sim Af^2 \frac{A}{L}$ , where  $f$  is the tail beat frequency. Keeping the sine of a local angle as  $A/L$ , we can obtain the thrust force component in longitudinal (swimming) direction as:

$$F_{tx} \sim ma \sim \rho A^3 f^2. \quad [A4]$$

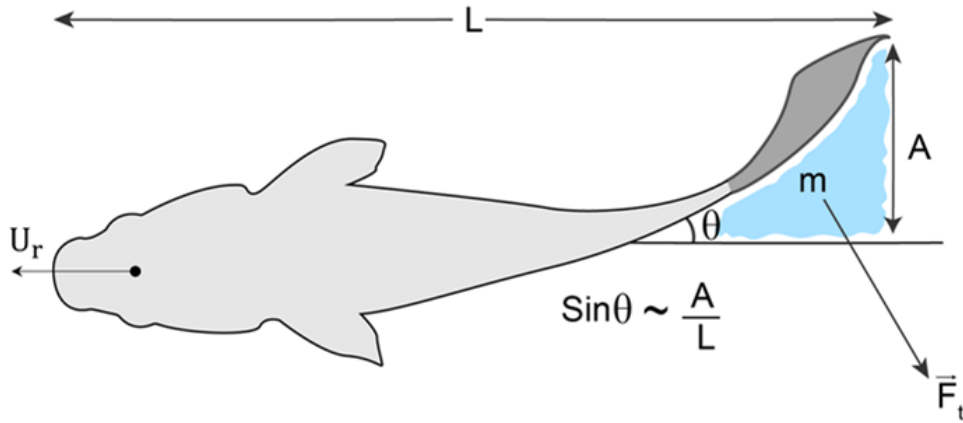


Figure A.1 Sketch of an idealized fish swimming at velocity  $U_r$ .  $L$  is the total length of the fish;  $A$  is the tail amplitude; the cyan area identifies the mass of displayed fluid per unit fish-depth during a tail beat;  $\vec{F}_t$  is the inertial force resulting from the displayed mass of fluid;  $\theta$  is the local angle between the tail and the direction of motion, in this case horizontal.

The dynamic equilibrium of resistance and thrust forces per unit depth (for turbulent boundary layer conditions, i.e.  $C_D \sim Re_L^{-1/5}$ ), leads to:

$$\rho \nu^{1/5} L^{4/5} U_r^{9/5} \sqrt{\frac{s}{L}} \sqrt{St} \sim \rho A^3 f^2. \quad [A5]$$

After some algebra, the following scaling relation can be derived:

$$St \sim \left(\frac{L}{A}\right)^{2/3} \left(\frac{S}{L}\right)^{1/3} Re_L^{-2/15}. \quad [A6]$$

By coupling Eq. A3 and A6, the average drag force for an undulating fish can be estimated as follows:

$$F_D = SF_{SD} \sim S\rho C_D \sqrt{\frac{S}{L}} \sqrt{St} LU_r^2 \sim S\rho Re_L^{-1/5} \sqrt{\frac{S}{L}} \left(\frac{L}{A}\right)^{1/3} \left(\frac{S}{L}\right)^{1/6} Re_L^{-1/15} LU_r^2, \quad [A7]$$

which can be summarised as  $F_D = \Gamma_3 U_r^{26/15}$ , where  $\Gamma_3 = \rho S^{5/3} L^{1/15} \left(\frac{L}{A}\right)^{1/3} \nu^{4/15}$ .

Experimental support for Eq. A6, which links  $St$  to  $Re_L$ , is provided by Figure A.2, displaying data specifically for fish as reported by Gazzola et al. (2014). The data presented in Figure A.2 include only fish swimming in turbulent boundary layer conditions i.e. at Reynolds number higher than the critical Reynolds number  $Re_{critical}$  of 2,500, as identified by Gazzola et al (2014). In contrast to the findings of Gazzola et al. (2014), where  $Re_L$  is reported to have no influence on  $St$  in turbulent regimes, the data in Figure A.2 show that there is a clearly visible dependence of  $St$  on  $Re_L$  for Reynolds number up to the order of  $10^6$ , which is consistent with the findings of Eloy (2012). Moreover, our theoretically derived scaling relation for turbulent boundary layer conditions, in Eq. A6, fit the experimentally collected data well within the range of  $Re_L$  where  $St$  displays  $Re_L$ -dependence, hence corroborating the proposed theory.

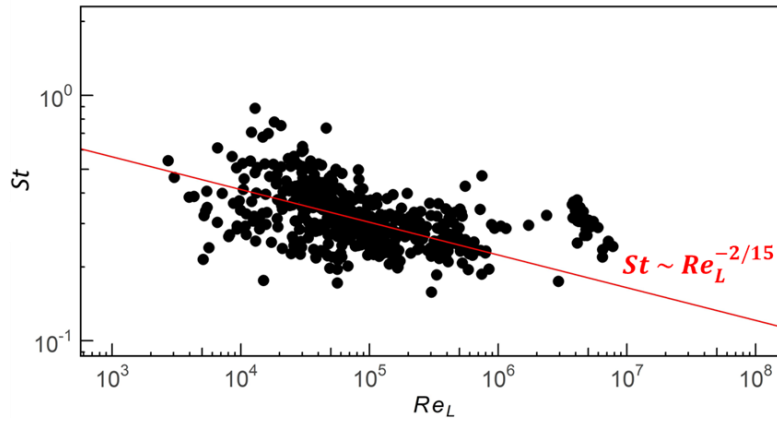


Figure A.2 Experimental data measurements highlighting the dependence of Strouhal number ( $St$ ) on Reynolds number ( $Re_L$ ) for fish swimming in turbulent boundary layer conditions. The red line has a slope of  $-2/15$ , which is the scaling exponent of the theoretically derived power law in Eq. A6, and is plotted for slope comparison with experimental data.

## References

- Anderson, E. J., McGillis, W. R., & Grosenbaugh, M. A. (2001). The boundary layer of swimming fish. *Journal of Experimental Biology*, 22.
- Blasius, H. (1908). Grenzsichten in Flussigkeiten mit kleiner Reibung. *Z. Math. Phys.* 56, 1–37.
- Ehrenstein, U., & Eloy, C. (2013). Skin friction on a moving wall and its implications for swimming animals. *Journal of Fluid Mechanics*, 718, 321–346. <https://doi.org/10.1017/jfm.2012.613>
- Ehrenstein, U., Marquillie, M., & Eloy, C. (2014). Skin friction on a flapping plate in uniform flow. *Philosophical Transactions of the Royal Society A: Mathematical, Physical and Engineering Sciences*, 372(2020), 20130345. <https://doi.org/10.1098/rsta.2013.0345>
- Eloy, C. (2012). Optimal Strouhal number for swimming animals. *Journal of Fluids and Structures*, 30, 205–218. <https://doi.org/10.1016/j.jfluidstructs.2012.02.008>
- Gazzola, M., Argentina, M., & Mahadevan, L. (2014). Scaling macroscopic aquatic locomotion. *Nature Physics*, 10(10), 758–761. <https://doi.org/10.1038/nphys3078>
- Schlichting, H., & Gersten, K. (2017). *Boundary-Layer Theory*. Springer Berlin Heidelberg. <https://doi.org/10.1007/978-3-662-52919-5>
- Webb, P. (1975). *Hydrodynamics and energetics of fish propulsion*. Bulletin of the fisheries Research Board of Canada 190, 1-156.

## Appendix B

This appendix describes the subsampling procedure of experimental data based on fish fork length ( $L_f$ ).

For all five fish species, the data did not conform to the  $\pm 10\%$  variation in  $L_f$  around its mean value, as per Katopodis & Gervais (2012). Figure B.1 shows the distribution of fish fork length for all available data on five fish species, without subsampling. To carry out subsampling following steps in their listed order were executed for all fish species:

- i. Within the range of fish fork length, a vector of mean fish length ( $L_{means}$ ) was generated by using an equal step spacing of 0.2 cm
- ii. A 10% variation around each element of the  $L_{means}$  vector was calculated and stored in a new vector ( $L_{variation}$ ). Note that both vectors,  $L_{means}$  and  $L_{variation}$ , are of similar length
- iii. Dataset was then subsampled based on fish fork length falling in the range of  $L_{means} \pm L_{variation}$
- iv. Lastly, in order to ensure that within each subsampled group the variation around true mean fish fork length was not more than 10%, the data was subset by eliminating the values that fell outside of the  $\pm 10\%$  of true mean  $L_f$

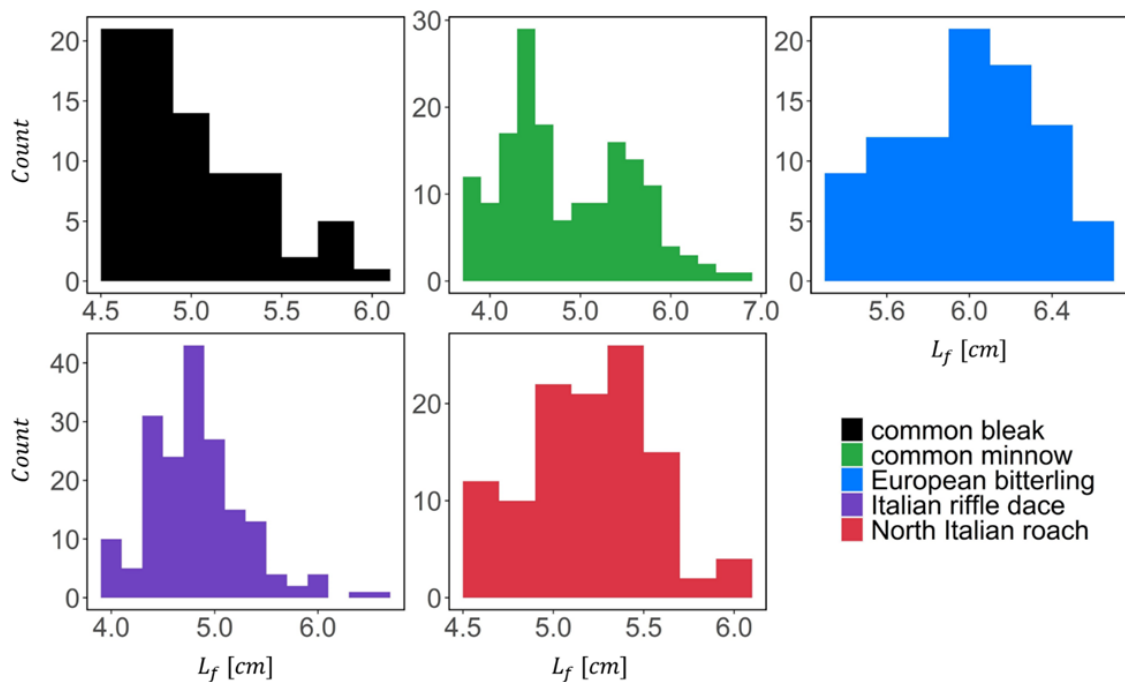


Figure B.1 Distribution plot of fish fork length ( $L_f$ ) for five fish species. Each panel shows the  $L_f$  data distribution for one fish species, as also highlighted using different colours (see legend).

Table B.1 gives a summary of subsampled groups analysed and report the number of subsampled groups for which the empirically estimated  $\beta$  values lie outside the theoretical range of  $\beta$  [1.73-2.0] as obtained from the linear regression analysis between  $\ln(\bar{T}_f)$  and  $\ln(U_f)$ , and  $\ln(\bar{T}_f'^2)$  and  $\ln(U_f)$ .

*Table B.1 Summary of subsampled groups reporting fish species, the total number of subsampled groups and the number of subsampled groups with  $\beta$  values outside theoretical range [1.73-2.0]. Asterisk symbol (\*) column reports number of groups with statistically significant scaling exponent whereas NS means not significant.*

Species	No. of subsampled groups	No. of subsampled groups with $\beta$ values outside theoretical range [1.73-2.0] obtained from linear regression between $\ln(\bar{T}_f)$ and $\ln(U_f)$				No. of subsampled groups with $\beta$ values outside theoretical range [1.73-2.0] obtained from linear regression between $\ln(\bar{T}_f'^2)$ and $\ln(U_f)$			
		Lower than 1.73		Higher than 2.0		Lower than 1.73		Higher than 2.0	
		NS	*	NS	*	NS	*	NS	*
<b><i>T. muticellus</i></b>	14	5	1	3	2	9	1	2	1
<b><i>P. phoxinus</i></b>	16	2	0	13	1	1	0	14	1
<b><i>R. amarus</i></b>	7	0	0	6	1	0	0	6	1
<b><i>L. aula</i></b>	8	0	0	7	1	2	0	3	2
<b><i>A. alborella</i></b>	8	0	0	6	2	2	0	5	1

## Reference

Katopodis, C., & Gervais, R. (2012). Ecohydraulic analysis of fish fatigue data. *River Research and Applications*, 28(4), 444–456. <https://doi.org/10.1002/rra.1566>

## Appendix C

For all collected experimental data, the allometric relationships for the fish fork length  $L_f$ , mass  $m$ , height  $h$ , and width  $w$  were plotted, for all five fish species, as power laws of the type  $Y = \gamma X^\theta$ , where  $Y$  stands for  $L_f$ ,  $w$ , and  $m$  and  $X$  stands for  $w$ ,  $h$ , and  $m$  (Figure C.1). The correlation coefficient  $R^2$  was determined from the linear regression of log-transformed values of  $L_f$ ,  $m$ ,  $h$ , and  $w$ . The highest  $R^2$  value of 75% was found for the allometric relation between  $L_f$  and  $m$  and no  $R^2$  value was lower than 50%.

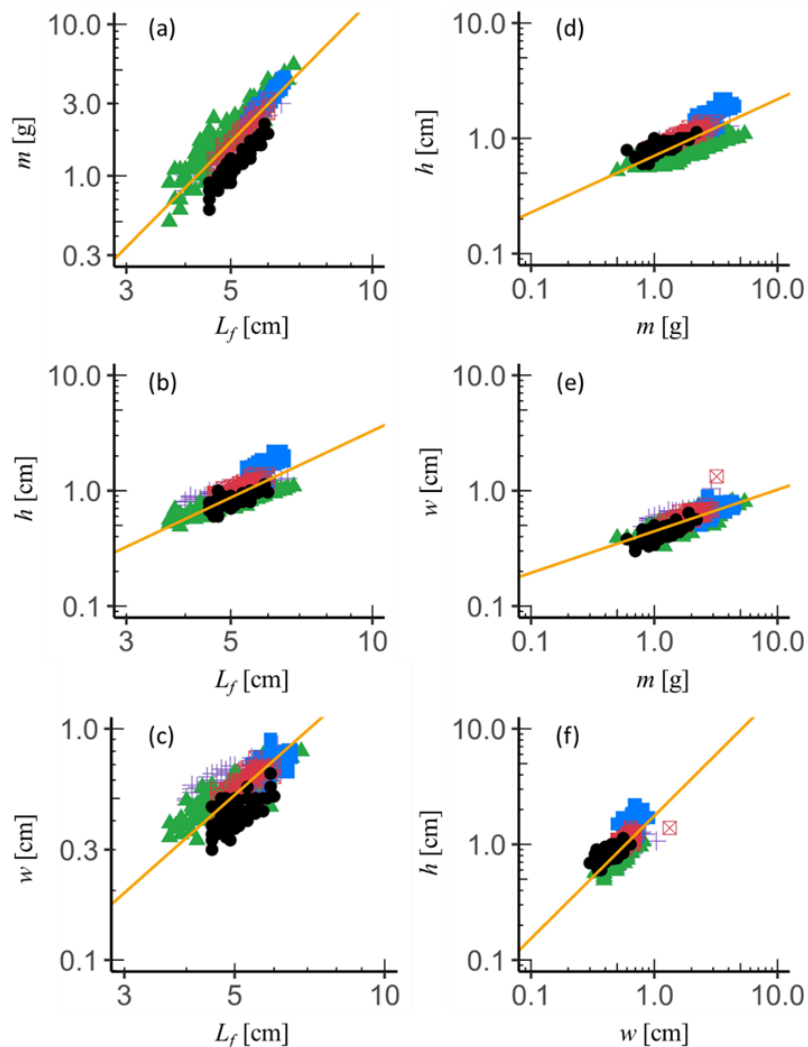


Figure C.1 Fish allometric relationships for five fish species between (a)  $L_f$  and  $m$ , (b)  $L_f$  and  $h$ , (c)  $L_f$  and  $w$ , (d)  $m$  and  $h$ , (e)  $m$  and  $w$ , and (f)  $w$  and  $h$ . Different symbols and colour marks are for different fish species: Plus purple mark (+) for Italian ruffle dace, green triangle ( $\blacktriangle$ ) for common minnow, blue square ( $\blacksquare$ ) for European bitterling, red crossed square ( $\boxtimes$ ) for North Italian roach, and black dot ( $\bullet$ ) for common bleak. Regression analysis is performed on all data from five fish species, and the regression lines for each allometric relationship are drawn in orange colour.



## Appendix D

From Eq. 4.9 ( $\overline{T_f^k} \sim U_r^{-k(\beta+1)}$ ), it is argued that the scaling of central moments (of any order) of  $T_f$  follows power law with exponent  $-k(\beta + 1)$ . In principle, the validity of this scaling relationship should be experimentally verified for any value of  $k$  (where  $k$  can be any positive integer). However, statistical robust estimation of central moments require an increasing sample size with increasing value of  $k$ , making it a difficult task to accurately estimate the central moments of higher order.

In this appendix, we demonstrate that for  $k = 3$  (and hence for any other value larger than 3), the estimation of central moments is characterised by an uncertainty that makes it meaningless to carry out data fitting to estimate the associated scaling exponent  $\beta$  in Eq. 4.9. This appendix reports the results obtained from the third-order central moment of time-to-fatigue ( $\overline{T_f^3}$ ) for the subsampled group with the highest *ReI* value for all fish species. Confidence intervals with 95% confidence level, for  $\overline{T_f^3}$ , were estimated from the 2.5<sup>th</sup> and 97.5<sup>th</sup> percentiles of the bootstrap distribution resulting from the bootstrapping procedure of data resampling with replacement using 10,000 replications.

Figure D.1 shows, for all fish species, the relationship between  $\overline{T_f^3}$  and  $U_f$ . While the 95% confidence intervals are very large and span up to four orders of magnitude, they are most often larger than the differences between the estimated values of  $\overline{T_f^3}$ , meaning such differences are not statistically significant. This is due to the limited sample size used to estimate the third-order central moment of  $T_f$  and its confidence interval. In conclusion, it is meaningless to identify trend using regression analysis and ultimately estimating the scaling exponent  $\beta$  in Eq. 4.9, for the scaling relationship between  $T_f$  and  $U_f$  for  $k = 3$  (or higher).

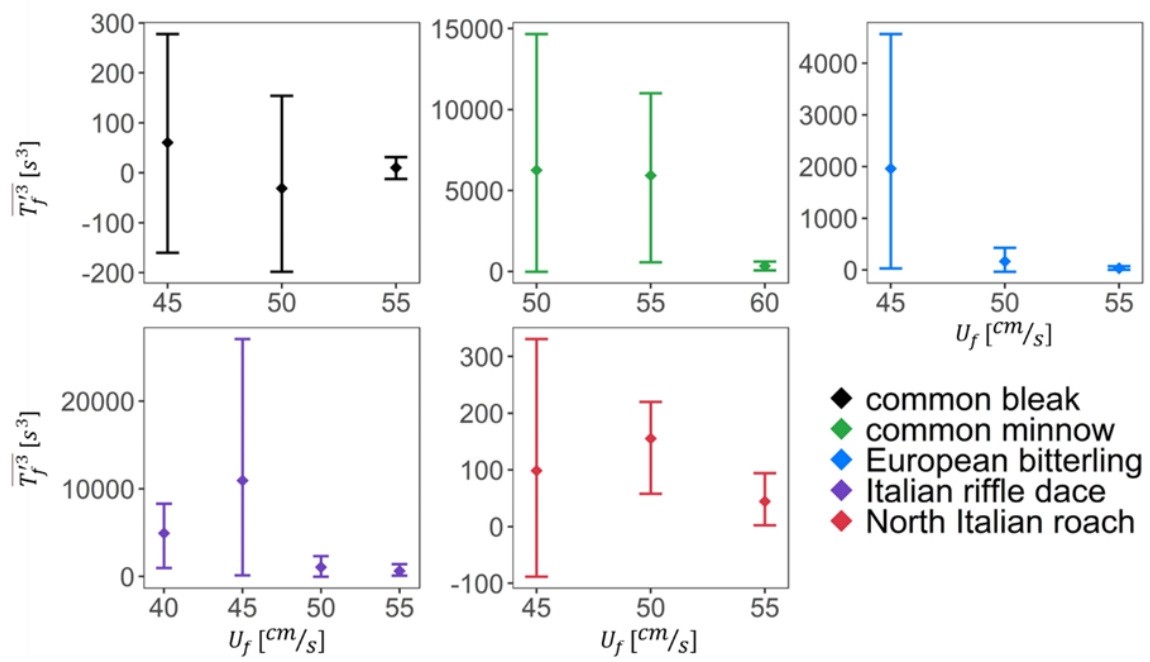


Figure D.1 Plots between  $\overline{T_f^3}$  and  $U_f$  for the subsampled data with the highest Reliability Index (Rel). Each panel correspond to different fish species as specified in the legend with a different colour code. Diamonds mark the third-order central moment values of time-to-fatigue data at a given test flow velocity and the error bars mark the 95% confidence interval for  $\overline{T_f^3}$ .

## Appendix E

This appendix contains a comprehensive list of all candidate models for both tapped and untapped fatigue definitions, for which the Akaike information criterion (AIC) values were calculated. The best (selected) model was the one with the lowest AIC value.

*Table E.1 List of candidate models for (a) Tapped and (b) Untapped fatigue definitions with their AIC values in ascending order. The plus (+) symbol between two predictor variables indicates that only the effect of each predictor variable was considered separately, whereas the asterisk (\*) symbol includes both the effect of each predictor variable and their interaction effect.*

(a)

<b>Tapped Fatigue</b>	
<b>Candidate models</b>	<b>AIC value</b>
Flume length + Flow velocity	245.49
Flow velocity	247.64
Flow velocity * Day	248.82
Flume length + Flow velocity + Day	248.99
Flume length * Flow velocity	250.71
Flow velocity + Day	250.87
Flume length * Flow velocity * Day	251.38
Day	300.49
Flume length	301.82
Flume length + Day	303.35
Flume length * Day	306.19

(b)

<b>Untapped Fatigue</b>	
<b>Candidate models</b>	<b>AIC value</b>
Flume length + Flow velocity + Day	303.75
Flume length * Flow velocity * Day	306.11
Flume length + Flow velocity	306.56
Flow velocity	307.59
Flume length * Flow velocity	307.60
Flow velocity + Day	308.43
Flow velocity * Day	310.35
Flume length + Day	333.41
Flume length * Day	335.29
Flume length	336.49
Day	338.12